Measure-preserving dynamical systems on $\mathbb{R}^3$ with all trajectories bounded

by

Jeffrey M. Ford

A dissertation submitted to the Graduate Faculty of
Auburn University
in partial fulfillment of the
requirements for the Degree of
Doctor of Philosophy

Auburn, Alabama
December 16, 2017

Keywords: Dynamical Systems

Approved by

Dr. Krystyna Kuperberg, Chair, Professor of Mathematics
Dr. Ziqin Feng, Assistant Professor of Mathematics
Dr. Huajun Huang, Associate Professor of Mathematics
Dr. Michel Smith, Professor of Mathematics

Abstract

We present here constructions, both smooth and piecewise-linear, of non-singular, measure-preserving dynamical systems on $\mathbb{R}^3$, with each trajectory contained in a bounded set. In the smooth case, we use a sequence of nested subsets of $\mathbb{R}^3$, and construct a measure-preserving flow where no trajectory escapes the set in which it originates. In the piecewise-linear case, we again employ a sequence of nested subsets, but rather than defining a flow using vector fields, we construct a measured 1-foliation, which gives rise to a measure-preserving dynamical system.

Acknowledgments

I would like to thank all of the people who have worked to make this dissertation possible. First I would like to thank Dr. Krystyna Kuperberg, for her support and encouragement over the past years. I would also like to thank Dr. Brian Martensen at Minnesota State University, for introducing me to Dr. Kuperberg. I am also grateful to Dr. Ziqin Feng, Dr. Huajun Huang, and Dr. Michel Smith for agreeing to serve on my committee.

I would like to thank Steven Clontz, Kat Perry, Ian Cero, and Joe Ozbolt for being excellent and supportive fellow students during my time at Auburn. I am especially thankful for the late Dr. Frank Sturm, who was a strong positive influence in my graduate career, and a very dear friend.

Finally, I would like to dedicate this dissertation to my spouse, Dr. Kristie Campana. Without her support and sacrifices, my pursuit of this degree and the completion of this dissertation would not have been possible.

Table of Contents

List of Figures

Chapter 1

Introduction

We begin with a non-technical overview of our results and motivations. A dynamical system can be thought of as a space (called the phase space) and a function (called the phase map) that describes how the points in that space move over time.

There are three major concepts necessary to state our results. First, we need the trajectories of the dynamical system. Starting with any point, we can find the location of that point at any time t, with t being positive or negative. We can think of a time t as being applied to a point x, moving x to some new point, tx. We require that if a point is moved by some time t_1, then another time t_2, that the action is the same as though the point was moved by time $t_1 + t_2$.

Given any point in our space, the set of all points which are reached by that point at any time is the trajectory of the point. For our construction, we need all trajectories to be bounded. Our constructions are in the 3-dimensional space of real numbers, $\mathbb{R}^3$. When we speak of a bounded subset of $\mathbb{R}^3$, we can think of a 3-dimensional solid ball of some finite radius. A trajectory is bounded if the entire trajectory can fit in some solid ball. For our constructions, we want each trajectory in the dynamical system to be bounded. If the sizes of all of the balls were capped by some diameter, we would say the bound is uniform.

All of our constructions have continuous trajectories; that is, they do not have any breaks. Depending on the dynamical system, the trajectories may or may not be smooth. We have one construction in which the entire system has smooth trajectories, one in which the trajectories are piecewise-smooth, and one in which the trajectories are piecewise-linear.

It is possible to create a dynamical system where some of the points never move, or where the function we use is undefined at certain points. Points where either of these behaviors occur are called singular points. We only want to work with non-singular dynamical systems, which have no singular points.

The third concept is the idea of a measure-preserving dynamical system. This is a generalization of the concept of an incompressible fluid, as described in [Ac] and [J]. For example, if a stone is dropped into a bucket of water, the water changes its shape to move around the stone, but the total volume remains the same. We can assign a function to our phase space, which we call the measure, that is analogous to measuring volume. If we pick some subset of our phase space, and find its measure, we would like that measure to be the same after all of the points in the space are moved by some time. The shape of our subset may dramatically change during the action by the phase map, but the total measure, or total volume, should remain the same.

The results in this dissertation each involve constructing non-singular, measure-preserving dynamical systems on $\mathbb{R}^3$.

We will construct three dynamical systems with this property. Two of these dynamical systems are constructed using vector fields. A vector field describes a dynamical system by telling each point which direction to move, and at what speed. The advantage to this is that we can immediately check whether or not the dynamical system is measure-preserving, via a straightforward calculation.

The third example will be constructed using a foliation. We find a way to break our phase space into a collection of 1-dimensional sets, which do not overlap with each other, and which cover every point in the space. These 1-dimensional sets, called leaves, can be shown to correspond with the trajectories of a dynamical system. Using this foliation, we can construct a piecewise-linear version of our theorem.

The motivation for this work arises from a question asked by G. Kuperberg, following his work in [GK]. As reported in [Ku], Kuperberg asked if there existed a non-singular dynamical system on $\mathbb{R}^3$, which was volume-preserving, and in which all trajectories were uniformly bounded.

It is shown in [JY] that there exists a non-singular dynamical system on $\mathbb{R}^3$ with all trajectories bounded, though the bound is not uniform. As a solution to Problem 110 in [Ma], it was shown by K. Kuperberg and Reed [KR], that there did exist a non-singular dynamical system on $\mathbb{R}^3$ with each trajectory uniformly bounded. We take ideas from each of these results in building something new.

G. Kuperberg's original question remains open, but our constructions in Theorems 2.4-2.6 make progress towards a solution. The difference is that the bounds on the trajectories here are not uniform.

In the second chapter, we give the formal definitions of dynamical systems and foliations, as well as how to determine if either is measure-preserving. In the third chapter, we use vector field constructions to find smooth and piecewise-smooth versions of our result. Chapter 4 shows how a foliation can be transformed into a dynamical system. In Chapter 5 we give further background on piecewise-linear constructions, and give the proof of the piecewise-linear version of our theorem.

Chapter 2

Preliminaries

We include the formal definitions here that are necessary to precisely state our results.

2.1 Dynamical Systems

A *topological manifold* M is a Hausdorff space with a countable basis, where for each point $p \in M$, there exists a neighborhood U about p which is homeomorphic to an open subset of $\mathbb{R}^n$. A *dynamical system* [BS] is a topological manifold X and continuous map $\pi : \mathbb{R} \times X \to X$, satisfying the properties,

- $\pi(0, x) = x$
- $\pi(t_1, (\pi(t_2, x)) = \pi(t_1 + t_2, x)$

X is called the *phase space* and π the *phase map*. When the map is acting on a subset of $\mathbb{R} \times X$, we refer to the dynamical system as a *flow*. The dynamical system may be written as $(X, \mathbb{R}, \pi)$, and can be thought of as an $\mathbb{R}$ group action on X. It may be written just as (X, π), when the group action is understood. When no confusion will arise, we abbreviate $\pi(t, x)$ by tx.

Given any $x \in X$, we define the *positive semi-trajectory* and *negative semi-trajectory* respectively as

$$\gamma^+(x) = \{tx : t \in \mathbb{R}_{\geq 0}\}$$

$$\gamma^-(x) = \{tx : t \in \mathbb{R}_{<0}\}.$$

The *trajectory* of x is the $\gamma(x) = \gamma^+(x) \cup \gamma^-(x)$. The trajectory is sometimes referred to as the *orbit* of x, while the positive and negative semi-trajectories are referred to as the *positive orbit* and *negative orbit* respectively.

A natural question is to ask the behavior of a sequence of points in X, determined by acting on a single point of X by all positive or negative values in $\mathbb{R}$. The *ω-limit set* of a point x is

$$\omega(x) = \{y \in X : \text{ there exists a sequence } \{t_n\} \subset \mathbb{R}, \text{ with } t_n \to \infty \text{ and } \{t_n x\} \to y\}.$$

Similarly, the *α-limit set* of a point x is

$$\alpha(x) = \{y \in X : \text{ there exists a sequence } \{t_n\} \subset \mathbb{R}, \text{ with } t_n \to -\infty \text{ and } \{t_n x\} \to y\}.$$

Given a point $x \in X$, we define the *positive orbit closure of x* by $\overline{\gamma^+(x)} = \gamma^+(x) \cup \omega(x)$ and the *negative orbit closure of x* by $\overline{\gamma^-(x)} = \gamma^+(x) \cup \alpha(x)$. The *orbit closure of x* is then just $\overline{\gamma(x)} = \overline{\gamma^+(x)} \cup \overline{\gamma^-(x)}$.

The phase map may also be applied to subsets of the phase space, rather than individual points. For a subset $Y \subseteq X$, $tY = \{tx : x \in Y\}$. Such a set is said to be *invariant* if, for all $t \in \mathbb{R}$, $tY \subseteq Y$. Equivalently, for each $x \in Y$, $\gamma(x) \subset Y$. A set may be *positively invariant* or *negatively invariant*, using similar definitions.

It is frequently the case that a flow is described by the vector field of a differential equation or system of differential equations. Observe that, for a phase map π, the vector field of the derivative $\frac{d\pi}{dt}|_{t=0}$ is parallel to the trajectories of the flow. This will be used to construct examples. We will find it convenient to switch between vector fields and flows.

There are a few special types of points in the system whose definitions we will need. A point $x \in X$ is a *fixed point* if, for all $t \in \mathbb{R}$, $tx = x$. A point $x \in X$ is a *periodic point* if

there exists $T \in \mathbb{R}$ such that $Tx = x$. If T is the smallest real such that $Tx = x$, x is said be *periodic of order* T. A fixed point is said to be periodic of order 0.

Lemma 2.1. Given a dynamical system $(X, \mathbb{R}, \pi)$, for each $x \in X$, $\gamma(x)$ is either a single point, homeomorphic to S^1, or homeomorphic to $\mathbb{R}$.

Proof. We consider two cases, when x is or is not a periodic point.

Case 1: Let x be a periodic point, with fundamental period t_0. Let $h : \gamma(x) \to [0, 1]$ be given by $h(x) = 0$ and $h(t_0 x) = 1$. Provided $t_0 \neq 0$, $[0, t_0]$ is homeomorphic to $[0, 1]$, h can be extended to all of $\gamma(x)$, and is a homeomorphism. As $x = t_0 x$, we identify the points 0 and 1 in the range, hence the range of h is actually S^1. If it is the case that $t_0 = 0$, x is fixed, and $\gamma(x)$ is a single point.

Case 2: If x is not periodic, assume $\gamma(x)$ is not homeomorphic to $\mathbb{R}$. Then there is some maximum value $T \neq 0$, such that for all $t > T$, $tx = Tx$. Then $x = 0x = (-t + t)x = (-t + T)x$, but as x is not periodic, we have a contradiction. We conclude that $\gamma(x)$ is homeomorphic to $\mathbb{R}$. □

Finally, we introduce the notion of a *minimal set*. A subset $Y \subseteq X$ is minimal if Y is non-empty, closed and invariant, and no subset of Y has these properties.

A convenient description of a minimal set is the following theorem [BS].

Theorem 2.2. Given a dynamical system (X, π), a non-empty set $Y \subset X$ is minimal if and only if $\overline{\gamma(x)} \subset Y$ for all $x \in Y$.

Proof. Assume Y is minimal, and $x \in Y$. Then Y is invariant, implying $\gamma(x) \subset Y$. Y is also closed, hence for any $\{t_n\} \subset \mathbb{R}$, the sequence $\{t_n x\}$ converges in Y. Therefore, $\alpha(x) \subset Y$ and $\omega(x) \subset Y$. We conclude that $\overline{\gamma(x)} \subset Y$.

Conversely, assume $\overline{\gamma(x)} \subset Y$ for each $x \in Y$. Y is given to be non-empty, so we need only check invariance and closure. $\gamma(x), \alpha(x)$, and $\omega(x)$ are each subsets of $\overline{\gamma(x)} \subset Y$, hence Y is invariant and closed. Therefore, Y is minimal. □

We will address a few different smoothness classes of dynamical systems here. A C^k *dynamical system*, is one in which the phase map π is k-times continuously differentiable. If a phase map is continuously differentiable for all k, the dynamical systems is C^∞, and we will refer to it as a *smooth dynamical system* [HSD].

Piecewise-linear dynamical systems are described in detail in Chapter 4.

2.2 Measure-preserving dynamical systems

Let Ω be a set. A σ-*algebra* $\mathcal{A}$ is a non-empty collection of subsets of Ω, which is closed under complements and countable unions. A *measure* μ on $\mathcal{A}$ is a function $\mu : \mathcal{A} \to \mathbb{R} \cup \{\infty\}$ satisfying the three conditions[Ro]:

1. $\mu(A) \geq 0$ for all $A \in \mathcal{A}$
2. $\mu(\emptyset) = 0$
3. If $A_1, A_2, \ldots$ are elements of $\mathcal{A}$, with $A_i \cap A_j = \emptyset$ for all $i \neq j$, then

$$\mu\left(\bigcup A_n\right) = \sum \mu(A_n).$$

A common measure on $\mathbb{R}^n$ is *Lebesgue measure*. Assume $S = \prod_{i=1}^n [a_i, b_i]$. Let $v(S) = \prod_{i=1}^n (b_i - a_i)$. For some $T \subset \mathbb{R}$, the *outer measure* of T[Ro] is given by

$$\lambda^*(T) = inf\{\sum_{S \in \mathcal{S}} v(S) : \mathcal{S} \text{ is a countable collection of sets that cover } T\}.$$

To distinguish Lebesgue measure in different dimensions, we will use λ_m to indicate the Lebesgue measure on m-dimensional subsets of $\mathbb{R}^n$.

A subset $T \subset \mathbb{R}^n$ is *measurable* if, for all $S \subset \mathbb{R}^n$,

$$\lambda^*(T) = \lambda^*(S \cap T) + \lambda^*(T \setminus S).$$

An outer measure restricted to the collection of measurable sets is the Lebesgue measure.

A measure μ on an n-manifold M is *locally Lebesgue* if, for a given subset $N \subset M$, $\mu(N)$ is equal to the Lebesgue measure of the image of N in $\mathbb{R}^n$ under the chart map.

The ordered triple $(\Omega, \mathcal{A}, \mu)$ consisting of a set, a σ-algebra on that set, and a measure on that sigma algebra, is a *measure space*.

Let $(\Omega, \mathcal{A}, \mu)$ be a measure space. Let $(\Omega, \mathbb{R}, \varphi)$ be a dynamical system as defined above. We define the inverse of φ by letting $\varphi^{-1}(t, x) = \varphi(-t, x)$. Let φ have the added condition that, for all $A \in \mathcal{A}$, $\varphi^{-1}(A) \in \mathcal{A}$. The measure μ is *invariant* with respect to φ if $\mu(A) = \mu(\varphi^{-1}(A))$ for all $A \in \mathcal{A}$. If μ is invariant with respect to φ, $(\Omega, \mathcal{A}, \mu, \varphi)$ is a *measurable dynamical system* [Ro].

A measure may also be defined in terms of differential forms. We borrow the notation here from [GP].

Given a manifold M and some point $x \in M$, the *tangent space at* x, $T_x(M)$ is the vector space of all vectors tangent to M at x. A *p-tensor* on a vector space V is a multilinear real valued function on V. A tensor T is *alternating* if the transposition of two variables changes the sign on T [GP], for example, if

$$T(v_1, v_2, v_3) = -T(v_1, v_3, v_2).$$

A p-form on M is a function ω that assigns to each point $x \in M$ an alternating p-tensor $\omega(x)$ which acts on $T_x(M)$.

In the case $M = \mathbb{R}^p$, a p-form is called a *volume form*. We will also refer to this as a Euclidean volume form, indicating that, if we label the coordinates $x_1, x_2, \ldots, x_p$ in $\mathbb{R}^p$, then $\omega = dx_1 \wedge dx_2 \wedge \cdots \wedge dx_p$.

A *Riemannian metric* [HK] on M is a collection of inner products $g_p : T_pM \times T_pM \to \mathbb{R}$, such that g_p applied to any smooth vector field on M yields a positive real number.

These inner products can be written as a matrix G. Then the *Riemannian volume form* [HK] is given by $\sqrt{|G|}dx_1 \wedge \cdots \wedge dx_n$, where $|G|$ is the absolute value of the determinant of G. Any Riemannian volume form gives rise to a measure which is a non-zero scalar multiple of Lebesgue measure [HK].

If a set $N \subset M$ is a member of some σ-algebra on M and ω is a volume form (Riemannian or not) on M, then we can define a measure

$$\mu(N) = \int_N \omega.$$

We have the following useful lemma to determine when a flow is volume-preserving.

Lemma 2.3. In the case that a measure μ given by a smooth volume form and the dynamical system is parallel to a smooth vector field $\vec{v}$ on $\mathbb{R}^n$, the measure-preserving condition is equivalent to the divergence equation [M2]

$$\nabla \cdot \vec{v} = 0.$$

Furthermore, any diffeomorphism which has Jacobian with determinant 1 preserves volume. It follows that translations and rotations in $\mathbb{R}^n$ preserve volume.

Such a dynamical system is called *volume-preserving*. This term will be used interchangeably with measure-preserving when it is clear that the measure comes from a volume form.

Take a manifold M, a measure μ on M, and a dynamical system $(\mathbb{R}, M, \pi)$, which is not necessarily measure preserving. The *likely limit set* $\mathcal{A}(M)$ of this dynamical system is the smallest closed subset of M such that $\omega(x) \subset \mathcal{A}(M)$, for all x in M, excluding a set of measure zero [M].

As stated by Milnor [M], if $(\mathbb{R}, M, \pi)$ is measure-preserving, then $\mathcal{A}(M) = M$. By contrapositive, if $\mathcal{A}(M) \neq M$, then $(\mathbb{R}, M, \pi)$ is not measure-preserving.

With the preliminary definitions out of the way, we can state our first two results. These will be proven in Chapter 3.

Theorem 2.4. There exists a C^0, measure-preserving dynamical system on $\mathbb{R}^3$, with all trajectories bounded.

Theorem 2.5. There exists a smooth, measure-preserving dynamical system on $\mathbb{R}^3$, with all trajectories bounded.

2.3 Foliations

Begin with an n-dimensional manifold M, and fix some indexing set A. Let $\mathcal{F} = \{L_\alpha : \alpha \in A\}$ be a collection of arcwise connected subsets of M. $\mathcal{F}$ is a *1-foliation of* M [T] if

(i) $L_\alpha \cap L_\beta = \emptyset$ for $\alpha \neq \beta$

(ii) $\bigcup_{\alpha \in A} L_\alpha = M$.

(iii) Given any point $p \in M$, there exists a chart $(U_\lambda, \varphi_\lambda)$ about p, with each φ_λ a homeomorphism $U_\lambda \to \mathbb{R}^n$, such that for L_α with $L_\alpha \cap U_\lambda \neq \emptyset$, each arcwise connected component of $\varphi_\lambda(L_\alpha \cap U_\lambda)$ is of the form

$$\{(x_1, x_2, \ldots, x_n) \in \varphi_\lambda(U_\lambda) : x_2 = c_1, x_3 = c_2, \ldots, x_n = c_{n-1}\}$$

where each c_i is a constant determined by L_α.

The manifold M is called the *support* of $\mathcal{F}$. The atlas $\{(U_\lambda, \varphi_\lambda)\}$ is called the *foliation atlas*.

Note that this definition requires that no points in M may exist outside of a leaf. It is possible to extend our definition to include a case where isolated points are not contained in leaves. Such points are called *singular* [FLP]. We will only consider non-singular foliations here.

We can also address the smoothness of a 1-foliation. A 1-foliation is said to be C^r if the chart maps are also C^r.

Since only one coordinate is not fixed in our definition of a 1-foliation, the image of a leaf under each chart map is homeomorphic to some interval in $\mathbb{R}$. A 1-foliation is *oriented* if the chart maps from the foliation to $\mathbb{R}^n$ preserves the usual orientation of $\mathbb{R}$. [T].

We have a choice of foliation atlas for a given foliation $\mathcal{F}$ with support M.

A *nice atlas* is a foliation atlas satisfying three conditions [Wa]:

1. The covering $\{U_\lambda\}$ is locally finite.

2. For any φ_λ, the set $\varphi_\lambda(U_\lambda) \subset \mathbb{R}^n$ is an open cube, $(-1, 1)^n$.

3. If φ_{λ_1} and φ_{λ_2} are each chart maps, with $U_{\lambda_1} \cap U_{\lambda_2} \neq \emptyset$, then there exists some φ_{λ_3}, such that $\varphi_{\lambda_3}(U_{\lambda_3})$ is an open cube, U_{λ_3} contains the closure of $U_{\lambda_1} \cup U_{\lambda_2}$, and $\varphi_{\lambda_1} = \varphi_{\lambda_3}|U_{\lambda_1}$.

For an arbitrary foliated manifold, a nice atlas always exists [Wa].

Given some U_λ in a nice atlas, and a leaf L in $(M, \mathcal{F})$, a *plaque* is the connected components of the intersection $L \cap U_\lambda$.

In a nice atlas, each plaque is diffeomorphic to (-1,1).

The other variation on the definition of a foliation, will be specifically for a foliation on a manifold with boundary. Assume M^n is an n-dimensional manifold with boundary. A foliation $\mathcal{F}$ on M^n, is a *1-foliation transverse to the boundary*[T] if the following conditions are satisfied:

(i) $L_\alpha \cap L_\beta = \emptyset$ for $\alpha \neq \beta$.

(ii) $\bigcup_{\alpha \in A} L_\alpha = M$.

(iii) Given any point $p \in M$, there exists a chart $(U_\lambda, \varphi_\lambda)$ about p, with each $\varphi_\lambda : U_\lambda \to \mathbb{R}^n_+$, a homeomorphism, such that for L_α with $L_\alpha \cap U_\lambda \neq \emptyset$, each arcwise connected component of $\varphi_\lambda(L_\alpha \cap U_\lambda)$ is of the form

$$\{(x_1, x_2, \ldots, x_n) \in \varphi_\lambda(U_\lambda) : x_2 = c_1, x_3 = c_2, \ldots, x_n = c_{n-1}\}$$

where each c_i is a constant determined by L_α.

This is illustrated in Figure 2.1, taken from [T]. The difference between this definition and our earlier definition is that the chart maps are strictly to the positive orthant in $\mathbb{R}^n$.

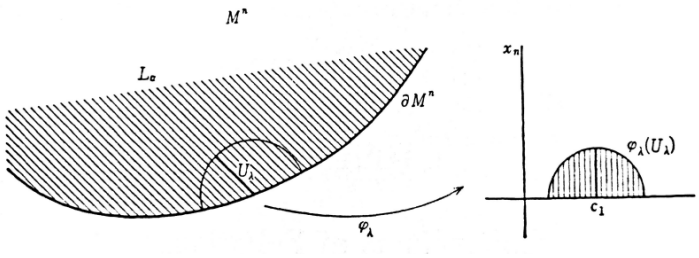

Figure 2.1: Example of chart map on a foliation transverse to the boundary of M^n.

For a foliated manifold with boundary $(M^n, \mathcal{F})$, we can also define the foliation $\partial\mathcal{F}$. Let A be the indexing set on the leaves as in our past two definitions, then $\partial\mathcal{F} = \{$ the connected components of $L_\alpha \cap \partial M^n : \alpha \in A\}$ [T]. This will be used in Chapter 4 in relating foliations to dynamical systems.

2.4 Measured foliations

To define a measure on a foliation, begin with an n-manifold M and a codimension $n-k$ foliation of M, denoted $\mathcal{F}$, with leaves $\mathcal{L}$. We take a collection of closed disks called *flow*

boxes of the form $D_k \times D_{n-k}$, whose interiors cover M. We want each $\mathcal{L}_\alpha$ passing through a flow box to intersect the box in a collection of horizontal disks $D_k \times \{y\}$. We then say the flow box is *transverse* to the foliation.

A *transversal* T is a smooth $(n-k)$-dimensional submanifold which is transverse to each $\mathcal{L}_\alpha$.

We are working only with 1-foliations here, so for all considerations above, $k = 1$. In this case, we can think of flow boxes like charts in an atlas, where the pre-image of each leaf under the chart map has all but one variable constant.

T is *small* if it can be surrounded by a single flow box. A *transverse measure* μ on $\mathcal{F}$ is a function which assigns each small transversal a finite non-negative number[RS]. Further, μ must be additive on a union of transversals. This additivity allows us to assign a measure to a transversal which is not small, by assigning it the sum of its measure in all flow boxes which contain it.

If α and β are two small transversals, an *isotopy* is a map $f : \alpha \times [0,1] \to \beta$, such that, for each $t \in [0,1]$, the restriction f_t which maps $x \in \alpha$ to $(x,t) \in \alpha \times [0,1]$ is an embedding. The *track* of the isotopy is the embedding $\hat{f} : \alpha \times [0,1] \to \beta \times [0,1]$, with $(x,t) \mapsto (f(x,t),t)$ [Hi]. For each $t \in [0,1]$, the isotopy is essentially constructing a path through the embeddings. We will be interested in isotopies where this path is parallel to the leaves of our foliation.

Let N be a submanifold of M, and $g : N \times [0,1] \to M$ an isotopy. Let g_0 and g_t represented the embeddings in M of $N \times \{0\}$ and $N \times \{t\}$ for some $t \in [0,1]$, respectively. When g_0 is the identity on N, and each g_t is a homeomorphism, then g is an *ambient isotopy*. [Hi]. An isotopy between two transversals in a 1-foliation is ambient, provided both transversals are small.

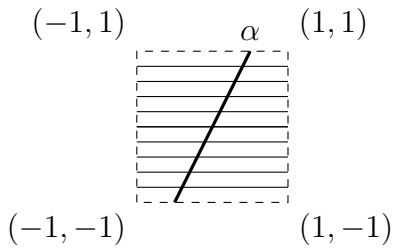

Figure 2.2: Small transversal α, $\mu(\alpha) = 2$.

Given two transversals, α, β, a measure μ is *invariant* if, when α and β are isotopic, with isotopy parallel to the foliation, then $\mu(\alpha) = \mu(\beta)$. Then the pair $(\mathcal{F}, \mu)$ is a *measured foliation*. [FLP]

In some sense we can think of this isotopy as moving one transversal onto another, with each point in the transversal remaining on the same leaf throughout the isotopy. The sets U_λ in the atlas for the foliation serve as flow boxes. To define a measure, let $(x_1, x_2, \ldots, x_n)$ be coordinates in $\mathbb{R}^n$, as in item (iii) in the definition of a 1-foliation. Given a small transversal α, let ω be the $n-1$ Euclidean volume form on $\mathbb{R}^n$. Define $\mu(\alpha) = ||\omega(\varphi_\lambda(\alpha))||$ [FLP]. This measure is locally Lebesgue, and provides convenient coordinates for our calculations.

We can think of the transverse measure on a small transversal as measuring the distance between the vertices of that transversal, after applying the chart map, in all directions except for the direction of the leaves.

For example, if $\mathcal{F}$ is a 1-foliation of a 2-manifold, Figure 2.2 shows the image of a small transversal α, with horizontal lines representing sample leaves. In this case, $\mu(\alpha) = |dy|$, the 1-dimensional Lebesgue measure of the intersection of α with the vertical axis. Note that from one vertex to the other there is a change of 2 in the y-values. There is a change in the x-values, but as this change is in the direction of the foliation, we ignore it.

For our third result, we will achieve the desired dynamics by first looking at a foliation. The following theorem will be proven in Chapter 5.

Theorem 2.6. There exists a piecewise-linear, measure-preserving dynamical system on $\mathbb{R}^3$, with all trajectories bounded.

Chapter 3

C^0 and C^∞ results

3.1 Motivation

We have several previous results that have motivated this work. The questions we investigate have their origins in the study of the fixed-point property. In some sense we can think of our search for non-singular dynamical systems to be akin to finding homeomorphisms of sets which do not have the fixed-point property.

The primary motivation for our construction is the result of Jones and Yorke [JY], proven in Theorem 3.5. We are also influenced by Wilson's construction for modifying flows [W], K. Kuperberg's construction of plugs [KK], and the work of G. Kuperberg on volume-preserving flows [GKK].

Some historical results of note should be mentioned first. We have 3 theorems of interest here. These address the notion of homeomorphisms without fixed-points. The restriction of these homeomorphisms to bounded sets relates them to the dynamical systems with bounded orbits we study here. The first result is due to Borsuk [Bo].

Theorem 3.1. There exists in the 3-dimensional Euclidean space $\mathbb{R}^3$ an acyclic Peano continuum which allows itself to be transformed topologically into itself without fixed-points.

Borsuk's result is based on constructing a 3-dimensional continuum. The second is due to Bing [B3], and is two dimensional.

Theorem 3.2. There is a continuous curve of dimension two which is the intersection of a decreasing sequence of topological cubes and which admits a fixed-point free homeomorphism onto itself.

The third result is due to Brechner and Mauldin [BM]. It is a modification of Bing's result above, extending his example to a construction that works on all of $\mathbb{R}^3$.

Theorem 3.3. There exists a fixed-point free, orientation preserving homeomorphism h of $\mathbb{R}^3$ onto itself, such that the orbits of bounded sets are bounded.

Borsuk's result starts with a cylinder, from which two open tubes are removed, each of which starts on the opposite ends of the cylinder, and without intersecting each other, approaches the base of the opposite tube, asymptotically. Essentially, these tubes becomes cones which spiral around each other, which is the heart of the constructions in both [B3] and [BM]. The parametric equations describing these sets are most clearly stated in [BM]. We include here a summary of the proof of Theorem 3.3, along with a motivating images. It should be noted that the surface in Figure 3.1, when combined with the same surface, but rotating down instead of up, is very similar to the idea used by Borsuk[Bo] (Theorem 3.1) and Bing [B3] (Theorem 3.2.). The main difference is that, in the first two cases, the circles in the spirals were tangent, while here, they are disjoint.

Proof of Theorem 3.3. Let S be the surface consisting of the union of a circle of radius 1 in R^3, lying parallel to the xy-plane, and centered at (0,0,1) and the parametric surface

$$R(u,v) = \left(\frac{u}{u+1}\cos(\frac{\pi}{2}u) + \frac{1}{1+2u}\cos(v), \frac{u}{u+1}\sin(\frac{\pi}{2}u) + \frac{1}{1+2u}\sin(v), \frac{u}{u+1} \right),$$

where $u \geq 0$ and $v \in \mathbb{R}$. We have a spiral originating at the unit disk in the xy-plane, and approaching the limit circle of radius 1 centered at (0,0,1). This is shown in Figure 3.1. We denote this the guiding spiral in the rest of the proof.

Assume $u \geq 0$, and let $\varphi(u) = u + \frac{u}{u+1}$. Then the function

$$\overline{h}(R(u,v)) = R(\varphi(u), v + \frac{\pi}{2})$$

is a fixed-point free homeomorphism of S, provided we extend $\overline{h}$ to our limit circle as a rotation of $\pi/2$.

Let M be S, unioned with the unit disk in the xy-plane, and the bounded complementary domain of S. Fix some $u \geq 0$, and define a function $\hat{h}$ on the disk at height $\frac{u}{u+1}$ in M. For each $a \in [0, 1)$, begin with the circle with parametric equation

$$P(v) = \left(\frac{u}{u+1} \cos(\frac{\pi}{2}u) + a\frac{1}{1+2u}\cos(v), \frac{u}{u+1}\sin(\frac{\pi}{2}u) + a\frac{1}{1+2u}\sin(v), \frac{u}{u+1} \right)$$

, let $u' = \varphi(u) + \frac{1-a}{u+1}$, and map the circle $P(v)$ to the circle on the guiding spiral at height $\frac{u'}{u'+1}$ and radius $\frac{a}{1+2u'}$, while rotating the circle by $\frac{\pi}{2}$.

Each disk in M at height $\frac{u}{u+1}$ is then mapped to a twisted cone, with the base of the code a circle on S at height $\frac{\varphi(u)}{\varphi(u)+1}$, and the vertex of the cone a point on the guiding spiral of height $\frac{u'}{u'+1}$. $\hat{h}$ is then a fixed-point free homeomorphism of M.

Brechner and Mauldin then extend $\hat{h}$ to all of $\mathbb{R}^3$. To define a map $h : \mathbb{R}^3 \to \mathbb{R}^3$, we first define it on all points where $z \in [0, 1)$. h is then defined for all integers n, to act on points with $z \in [n, n+1)$ by translation from the action when $z \in [0, 1)$.

While our guiding spiral S was a twisted cone approaching a limit circle of radius 1 with $z = 1$, we now let S' be the same equation, but twisting down. Then S' has the limit circle of S as its base, and approaches the base of S, and circle with radius 1 and $z = 0$, as its limit circle. This is shown in Figure 3.2. By construction, at each height z, the discs in S and S' are disjoint.

To define h, start with points where $x^2 + y^2 \geq 1$ and $z = \frac{u}{u+1}$. In this case, $h(x, y, z) = (-y, x, \frac{\varphi u}{\varphi(u)+1}$. This changes the height of the point, while rotating counter-clockwise.

We can extend $\hat{h}$ to S', by taking each circle on S' at height $\frac{u}{u+1}$ to a circle on S' at height $\frac{\varphi u}{\varphi u+1}$. $\hat{h}$ also extends to the interior of S' by taking discs to twisted cones, as before, just in the opposite direction.

This gives us a map on all points with $z \in [0, 1)$. Extension to $\mathbb{R}^3$ occurs as above, and h is a fixed-point free homeomorphism.

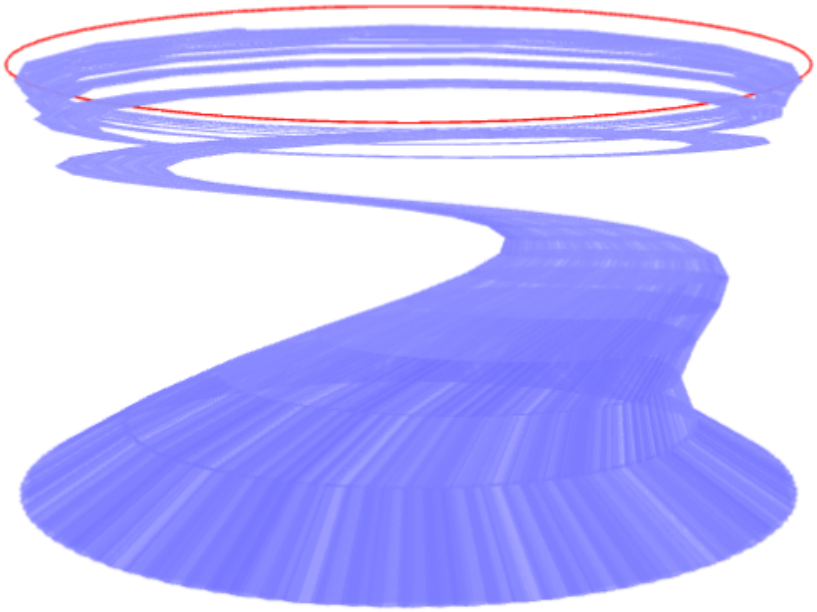

Figure 3.1: The surface S from Theorem 3.3

□

These first three theorems give us some idea of how such constructions develop from early ideas. From the notion of a fixed-point-free homeomorphism, we move to constructing dynamical systems from non-singular vector fields. Our most important influence is the Jones-Yorke construction. We will begin with their construction, modified to suit our needs. As we refer to the Jones-Yorke construction frequently moving forward, we take time to prove it in detail here.

This first lemma is necessary to state the proof from [JY].

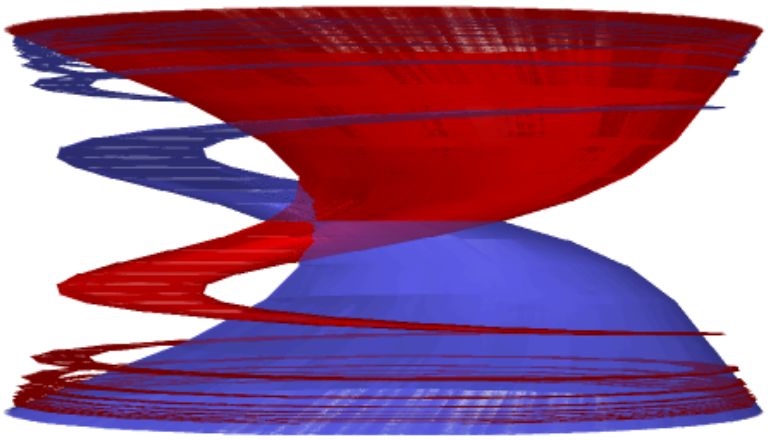

Figure 3.2: The union of S and S'.

Lemma 3.4. The finite sums and products of Lipschitz functions are locally Lipschitz.

Proof. Let f_1 and f_2 be Lipschitz functions on a compact set X, with Lipschitz constants k_1 and k_2 respectively. Let

$$K = k_1(\sup_{x \in X} |f_2(x)|) + k_2(\sup_{x \in X} |f_1(x)|).$$

Then for any $x_1, x_2 \in X$, we have

$$\begin{aligned}
|f_1(x_1)f_2(x_1) - f_1(x_2)f_2(x_2)| &= |f_1(x_1)f_2(x_1) - f_1(x_2)f_2(x_1) + f_1(x_2)f_2(x_1) - f_1(x_2)f_2(x_2)| \\
&\leq |f_1(x_1)f_2(x_1) - f_1(x_2)f_2(x_1)| + |f_1(x_2)f_2(x_1) - f_1(x_2)f_2(x_2)| \\
&= |f_2(x_1)||f_1(x_1) - f_1(x_2)| + |f_1(x_2)||f_2(x_1) - f_2(x_2)| \\
&\leq k_1|f_2(x_1)||x_1 - x_2| + k_2|f_1(x_2)||x_1 - x_2| \\
&\leq K|x_1 - x_2|
\end{aligned}$$

Therefore, the finite product of Lipschitz functions is Lipschitz. For any finite sum of Lipschitz functions, we have

$$|f_1(x_1) + f_2(x_1) - f_1(x_2) + f_2(x_2)| = |f_1(x_1) - f_1(x_2) + f_2(x_1) - f_2(x_2)| \leq (k_1 + k_2)|x_1 - x_2|$$

and the Lipschitz condition holds. □

Theorem 3.5. There exists a non-singular flow on $\mathbb{R}^3$, with all trajectories bounded [JY].

Proof. Define the function $c(r) = \frac{2}{3}(4^{r+1} - 4)$. Construct a set of tori, $\{T^r : r \in 0, 1, 2, \ldots\}$, where T^r is the region bounded by the parametric surface

$$x = 4^r(2 + \cos(u))\cos(v)$$
$$y = 4^r(2 + \cos(u))\sin(v) + c(r)$$
$$z = 4^r \sin(u)$$

if r is even, and

$$x = 4^r \sin(u)$$
$$y = 4^r(2 + \cos(u))\sin(v) + c(r)$$
$$z = 4^r(2 + \cos(u))\cos(v)$$

if r is odd

for $u, v \in [0, 2\pi]$.

Each solid torus T^i is then completely contained in T^{i+1}, with the even indexed tori in the xy-plane, and the odd indexed tori in the yz-plane. Each T^r is centered at $(0, c(r), 0)$. The nesting of the first three tori is shown in Figure 3.1.

Let $p = (x, y, z)$ be a point in $\mathbb{R}^3$. Let $i(r) = \frac{1-(-1)^r}{2}$ so that the function i returns 0 if r is even, and 1 if r is odd. Let $G_0(p) = (y, -x, 0)$ and $G_1(p) = (0, -z, y)$. Let $h_0(p) = \min\{1, 1 - d(T^0, p)\}$ and $h_r(p) = \min\{1, 1 - d(T^r, p), d(T^{r-1}, p)\}$.

Define a flow on $\mathbb{R}^3$, by

$$\dot{p} = \sum_{r=0}^{\infty} G_{i(r)}(p - (0, c(r), 0))h_r(p). \tag{3.1}$$

The proof given in [JY] showing that this flow is non-singular includes the statement that, if, for a given point p, r is the smallest index such that $p \in T^r$, then for all $m < r$, with

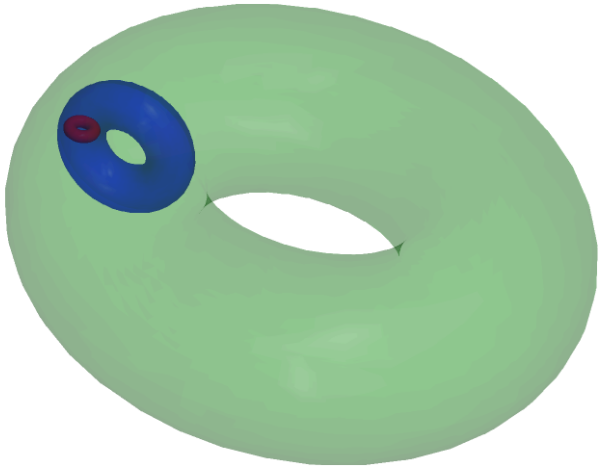

Figure 3.3: Nested tori in $\mathbb{R}^3$

$d(p, T^m) \geq 1$, $h_m(p) = 0$. It is necessary that we not allow negative values for h. We therefore modify the functions to $h_0(p)$ =max$\{0$,min$\{1, 1 - d(T^0, p)\}\}$ and $h_r(p)$ =max$\{0$,min$\{1, 1 - d(T^r, p), d(T^{r-1}, p)\}\}$.

Clearly all trajectories in T^0 are circles, and so remain bounded in T^0. We can also visualize the flow near the boundary of T^0 with trajectories through T^1, as shown in Figure 3.2.

For any point in T^n, the omega limit set of that point is in T^n, either by remaining in a periodic orbit in T^n, or by attracting to the surface of T^{n-1}. Hence, each T^n is invariant, and as $\mathbb{R}^3 = \cup_{n=0}^{\infty} T^n$, all trajectories are bounded.

We now show that the flow is non-singular. We first show that all solutions of (1) are unique.

For each natural r, if $p \in T^r$, $h_m(p) = 0$ for all $m > r$. Therefore, (1) is always computed as a finite sum. (1) is therefore locally Lipschitz on each T^r, and as $\mathbb{R}^3 = \cup_{i \in \mathbb{N}} T^r$, it is locally Lipschitz on $\mathbb{R}^3$. Therefore, solutions of (1) exist are are unique [CL].

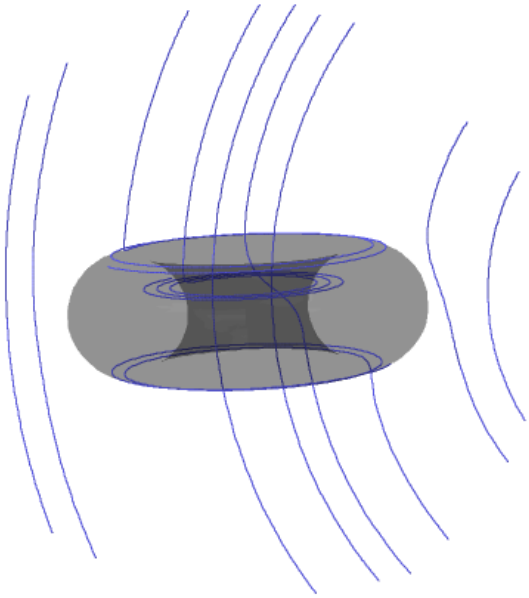

Figure 3.4: Flow near the boundary of T^0

To verify that $\dot{p} \neq 0$, for all $p \in \mathbb{R}^3$, first fix p and let $r = \min\{s : x \in T^s\}$. As above, $h_m(p) = 0$ for all $m > r$. If $d(p, T^{r-1})n \geq 1$, then $h_r(p) = 1$. If $0 < d(p, T^{r-1}) < 1$, then $h_r(p) = h_{r-1}(p) = d(p, T^{r-1}) \neq 0$. If $m < r - 1$, $d(p, T^m) > d(p, T^r)$, which implies $1 - d(p, T^m) < 0$, and therefore $h_m(p) = 0$. We need only consider the r and $r - 1$ terms of the sum to determine that the flow is non-singular.

If $r = 0$, $\dot{p} = (y, -x, 0)$, which is non-zero for all points in T^0. If $r > 0$, $\dot{p} = (y - c(r), -x - z, y - c(r-1)$ when r is even, and $\dot{p} = (y - c(r-1), -x - z, y - c(r)$ when r is odd. In either case, $\dot{p} = 0$ iff $y = c(r-1)$ and $y = c(r)$. By the definition of $c(r)$, this is never true, and we conclude that the flow is non-singular. □

As constructed, this flow is not measure-preserving. The boundary of T^n is an attractor for a subset of T^{n+1} of non-zero measure, and by a result of Milnor [M], cannot preserve measure. This can also be verified directly by writing the function h explicitly for points

whose distance from T^0 is less than or equal to 1. It is easy to check that the explicit construction of this flow has non-zero divergence.

3.2 Modifying dynamical systems

One method for modifying dynamical systems is the insertion of plugs. We give here the definition of a plug as in [KK].

Let F be a compact, orientable 2-manifold, with non-empty boundary. Let $I = [0, 1]$. Let φ be a flow on $F \times I$, generated by a non-singular vector field $\mathcal{V}$. Additionally, assume that on some neighborhood of the boundary of $F \times I$, the vector field is parallel to the boundary, and oriented in the positive direction of I. F is called the *base* of $\mathcal{V}$. We have three conditions we wish the flow to satisfy:

(i) If a trajectory of φ passes through a point $(p, 0)$ and a point $(q, 1)$, then $p = q \in F$.

(ii) The reflection of $\mathcal{V}$ through the layer $F \times \{1/2\}$ is the negative of $\mathcal{V}$.

(iii) There exists at least one trajectory of φ passing through $F \times \{0\}$, which does not intersect $F \times \{1\}$.

If condition (i) is satisfied, the flow has *matched ends*. If condition (ii) is satisfied, the flow has the *mirror image property*. If $\mathcal{V}$ satisfies conditions (i) and (iii) it is a *plug*. It is a *semi-plug* if it satisfies (iii) but not (i). It is an *un-plug* if it has matched ends, but does not satisfy (iii), and it is a *semi-un-plug* if it fails to meet any criteria. If it satisfies all 3 conditions, it is a *mirror-image plug*.

A construction by Wilson [W] will turn a plug into a mirror-image plug. Simply by concatenating a plug with the image of itself, such that the upper half is the negative of the reflection of the lower half, will create a plug with the mirror-image property. This will ensure that any trajectory through $(p, 0)$ and $(q, 1)$, with $p \neq 1$, continues through the point $(p, 2)$, so the mirror-image property is satisfied.

An important consideration when constructing a plug is the ability to use it to smoothly change a given flow on a manifold. Again referring to [KK], let $\mathcal{V}$ be a plug with base F, and $\mathcal{X}$ a flow on some 3-manifold M. Let $f : F \times I \to M$ be an embedding, that is, f is continuous, injective, and $F \times I$ is homeomorphic to $f(F \times I)$. We require also that $f(\{p\} \times I)$ is contained in the trajectory of $f(p, 0)$. The direction of $\mathcal{V}$ and the direction of $\mathcal{X}$ must agree on the boundary of $F \times I$. We refer to this situation as the flow generated by $\mathcal{X}$ being *parallel* to the boundary of $F \times I$. If these conditions are satisfied, $F \times I$ is *inserted* into the parallel flow. If $F \times I$, $\mathcal{V}$, $\mathcal{X}$, M, and f are each C^r (where r may be ∞), then we smoothly change the vector lengths around the image of the boundary of $F \times I$ to obtain a new vector field $\mathcal{Y}$, which agrees with $\mathcal{V}$ inside of the image of $F \times I$ under f, and agrees with $\mathcal{X}$ everywhere else. This process is referred to as an *insertion*.

3.2.1 Dehn Surgery

Insertion as defined in [KK] is not quite sufficient for the proof we wish to construct here. Instead of removing a region from an existing flow which is homeomorphic to our plug by finding an embedding of $F \times I$, we will have to first remove a region from the existing flow which is homeomorphic to the plug, with a torus removed from the interior of the plug. The insertion will then take place around a torus that exists in the un-modified flow. If this is not done correctly, it would be possible for us to change the manifold into which the plug is inserted. This would be problematic, as the manifold would no longer be $\mathbb{R}^3$, and our theorem would not be satisfied. We can address this via Dehn surgery.

If we begin with a closed 3-manifold M , remove the interior of a solid torus T_1 from its interior, and glue in a new solid torus T_2, we say the new manifold is obtained by *Dehn surgery*.

We follow the definitions of [G] here. This reference generalizes the construction to the neighborhood of knots in S^3. We restrict ourselves to the unknot (a circle) here, as that is sufficient for the proofs that follow.

Begin with a solid torus $T = S^1 \times D^2$ in M. For some point $* \in S^1$, let $m = * \times \partial D^2$ be a *meridian* of T. This is a curve in the boundary of T, which bounds a solid disk in T. Given a meridian m, a *longitude* l is a simple closed curve in the boundary, which may or may not equal the meridian. Denote by $[m]$ and $[l]$ the isotopy classes of m and l respectively. $[l]$ is referred to as the *framing* of the torus. The framing is *integral* if it only crossed the meridian once. A simple closed curve in the boundary of T is *essential* if it does not bound a disk in the boundary of T. A *slope* on the boundary of T is an isotopy class of unoriented, essential, simple closed curves on the boundary of T. If α is a slope on the boundary of T, then for some coprime integers p and q, $[\alpha] = p[m] + q[l]$. The slope is often referred to as $\alpha = \frac{p}{q}$.

Now return to our closed 3-manifold M, and the tori T_1 and T_2 as above. Assume m is a meridian on T_1, and α a slope on T_2. Remove the interior of T_1 from the interior of M, and glue in T_2, identifying α with m. This operation is the Dehn surgery.

As an example, consider the solid torus in Figure 3.3, with the indicated meridian and longitude.

The boundary of T_1 can be visualized as a rectangle with sides identified. We cut along l and m to get this rectangle. Suppose we take a slope of $\alpha = \frac{2}{3}$, as in Figure 3.4. We obtain α by dividing the length of m into 2 pieces, and l into 3 pieces. Looking at α on the surface of the torus, as in Figure 3.5, we see that a homeomorphism that identified α with m would not yield the same manifold as the one we started with.

The Lickorish-Wallace Theorem states that any orientable closed 3-manifold can be obtained from S^3 be a series of Dehn surgeries [L]. We need to ensure that the topology of the plugs in our proofs are not changed by the Dehn surgery. To that effect, we will require

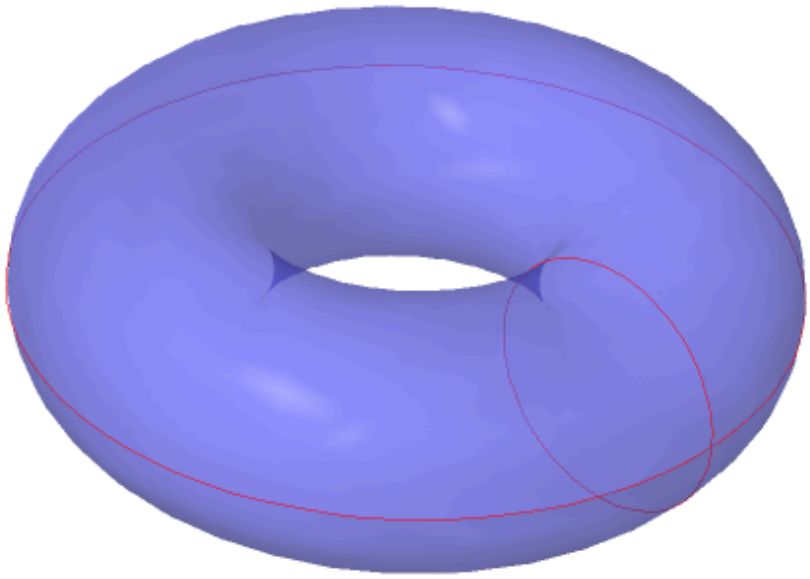

Figure 3.5: Solid torus with meridian m and longitude l indicated

that $\alpha = \frac{1}{1} = 1$, so the slope of our surgery is 1. This will be used in all plug insertions and the accompanying surgeries for the remainder of this paper.

Essentially, we will always have a longitude equal to our original meridian. To do this, whenever a torus needs to be removed from the interior of a flow bordism, we first locate a meridian on the existing torus in the flow. Choose the coordinates for the flow bordism so that the meridian on the torus being excised from the flow bordism is the same as the meridian on the existing torus. This will always avoid a Dehn twist in the insertion.

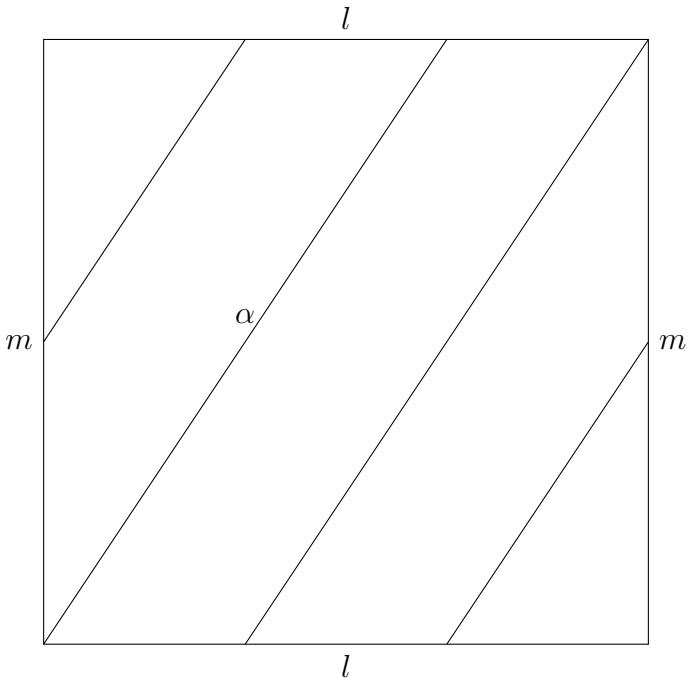

Figure 3.6: Meridian, longitude, and slope on the boundary of a torus

It should be noted that, in the measure-preserving case, insertion is a bit more complicated. We need to be certain that any smooth change in the length of the vectors remains measure-preserving. We will work around this by explicitly constructing modifications of vector fields that agree precisely with the original vector field, without any need to change lengths. That is, we will first create a vector field with specific properties, then at any point where we wish to insert a semi-plug, we will guarantee that the vector field in the boundary of the semi-plug agrees with the vector field at the areas where insertion takes place.

We now have the tools necessary to prove Theorem 2.4.

3.3 Proof of Theorem 2.4

Proof. Begin with the Jones-Yorke construction of Theorem 3.5. Let $\vec{F}$ be the flow in Theorem 3.5. We will construct a volume-preserving semi-plug containing a torus, with the flow on the torus composed of entirely circular orbits.

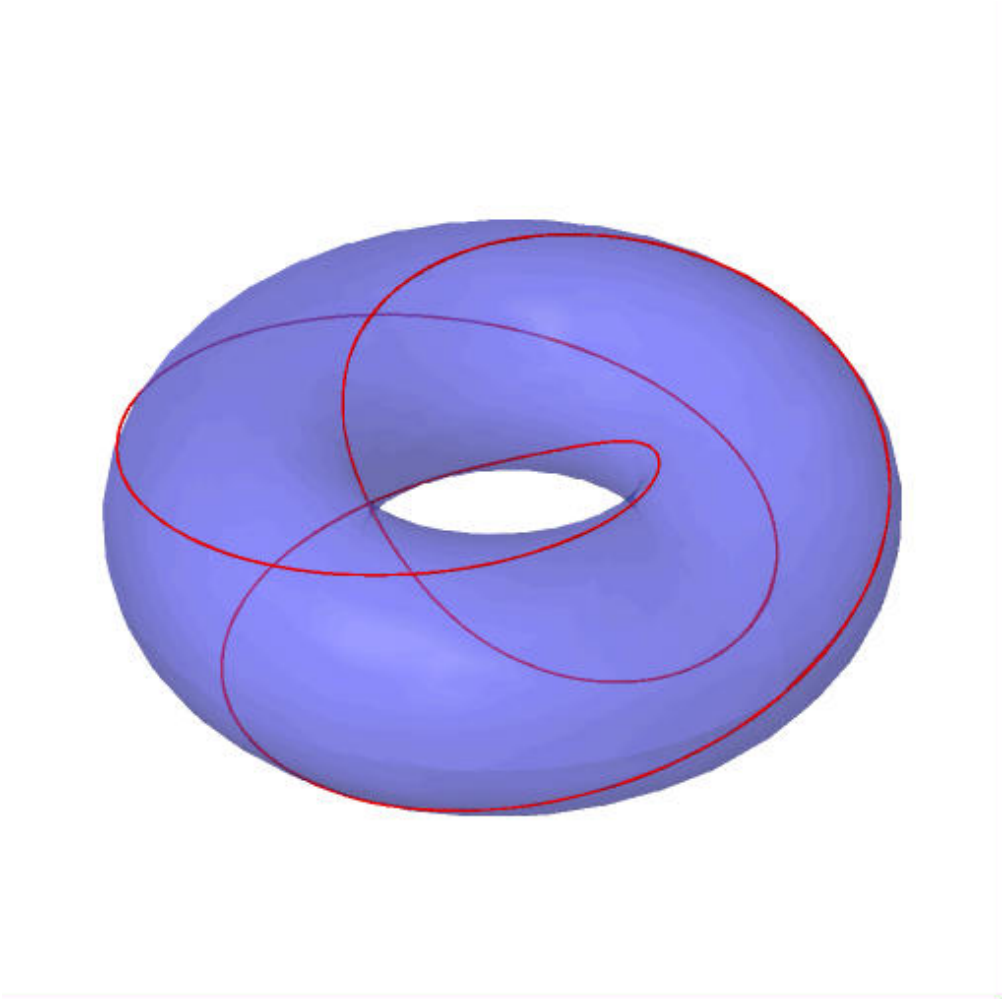

Figure 3.7: Solid torus with meridian α indicated

We can then modify the flow in a neighborhood of each T_n, which is contained in T_{n+1}, and which does not affect the flow on the boundary of T_{n+1} or T_n.

Define a function

$$h_n(r, z) = z^2 + (r - 2 \cdot 4^n)^2 - 4^n.$$

Note that this is the square of the distance function from a point to the boundary of T_n.

We will need a smooth ramp functions in our construction, as well as its derivative. Begin with

$$b(x) = e^{-1/x}.$$

We then define

$$b_1(x) = \begin{cases} 0 & \text{if } x \leq 0 \\ \frac{b(x/3)}{b(x/3)+b(1-x/3)} & \text{if } x \in (0,3) \\ 1 & \text{if } x \geq 3 \end{cases}$$

$$b_2(x) = \frac{db_1}{dx} = \begin{cases} 0 & \text{if } x \leq 0 \text{ or } x \geq 3 \\ \frac{b(x/3)b(1-x/3)[\frac{9}{x^2}+\frac{9}{(x-3)^2}]}{3[b(x/3)+b(1-x/3)]^2} & \text{if } x \in (0,3) \end{cases}$$

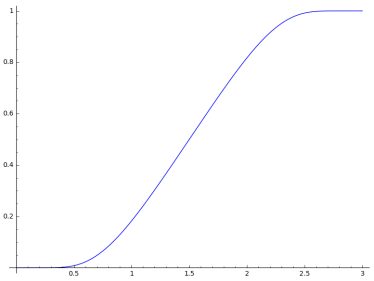

(a) Ramp function b_1

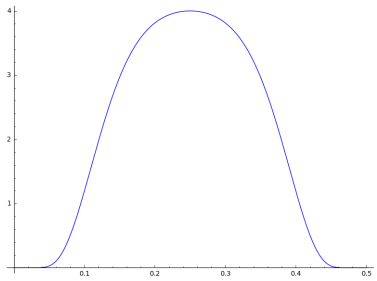

(b) Bump function b_2, the derivative of b_1

Figure 3.8: The function b_1 and its derivative b_2.

Let $\mathfrak{C}_n$ be a cylinder with radius $3 \cdot 4^n + 1$ and height $2 \cdot 4^n + 2$. Note that a torus with the same dimensions as T_n, centered at the origin and lying in the xy-plane, will fit inside $\mathfrak{C}_n$.

Construct a vector field P_n in cylindrical coordinates (r, θ, z) on $\mathfrak{C}_n$ such that

1. P_n is non-singular.
2. As $h_n \to 0$, $P_n \to \langle 0, -1, 0 \rangle$
3. As $h_n \to 3$, $P_n \to \langle 0, 0, -1 \rangle$
4. P_n is divergence-free.

Define P_n in cylindrical coordinates (r, θ, z). Let $h = h_n(r, z)$, and note that $h = 0$ for points on the boundary of T_n and returns 3 for points distance 1 from the boundary of T_n.

Then

$$P_n = \begin{cases} \langle 0, -1, 0 \rangle & \text{if } h \leq 0 \\ \langle zrb_2(h), -1 + b_1(h), -b_1(h) - r(r-2)b_2(h) \rangle & \text{if } h \in (0,3) \\ \langle 0, 0, -1 \rangle & \text{if } h \geq 3 \end{cases}$$

Each function in P_n is always defined when $h_n \in [0,3]$, and $P_n \neq \langle 0,0,0 \rangle$ for all points in $\mathfrak{C}_n$. As all partial derivatives of the components of P_n are bounded (by construction of the bump functions), the differential equation $\dot{p} = P_n$ has a unique solution [CL]. Therefore, P_n is non-singular, and condition 1 is satisfied.

Looking at the behavior of P_n as h changes, we satisfy conditions 2 and 3, since

- As $h \to 0$, $b_1(h) \to 0$, $b_2(h) \to 0$
- As $h \to 3$, $b_1(h) \to 1$, $b_2(h) \to 0$

In cylindrical coordinates, denote the components of the vector field $P_n = \langle P_r, P_\theta, P_z \rangle$. The divergence equation in cylindrical coordinates yields

$$\begin{aligned} \nabla \cdot P_n &= \frac{1}{r}\left(\frac{\partial}{\partial r} r P_r\right) + \frac{1}{r}\left(\frac{\partial}{\partial \theta} P_\theta\right) + \frac{\partial}{\partial z} P_z \\ &= \frac{1}{r}\left(\frac{\partial}{\partial r} z r^2 b_2(h)\right) + \frac{1}{r}\frac{\partial}{\partial \theta}\left(-1 + b_1(h)\right) + \frac{\partial}{\partial z}\left(-b_1(h) - r(r-2)b_2(h)\right) \\ &= \frac{1}{r}\left(2zrb_2(h) + zr^2 \frac{\partial b_2}{\partial h}\frac{\partial h}{\partial r}\right) + 0 - \frac{\partial b_1}{\partial h}\frac{\partial h}{\partial z} - r(r-2)\frac{\partial b_2}{\partial h}\frac{\partial h}{\partial z} \\ &= 2zb_2(h) + zr\frac{\partial b_2}{\partial h}(2(r-2)) - b_2(h)(2z) - r(r-2)\frac{\partial b_2}{\partial h}(2z) \\ &= 0 \end{aligned}$$

and we have satisfied all 4 conditions. We have two components to the boundary of the cylinder. The vector field is always $\langle 0, 0, -1 \rangle$. This flow is on a cylinder, so we can think of the boundary at the top and bottom as disks, on which the flow is either transverse in, or transverse out. On the sides of the cylinder, the flow is just vertical trajectories.

For each n, let $\hat{T_n} = \{(r, \theta, z) \in \mathbb{R}^3 : h_n(r, z) \in (0, 1)\}$. Since $\mathfrak{C}_n$ contains a copy of T_n, it also contains a copy of $\hat{T_n}$. We can therefore consider $\hat{P_n}$ to be the portion of P_n restricted to $\hat{T_n}$.

We insert each $\hat{P_n}$ into $\vec{F}$ in two different ways. If n is even, insert $\hat{P_n}$ into $\vec{F}$ by translating $c(n)$ units along the $y-$axis. If n is odd, inset $\hat{P_n}$ into $\vec{F}$ by translating $c(n)$ units along the $y-$axis and rotating $\hat{P_n}$ about the $x-$axis by an angle of $\pi/2$. In either case, the Dehn surgery in the insertion is performed with slope 1, so the topology of the underlying manifold (in this case, $\mathbb{R}^3$, is not changed.

Denote the modified vector field on $\mathbb{R}^3$ by $\vec{W}$.

We now verify that the solution to differential equation $\dot{p} = \vec{W}$ satisfies the conditions of Theorem 2.4.

It follows from the facts that $\vec{F}$ and P_n are each non-singular that $\vec{W}$ is non-singular.

The partial derivatives of P_n are all bounded, and therefore P_n satisfies the Lipschitz condition, and the equation $\dot{p} = P_n$ has a solution.

Let S_n be the set of all points p such that $h_n(p) = 1$. Denote this the *switching manifold* on T_n [DBCK]. This is the set of points where the insertion of $\hat{P_n}$ meets the existing vector field $\vec{F}$. In our definition of insertion above, we considered smoothly changing the lengths of the vectors in a neighborhood of this switching manifold. Here instead, we can consider a piecewise-smooth construction.

We can define the *degree of smoothness* [DBCK] at each point $p \in S_n$, as the highest order r such that the Taylor Series expansions of the dynamical systems determined by the vector fields on either side of the switching manifold, evaluated at zero, agree up to the $(r-1)$-st term. Our vector fields are not gradient fields, but they do agree after one partial derivative is taken. Therefore, the degree of smoothness in our switching manifold is zero, and $\vec{W}$ is C^0.

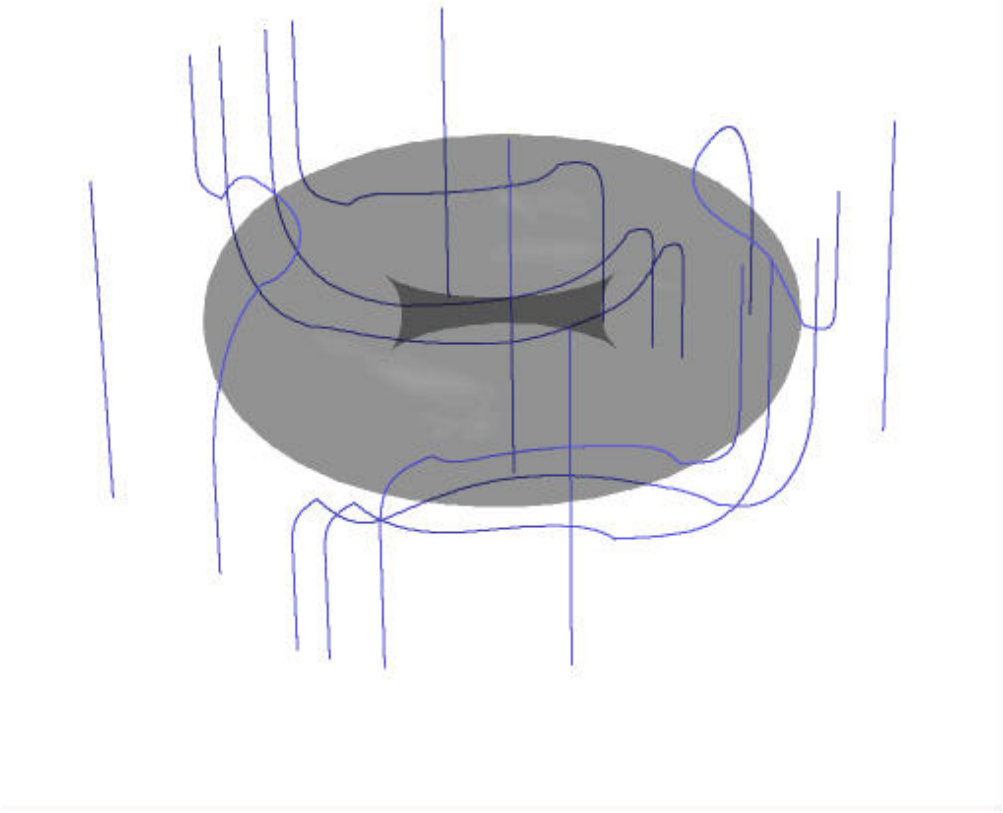

Figure 3.9: $\vec{W}$ in a neighborhood of T_0

As translations and rotations are volume preserving, and those are the only operations needed during our insertions, the vector field $\vec{W}$ is divergence-free whenever P_n is divergence free.

That fact that all trajectories are bounded follows immediately the embedding of P_n, which will touch the boundary of T_n only in the case of T_1, but in this case, the embedded vector field agrees with $\vec{F}$.

In all other cases, the embedded field does not touch the boundary of T_{n+1}, hence the property of bounded trajectories from [JY] is preserved.

We conclude that the solution to the differential equation $\dot{p} = \vec{W}$ is a non-singular, measure-preserving dynamical system on $\mathbb{R}^3$, with all trajectories bounded. □

We need one additional definition and an additional lemma before we proceed.

Given a diffeomorphism between two manifold $g : M \to N$, and a vector field $\vec{V}$ on M, let $g_*(\vec{V})$ be the vector field on N given by operating on each vector in $\vec{V}$ by the Jacobian of g.

Lemma 3.6. If $\vec{V}$ is a vector field that yields a volume-preserving dynamical system on a manifold M, and $g : M \to N$ is a diffeomorphism whose Jacobian has determinant of absolute value 1 at all points in M, then $g_*(\vec{V})$ yields a volume-preserving dynamical system on N [M2].

3.4 Proof of Theorem 2.5

Proof. Define an *obround* of radius R as the set of points in $\mathbb{R}^2$

$$\{(x, y) \in \mathbb{R}^2 : x \in [-R, R], y = \pm R\} \cup \{(x, y) \in \mathbb{R}^2 : (x \pm 2R)^2 + y^2 = R^2\}.$$

An obround is the boundary of a square of side length $2r$, with semi circles of radius r appended to the right and left sides. This is shown in Figure 3.10.

A *tobround* of major radius R and minor radius r, with $r < R$, is the Cartesian product of a solid disk of radius r and an obround of radius R. This is shown in Figure 3.11.

The process of constructing the flow that satisfies this theorem is as follows:

1. Construct a nested sequence of tobrounds, whose union is $\mathbb{R}^3$.

2. Define a flow in each tobround with non-singular trajectories that are contained in the tobround in which they originate.

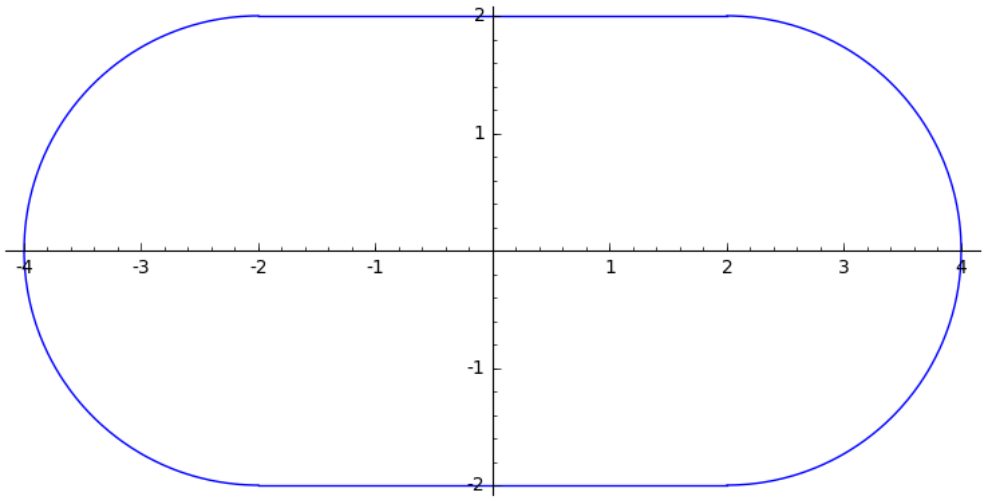

Figure 3.10: Obround with radius 2

3. The distance from the boundary of a tobround to the boundary of the larger tobround in which it is nested must always be greater than or equal to 2.

4. Construct a volume-preserving diffeomorphism from a solid torus to a tobround for each tobround in the construction.

5. Construct a smooth, volume-preserving flow around the torus, which is vertical at distance 1 from the boundary of the torus.

6. Apply the Jacobian of the diffeomorphism from point 4 above to the vector field around the torus to obtain a flow in a neighborhood of each tobround.

7. The resulting flow agrees with the existing flow on the nested tobrounds, is non-singular, has all trajectories trapped within a particular tobround, and preserves volume.

To define a sequence of tobrounds whose union is $\mathbb{R}^3$, let $\mathcal{O}_0$ be a tobround with minor radius 1 and major radius 2. If $n > 0$ is even, let $\mathcal{O}_n$ be the tobround with minor radius $6 \cdot 2^{2n-1}$ and major radius $6 \cdot 2^{2n}$, shifted $6 \cdot 2^{2n}$ units positively along the y-axis. If $n > 0$ is

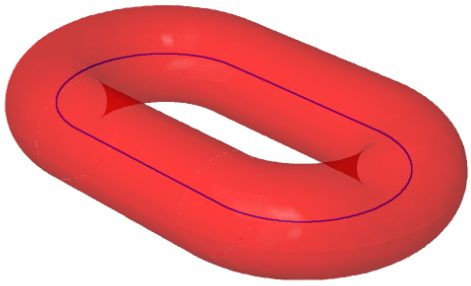

Figure 3.11: Tobround with major radius 2, and minor radius 1

odd, the major and minor radii are as defined above, as is the shifting along the y-axis, but the entire obround is rotated about the $y-$axis by an angle of $\pi/2$. This is shown in Figure 3.12.

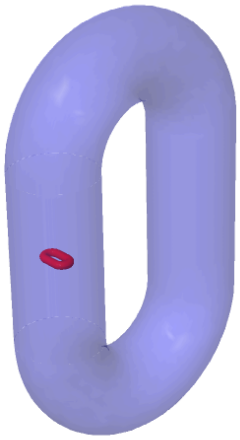

Figure 3.12: $\mathcal{O}_0$ nested in $\mathcal{O}_1$

Note that

$$\bigcup_{n\in\mathbb{N}} \mathcal{O}_n = \mathbb{R}^3.$$

We can construct a flow on $\mathbb{R}^3$ by defining it on each tobround. For each $p \in \mathbb{R}^3$, let $d(p, \mathcal{O}_n)$ be the usual distance function. For each $\mathcal{O}_n$, let $o_n(d(p, \mathcal{O}_n)$ be the smooth bump function which returns 1 on the boundary of $\mathcal{O}_n$ and 0 for all points whose distance from $\mathcal{O}_n$ is greater than or equal to 1.

Define a piecewise vector field in Cartesian coordinates on $\mathcal{O}_0$ by

$$\dot{p} = \begin{cases} \langle y, 0, 0 \rangle & \text{if } x \in [-2, 2] \\ \langle y, 2 - x, 0 \rangle & \text{if } x > 2 \text{ and } (x-2)^2 + y^2 \in [1, 9] \\ \langle y, -x - 2, 0 \rangle & \text{if } x < -2 \text{ and } (x+2)^2 + y^2 \in [1, 9] \end{cases}$$

The trajectories are then clockwise oriented obrounds, within the tobround $\mathcal{O}_\prime$. Sample trajectories are shown in Figure 3.13. This is clearly non-singular, and all trajectories are bounded.

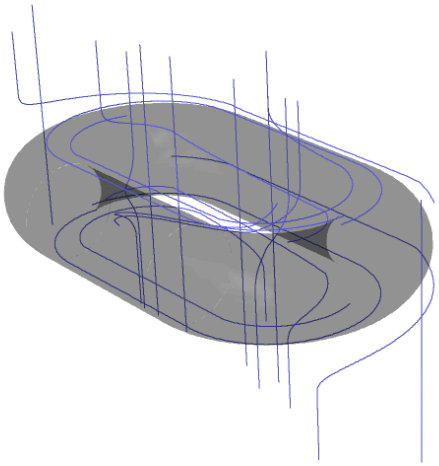

Figure 3.13: Trajectories near $\mathcal{O}_0$

Let o_0 be the bump function above, with argument assumed to be $d(p, \mathcal{O}_0)$. Extend our flow to $\mathcal{O}_1$ by

$$\dot{p}= \begin{cases} \langle o_0 y, 0, (1-o_0)(y-24)\rangle \\ \qquad\qquad \text{if } z \in [-24, 24] \\ \langle o_0 y, o_0(2-x) + (1-o_0)(24-z), (1-o_0)(y-24)\rangle \\ \qquad\qquad \text{if } z > 24 \text{ and } (z-24)^2 + (y-24)^2 \in [12, 36] \\ \langle o_0 y, o_0(-x-2) + (1-o_0)(-z-24), (1-o_0)(y-24)\rangle \\ \qquad\qquad \text{if } z < -24 \text{ and } (z-24)^2 + (y-24)^2 \in [12, 36] \end{cases}$$

This gives us the first steps towards an analogous result to Jones and Yorke, but with nested tobrounds. The bump function ensures that this flow is smooth with respect to the existing flow on $\mathcal{O}_0$. It is non-singular, and all trajectories are bounded within $\mathcal{O}_1$. The flow at distance 1 from the boundary of $\mathcal{O}_0$ is $\langle 0, 0, y-24\rangle$. As $\mathcal{O}_0$ is an attractor, this flow is not currently measure-preserving.

To generalize this, assume n is odd, as the case that n is even immediately follows. Then the vector field on $\mathcal{O}_n$ is given by

$$\dot{p}= \begin{cases} \langle o_{n-1}(y-6\cdot 2^{2n-1}), 0, (1-o_{n-1})(y-6\cdot 2^{2n})\rangle \\ \qquad\qquad \text{if } z\in[-6\cdot 2^{2n}, 6\cdot 2^{2n}] \\ \langle o_{n-1}(y-6\cdot 2^{2n-1}), \\ \quad o_{n-1}(6\cdot 2^{2n-1}-x)+(1-o_{n-1})(6\cdot 2^{2n}-z), \\ \quad\quad (1-o_{n-1})(y-6\cdot 2^{2n})\rangle \\ \text{if } z>6\cdot 2^{2n} \text{ and } (z-6\cdot 2^{2n})^2+(y-6\cdot 2^{2n})^2\in[6\cdot 2^{2n-1}, 18\cdot 2^{2n-1}] \\ \langle o_{n-1}(y-6\cdot 2^{2n-1}), \\ \quad o_{n-1}(-x-6\cdot 2^{2n-1})+(1-o_{n-1})(-z-6\cdot 2^{2n}), \\ \quad\quad (1-o_{n-1})(y-6\cdot 2^{2n})\rangle \\ \text{if } z<-6\cdot 2^{2n} \text{ and } (z-6\cdot 2^{2n})^2+(y-6\cdot 2^{2n})^2\in[6\cdot 2^{2n-1}, 18\cdot 2^{2n-1}] \end{cases}$$

In order to make this volume-preserving, we insert a vector field around each tobround, which agrees with the existing flow on the boundary of the tobround, and with the vertical flow at distance 1 from the boundary of each tobround.

This vector field is built by first constructing a volume-preserving flow around a solid torus, then use a volume-preserving diffeomorphism between the torus and the tobround to get the appropriate flow around the tobround.

For a given $\mathcal{O}_n$, denote the major radius M and minor radius m, and central obround O_n Let $\mathcal{T}_n$ be a solid torus with major radius $M(1+\frac{2}{\pi})$ and minor radius m and central circle T_n

Define a diffeomorphism g_n on from the central circle of $\mathcal{T}_n$ (in polar coordinates) to the central obround of $\mathcal{O}_n$ (in Cartesian coordinates).

For brevity, let $\hat{M} = \sqrt{2r + M^2 - \frac{2}{\pi}(\pi+2)M}$, then

$$g_n(r,\theta) = \begin{cases} (-\frac{M}{\pi}(\pi+2)\theta + M, \frac{r\pi}{M(\pi+2)} + M - 1) \\ \qquad\qquad \text{if } \theta \in [0, \frac{2\pi}{\pi+2}) \\ (\hat{M}\cos(\frac{\pi+2}{\pi}\theta + \frac{\pi}{2} - 2) - M, \hat{M}\sin(\frac{\pi+2}{\pi}\theta + \frac{\pi}{2} - 2)) \\ \qquad\qquad \text{if } \theta \in [\frac{2\pi}{\pi+2}, \pi) \\ (\frac{M}{\pi}(\pi+2)(\theta - \pi) - M, \frac{r\pi}{M(\pi+2)} - M - 1) \\ \qquad\qquad \text{if } \theta \in [\pi, \pi(\frac{\pi+4}{\pi+2})) \\ (\hat{M}\cos(\frac{\pi+2}{\pi}\theta - \frac{3\pi}{2} - 4) + M, \hat{M}\sin(\frac{\pi+2}{\pi}\theta - \frac{3\pi}{2} - 4) \\ \qquad\qquad \text{if } \theta \in [\pi(\frac{\pi+4}{\pi+2}), 2\pi) \end{cases}$$

Both the torus and the tobround have the same minor radius and are each oriented in the xy-plane. Let D_m be a solid 2-disk of radius m, then

- $\mathcal{T}_n = T_n \times D_m$.
- $\mathcal{O}_n = O_n \times D_m$.

Extend g_n by defining $G_n : \mathcal{T}_n \to \mathcal{O}_n$ as $G_n(\mathcal{T}_n) = g_n(T_n) \times D_m$. G_n is then a diffeomorphism. As the Jacobian of each piece of g_n has determinant 1, and the map is the identity on D_m, G_n is volume preserving.

Now we define a flow in a neighborhood of $\mathcal{T}_n$ using cylindrical coordinates. This is the nearly the same flow used in the proof of Theorem 2.4. The main difference is that we replace our distance function h with

$$\tilde{h}(r,z) = (r - 6 \cdot 2^{2n})^2 + z^2 - 6 \cdot 2^{2n-1}.$$

The bump functions $b_1(\tilde{h})$ and $b_2(\tilde{h})$ are the same as before.

The flow is then given by

$$P_{\mathcal{T}_n} = \langle 6{\cdot}2^{2n-1} zr b_2(\tilde{h}), -1+b_1(\tilde{h})-2b_2(\tilde{h})zr\cos(\theta), -b_1(\tilde{h})(r\sin(\theta)-6{\cdot}2^{2n-1})-r(-6{\cdot}2^{2n})b_2(\tilde{h})\rangle.$$

We have the following necessary conditions which are satisfied:

1. $P_{\mathcal{T}_n}$ is divergence free.
2. $P_{\mathcal{T}_n}$ is smooth with respect to a flow on $\mathcal{T}_n$ by circular orbits.
3. $P_{\mathcal{T}_n}$ is vertical at distance 1 from the boundary of $\mathcal{T}_n$.
4. $P_n = G_{n,*}(P_{\mathcal{T}_n})$ is a divergence-free flow.
5. The extended diffeomorphism G_n is the identity on the z-coordinate, P_n is vertical at distance 1 from the boundary of $\mathcal{O}_n$.

Each of these is quickly checked. We can verify 1, using the same notation for the components as in the proof of 2.4, via

$$\begin{aligned}
\nabla \cdot P_n &= \frac{1}{r}\left(\frac{\partial}{\partial r} r P_r\right) + \frac{1}{r}\left(\frac{\partial}{\partial \theta} P_\theta\right) + \frac{\partial}{\partial z} P_z \\
&= \frac{1}{r}\left(\frac{\partial}{\partial r} 6\cdot 2^{2n-1} z r^2 b_2(\tilde{h})\right) + \frac{1}{r}\left(\frac{\partial}{\partial \theta}\left(-1 + b_1(\tilde{h}) - 2b_2(\tilde{h}) zr\cos(\theta)\right)\right) \\
&\quad + \frac{\partial}{\partial z}\left(-b_1(\tilde{h})(r\sin(\theta) - 6\cdot 2^{2n-1}) - r(-6\cdot 2^{2n}) b_2(\tilde{h})\right) \\
&= \frac{1}{r}\left(6\cdot 2^{2n} zr b_2(\tilde{h}) + 2r(r - 6\cdot 2^{2n}) z \frac{\partial b_2}{\partial h}\right) + 2zr b_2(\tilde{h})\sin(\theta) - 2zr b_2(\tilde{h})\sin(\theta) \\
&\quad + 6\cdot 2^{2n} z b_2(\tilde{h}) - 2r(r - 6\cdot 2^{2n-1}) \frac{\partial b_2}{\partial h} z = 0
\end{aligned}$$

For 2 and 3, as $\tilde{h} \to 0$, the flow approaches $\langle 0, -1, 0\rangle$, and as $\tilde{h} \to 1$, the flow approaches $\langle 0, 0, -1\rangle$. Conditions 4 and 5 follow from the construction of g_n and G_n respectively.

Inserting this flow around each tobround $\mathcal{O}_n$ in our construction results in a volume-preserving flow inside of each tobround $\mathcal{O}_{n+1}$. This is shown around $\mathcal{O}_0$ in Figure 3.14 and 3.15.

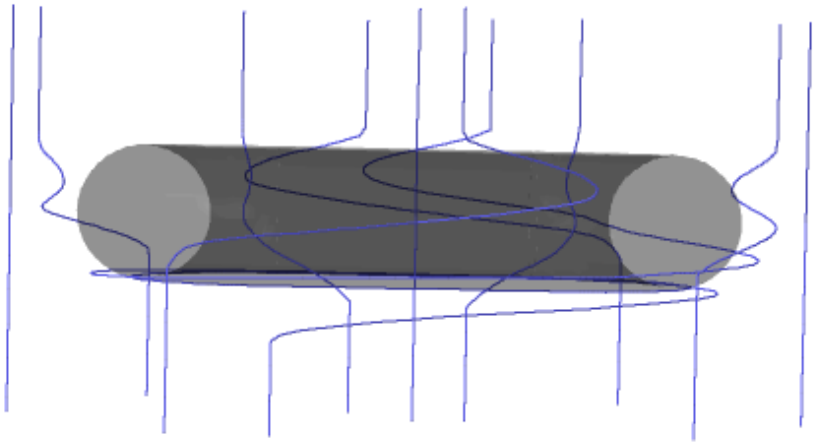

Figure 3.14: Trajectories near $\mathcal{O}_0$ after modification

This can be inserted with a rotation if n is odd. The flow has not caused any trajectories contained in a tobround to leave that tobround, since the modification only exists up to a distance 1 from the boundary of a tobround, and the boundary of the next largest tobround is at least 2 units away. As the flow on this modified region agrees with the flow previously

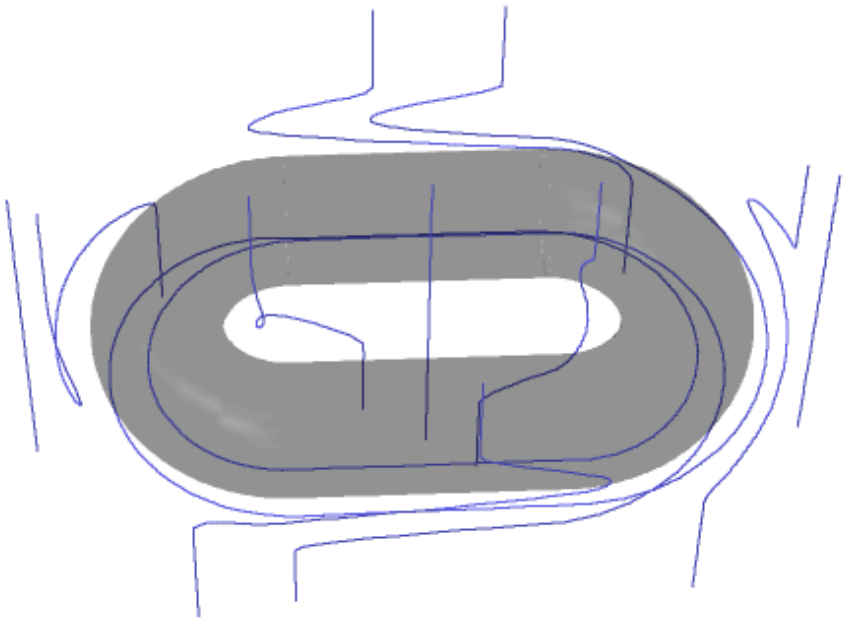

Figure 3.15: Trajectories near $\mathcal{O}_0$ after modification, side view

constructed, and the modification is C^∞, we have a C^∞, non-singular, measure-preserving dynamical system on $\mathbb{R}^3$, with all trajectories bounded.

□

Chapter 4

Foliations of $\mathbb{R}^3$ and their relationship to dynamical systems

4.1 Relating foliations to dynamics

In this chapter we start with foliations, and see how they can be used to construct dynamical systems.

The relationship between measured foliations and measure-preserving dynamics has been explored in a variety of works, such at [H, LN], [P], [RS], [T], and [Wa]. In most cases, the notion of transverse invariant measure is defined differently, so that it is appropriate for foliations where the leaves have dimension greater than one. Additionally, these references tend to have proofs which are non-constructive. We therefore present a new proof, which is specific to our needs.

We will start with an example, then prove a general theorem for constructing a volume-preserving dynamical system from a measured 1-foliation (Theorem 4.2.). After a few new definitions, we will show how the analog of a semi-plug from Chapter 3, when constructed from a foliation, can be regarded as a dynamical system (Theorem 4.7).

To begin, given an n-dimensional manifold M, let $(M, \mathcal{F})$ be an oriented 1-foliation.

We can think of a leaf in a 1-foliation as being sent by the chart maps to the image of the plaques, which are all open intervals in $\mathbb{R}^n$, with the overlap of the chart maps allowing the image of the leaf under the chart map to straighten out. This allows for a nice way to think of distance traveled along a leaf. This is illustrated well in this image from Hurder [H, LN].

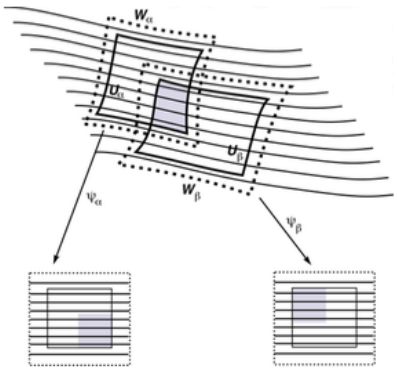

Figure 4.1: Leaves in a 1-foliation after application of chart maps.

Given two points $x, y \in M$, lying on the same leaf L, a *plaque chain* [CC] is a sequence of plaques, $P_0, P_1, \ldots P_p$, such that $x \in P_0$, $y \in P_p$, and for each integer $i \in \{1, 2, \ldots, p\}$, $P_i \cap P_{i-1} \neq \emptyset$. We can use plaque chains to follow the image of leaves through multiple charts in our foliation atlas.

The use of plaques can also give use the *complete transversal* of a foliation [Wa]. Assume the set $\{U_\lambda, \varphi_\lambda\}$ is a nice atlas for $(M, \mathcal{R})$. For a given leaf $L \in \mathcal{F}$, and each U_λ, let T_{U_λ} be the set of all plaques of $L \cap U_\lambda$. Let T be the disjoint union of all T_{U_λ}. Then T is a complete transversal of $\mathcal{F}$. It is a bit of a misnomer, because the sets which make up T are not themselves transverse to the foliation, but each T_U is homeomorphic to a set T'_U, which is transverse to the foliation. Furthermore, each leaf in $\mathcal{F}$ intersects at least one element of the set of all T'_U [Wa].

It will be the set of all T'_U that we are interested in. In Example 4.1 we will find this set and use it in constructing a phase map.

For the next example and the proof that follows, we will assume that each of the foliations has a nice atlas, given by the flow boxes, enclosing the small transversals. We will assume that, under the chart maps, the foliation lies in the x direction, and that all other coordinates are constant under the image of every plaque.

Example 4.1. Let M be the hyperboloid of one sheet in $\mathbb{R}^3$, given by the parametric equations

$$x = \sqrt{u^2 + 1}\cos(v)$$
$$y = \sqrt{u^2 + 1}\sin(v)$$
$$z = u$$

for $u \in [-1, 1]$ and $v \in [0, 2\pi]$. Assume M is foliatied by circular leaves, lying parallel to the xy-plane, as in Figure 4.2.

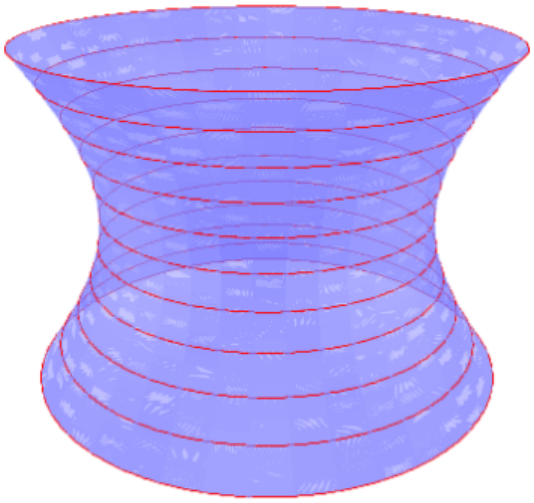

Figure 4.2: Foliation of M by circular leaves

First, note that this foliation is measured. Let ω_1 be the Euclidean 1-form on $\mathbb{R}^2$, on the y-coordinate. Let $(U_\lambda, \varphi_\lambda)$ be a nice atlas for $\mathcal{F}$, which arises from the flow boxes. We can define a transverse measure, as in section 2.4.

Given a small transversal α, define $\mu(\alpha) = ||\omega_1(\varphi_i(\alpha))||$ [FLP]. We are assuming here that the x-coordinate in $\mathbb{R}^2$ is kept constant on the image of each plaque under every chart map.

Let α be a transversal on M. Here α is essentially a 1-dimensional subset of M which is not parallel to any leaves in $\mathcal{F}$, and which is the union of small transversals. Assume there exists a transversal β, with α isotopic to β. We must show that their transverse measures are equal.

Since our leaves are circular and parallel to the xy-plane in $\mathbb{R}^3$, when the chart map is applied, the change in the y coordinate on each small transversal that makes up α will be kept constant during an isotopy parallel to the leaves that moves α to β. Therefore, $\mu(\alpha) = \mu(\beta)$.

To give a specific example, let α be the transversal connecting the points $(\sqrt{2}, 0, 1)$ and $(\sqrt{2}, 0, -1)$, and β connect the points $(0, \sqrt{2}, 1)$ and $(0, \sqrt{2}, -1)$, as in Figure 4.3.

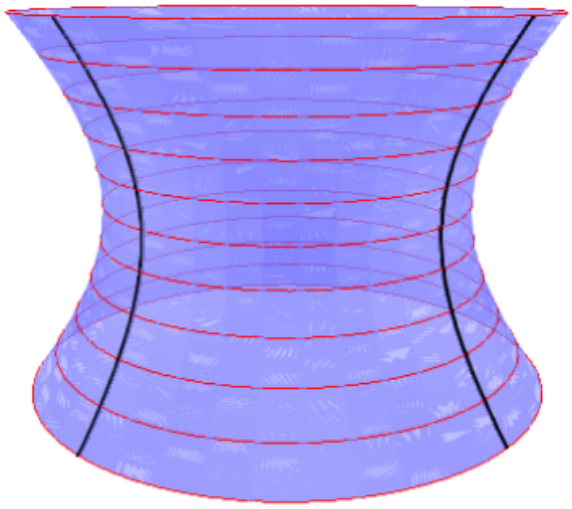

Figure 4.3: M with transversals α and β shown.

The function $f : \alpha \times [0, 1] \to \beta$ is $f(x, y, z, t) = (\sqrt{2}\cos(\frac{t\pi}{2}), \sqrt{2}\sin(\frac{t\pi}{2}), z)$. This gives α when $t = 0$, β when $t = 1$, and is an isotopy.

We can also see that $\mu(\alpha) = \mu(\beta)$. The total change in the z-coordinate between α and β is the same when viewed on M. For our choice of nice atlas, α will have some finite measure, determined by the number of flow boxes which contain a small transversal in α,

and the change in the y-coordinate on the portion of α in the image of each flow box under the chart map. The measure of each of these small transversals will be calculated just as in Figure 2.1. As α is moved across the leaves via the isotopy f, the total displacement along the y-coordinate must remain the same as α is moved into new flow boxes. This follows from the fact that all leaves on M are parallel. Therefore the measure of β must be equal to the measure of α.

We conclude that $(M, \mathcal{F})$ is a measured foliation.

We now construct a volume-preserving dynamical system from $(M, \mathcal{F})$. Our first intuition here is to simply take a point p_0 in M and any $t \in \mathbb{R}$, apply the appropriate chart maps to get a chain of plaques, then shift p_0 to $p_0 + t$, and apply the inverse of the chart map. We will do so to start, and define the map $\pi_0 : \mathbb{R} \times M \to M$. To define $\pi_0(t, p_0)$, first apply the appropriate chart maps to get a plaque chain, starting at p_0. Apply the first chart map in the chain, and add t to the x-coordinate of p_0. Apply the inverse chart map at the end of the plaque chain, and define this to be $\pi_0(t, p_0)$. Since the map π_0 only acts by translation in $\mathbb{R}^2$, it satisfies our definition for a phase map. Note also that, since π_0 only moves subsets of M along leaves of the foliation, for any transversal $\alpha \in M$ and any $t \in \mathbb{R}$, $\pi_0(t, \alpha)$ is an isotopy.

This may cause an issue, depending on what dynamical system we are hoping to construct, and which measure we want the dynamical system to preserve.

If we were to start with a dynamical system, and define the leaves of an oriented 1-foliation by its orbits, we would have the same structure of the orbits, but we would lose the parametrization of how points traverse those orbits.

Essentially, this construction would lose the time component of the dynamical system. We seek to remedy this here.

For example, if transversal α were as in Figure 4.3, and β' was a transversal starting at the point in α with z-coordinate -1, but sharing the point in β with z-coordiante 1, then α and β' would have the same transverse measure, but different Lebesgue measure.

Let ω_2 be the Euclidean 2-form on $\mathbb{R}^2$. We can use this to construct a measure on M, which is invariant under our dynamical system.

Since we have a nice atlas for M, and M is compact, choose a finite subcover of the atlas, $\{(V_0, \varphi_0), \ldots, (V_n, \varphi_n)\}$ which covers M. Let $A \subset M$.

Define

$$\eta(A) = \sum_{i=0}^{n} \omega_2(\varphi_i(A \cap V_i)).$$

η is then a measure on M. η is defined by a volume form, but it is a volume form on the subsets of $\mathbb{R}^2$ that are in the image of each of the chart maps, not M.

Since our transverse measure preserves the change in the y-coordinate of transversals under isotopy, and the translation from π_0 preserves the change in the x-coordinate, we can conclude that the Euclidean 2-form ω_2 is preserved under $pi_0^{-1}(t, A)$ for any $t \in \mathbb{R}$.

We then have $(M, \mathbb{R}, \pi_0, \eta)$ is a measure preserving dynamical system, though η is not the Lebesgue measure.

We can go a bit further, and see how a Riemannian volume form on M can be preserved under a different choice of phase map.

Each leaf in this foliation is circular. Fix the set α as above, and define the length of a leaf by fixing a point on the leaf in α and measuring the metric distance along the leaf, following the orientation, until the leaf intersects α again. If α was decomposed as a set of small transversals, these would play the role of the sets T'_U in the definition of a complete transversal from the beginning of the chapter. α is transverse to all of $\mathcal{F}$, and each leaf in $\mathcal{F}$ intersects α at least once.

For a given $p_0 \in M$, let $l(p_0)$ be the length of the leaf containing p_0. For example, $l(\sqrt{2}, 0, 1) = 2\sqrt{2}\pi$, while $l(1, 0, 0) = 2\pi$.

Keeping our chosen nice atlas $(U_\lambda, \varphi_\lambda)$, for a point $p_0 \in M$, define $\pi_1 : \mathbb{R} \times M \to M$, by letting $\pi_1(t, p_0)$ be pre-image (under the chart map) of the point $\varphi_\lambda(p_0) + l(p_0)t$, which shifts the point along the image of the leaf $\updownarrow(p_0)t$ units. Since the chart maps in the foliation are continuous, π_1 is continuous. Just as in the case with π_0, we have that $\pi_1(0, p_0) = p_0$ (since it is not translated along the leaf at all), and that $\pi_1(t_1, (\pi_1(t_2, p_0)) = \pi_1(t_1 + t_2, \pi_1)$ (since two translations along $\mathbb{R}$ are easily composed). Therefore, the definition of a dynamical system is satisfied by $(M, \mathbb{R}, \pi_1)$.

We next verify that this dynamical system preserves volume. We have μ as the transverse measure on $\mathcal{F}$. Let $A \subset M$. Let ω_M be the Riemannian volume form on M. If the dimension of A is less than 2, then $\omega_M(A) = 0$, and the measure will be preserved.

If the dimension of A is 2, decompose A as a union of small transversals. Think of points on M in cylindrical coordinates. Our chart maps preserve the orientation of leaves in the x direction, so $\pi_1^{-1}(t, A)$ will rotate A around M, scaled by the length of each leaf going through each point in A, so the change in θ between any two points in A is preserved under π_1^{-1}. For any fixed θ the metric on M is determined by r and z, and that distance is represented by changes in the y-coordinates under the chart map. The invariance of μ with respect to the y-direction after the chart map is applied, will preserve the change in the remaining components of ω_M under $\pi_1^{-1}(t, A)$.

Therefore, each point in A will have its r and z coordinates preserved under $f^{-1}(t, A)$, and while each point will move a different distance, the change in the angle θ will be the same for each point. We conclude that ω_M is preserved under $\pi_1^{-1}(t, A)$ for any choice of $t \in \mathbb{R}$.

Since any Riemannian volume form is a non-zero scalar multiple of the Lebesgue measure [HK], let ν be the measure associated with ω_M, then, $(M, \mathbb{R}, f, \nu)$ is a measure-preserving dynamical system.

We follow the steps of this example to get a general proof of this fact for compact, connected, orientable, 3-manifolds. This will be useful later, when we construct measured foliations, then use them to create measure-preserving dynamical systems. Note that the dynamical system in Theorem 4.2 does preserve measure, but it is not Lebesgue measure. We will introduce supporting theorems after the proof of Theorem 4.2. This will allow us to prove a version of Theorem 4.2 in Theorem 4.7, which is specifically applicable to the proof of Theorem 2.6 in Chapter 5.

Theorem 4.2. A smooth, oriented, measured, 1-foliation $(\mathcal{F}, \mu)$ on a smooth, compact, connected, orientable 3-manifold, yields a volume-preserving dynamical system.

Proof. Assume M is as in the statement of the theorem , and let $(M, \mathcal{F}, \mu)$ be an oriented, measured 1-foliation of M, with a nice foliation atlas $\{(U_i, \varphi_i)\}$. μ is the transverse measure on the foliation, which is invariant when applied to isotopic transversals. We assume that the images of the plaques are open intervals, with both the y and z coordinates fixed.

Beginning as in example 4.1, we define a phase map $\pi : \mathbb{R} \times \mathbb{R}^3 \to \mathbb{R}^3$ on a point (t, x) by applying the appropriate chart maps to get a chain of plaques. Let $x_0 = \varphi_i(x)$, for the appropriate choice of chart map. Let $x_p = x_0 + t$. Then x_p is in the same leaf as x_0, so there is a plaque chain connecting x to $\pi(t, x) = \varphi_j^{-1}(x_p)$, where φ_j^{-1} is the last chart map in the plaque chain. This satisfies the definition of a dynamical system, but, as above, we cannot guarantee that this preserves Lebesgue measure, or equivalently, Euclidean volume.

Instead, introduce a new measure, η. Let $A \subset M$. Since M is compact, our nice atlas reduces to a finite subcover. Choose some finite subset of the charts $\{(V_0, \varphi_0), \ldots, (V_n, \varphi_n)\}$ which covers M.

Let ω be the Euclidean volume form on $\mathbb{R}^3$. As in our last example, define

$$\eta(A) = \sum_{i=0}^{n} \omega(\varphi_i(A \cap V_i)).$$

η is then a measure on M. η is defined by a volume form, but it is a volume form on the subset of $\mathbb{R}^3$ that comes from the chart maps, not M.

We next verify that $(M, \mathbb{R}, \pi, \eta)$ is a volume-preserving dynamical system. Assume $A \subset M$, and let $t \in \mathbb{R}$. If the dimension of A is less than 3, $\eta(A) = 0$. Otherwise, the invariance of μ ensures that $\pi^{-1}(t, A)$ will not change the differences in the y or z coordinate where the volume is taken, and the dynamics will preserve the change in the x coordinate. Therefore, ω is preserved on each small transversal in A. From our definition of η, $\eta(A) = \eta(\pi^{-1}(t, A)$ for all $A \subset M$.

We conclude that $(M, \mathbb{R}, \pi, \eta)$ is a volume- preserving dynamical system.

□

We have one additional result, which can be helpful in determining if a foliation is measured. This corollary follows from the result in [M] stated in Chapter 3, in combination with Theorem 4.2.

Corollary 4.3. Let M be an compact, connected, orientable, smooth 3-manifold, with measure η, and $\mathcal{F}$ an oriented 1-foliation of M with transverse measure μ. Let $(\mathbb{R}, M, \pi)$ be the dynamical system induced by $\mathcal{F}$, as in Theorem 4.2. If $\mathcal{A}(M) \neq M$, then $(\mathcal{F}, \mu)$ is not a measured foliation.

4.2 Flow bordisms

The plugs discussed in Chapter 3 were constructed from a flow. Plugs can also be constructed from foliations.

We will begin with some background from Tamura [T], on *foliation cobordisms*, then move to the definitions from Kuperberg and Kuperberg [GKK] of a *flow bordism*, and show how this relates to the plugs from [KK], [GKK] discussed in Chapter 3.

In Tamura [T], the definitions are given in terms of a general q-dimensional foliation on an n-dimensional manifold. As we are only considering $1-$foliations here, we restated the definitions appropriately.

Assume M_1^n and M_2^n are two n-dimensional, closed, oriented, manifolds. Let $\mathcal{F}_1$, and $\mathcal{F}_2$ be 1-foliations of M_1^n and M_2^n respectively. Let $-M_2^n$ denote the reversed orientation of M_2^n. If there exists an $n+1$-dimensional manifold W^{n+1}, along with a 1-foliation $\hat{\mathcal{F}}$, transverse to ∂W^{n+1}, such that

$$\partial W^{n+1} = M_n^1 \cup (-M_2^n)$$

and

$$(\partial W^{n+1}, \partial \hat{\mathcal{F}}) = (M_1^n, \mathcal{F}_1) \cup (-M_2^n, \mathcal{F}_2)$$

then $(W^{n+1}, \hat{\mathcal{F}})$ is a *foliated cobordism* between $(M_1^n, \mathcal{F}_1)$ and $(M_1^n, \mathcal{F}_2)$. The two foliated manifolds $(M_1^n, \mathcal{F}_1)$ and $(M_1^n, \mathcal{F}_2)$ are said to be *cobordant*.

Using the definitions in [GKK], we have three types of boundary we wish to consider for a n-manifold M with a 1-foliation $\mathcal{F}$. The *transverse boundary* is the portion of the boundary of M where $\mathcal{F}$ is locally modeled by the foliation of $\mathbb{R}^n$ by vertical lines. The *parallel boundary* is the portion of the boundary of M where $\mathcal{F}$ is locally modeled by the foliation of the upper half-space of $\mathbb{R}^n$ by horizontal lines. *Corners* occur at points on the boundary which are neither parallel boundary, nor transverse boundary.

A helpful visual for this, is to think of a cylinder, in cylindrical coordinates, $\{(r, \theta, z) : 1 \leq r \leq 2, \theta \in [0, 2\pi), z \in [-1, 1]\}$, and which is foliated by vertical lines. The parallel

boundary would be the components where $r = 1$ or $r = 2$, and the transverse components would be where $z = \pm 1$.

Given a connected, compact manifold P, a *flow bordism* $\mathcal{P}$ is an oriented 1-foliation of P, such that all boundary of P is either transverse, parallel, or corners [GKK].

We can see how this is related to the cobordism discussed above. The transverse and parallel boundary components of the bordism can be through of as the cobordant manifolds, though we do not have the condition that the orientation is reversed in one of the manifolds when the union is taken.

The remaining definitions are equivalent to those in Chapter 3, but modified for the use of foliations.

Let F_- be the closure of the transverse boundary oriented inwards, and F_+ be the closure of the transverse boundary oriented outwards. We have two additional properties in which we are interested.

(i) There exists an infinite leaf with an endpoint in F_-

(ii) There exists a manifold F and two homeomorphisms $\alpha_- : F \to F_-$, $\alpha_+ : F \to F_+$ such that if $\alpha_+(p)$ and $\alpha_-(q)$ are endpoints of a leaf of $\mathcal{P}$, then $p = q$.

If a flow bordism satisfies condition (i), but not condition (ii), it is a *semi-plug*. It is has condition (ii), it has *matched ends*. A flow bordism which satisfies (ii) but not (i) is an *un-plug*. If $\mathcal{P}$ has properties (i) and (ii), it is a *plug* [GKK].

If $\mathcal{P}$ is a plug, the manifold P is the *support* of P. This is equivalent to our notation of a manifold being the support of a suspension above.

If $\mathcal{P}$ has matched ends, then F is the *base* of $\mathcal{P}$. The set of all points in F_- which are endpoints of infinite leaves is the *entry stopped set* of $\mathcal{P}$. Similarly, the points in F_+ which are endpoints of infinite leaves is the *exit stopped set*. Whenever $\mathcal{P}$ has matched ends, the

set $S = \alpha_-^{-1}(S_-) = \alpha_+^{-1}(S_+)$, is called the *stopped set*. If S has non-empty interior, then $\mathcal{P}$ *stops content*.

Modification of a foliation using a plug requires the operation of *insertion*. Let $\mathcal{P}$ be a flow bordism, and $\mathcal{X}$ a foliation on some manifold M. An *insertion map* is an embedding of the base of $\mathcal{P}$, which is transverse to $\mathcal{X}$. Denote the embedding map σ. A flow bordism $\mathcal{P}$ is *insertible* if there is an embedding of $\mathcal{P}$ into $\mathbb{R}^n$ which is transverse to vertical lines [GKK].

In essence, we are looking for the base of $\mathcal{P}$ to be entirely transverse boundary. That will ensure that, when a leaf from $\mathcal{X}$ intersects the base of the flow bordism, that leaf will only intersect a single leaf in the base of the flow bordism. The parallel boundary will guarantee that when a leaf exits the bordism, it will also intersect a single leaf. Without these conditions, it would be possible that a single leaf could be intersected by multiple leaves. This would either create singular points, or a 2-dimensional leaf, either of which would not be compatible with our proof of foliations giving rise to dynamical systems.

The next component we need to consider, is attachability. As per [GKK], a plug is *attachable* if every leaf in the parallel boundary is finite. Assume we have a plug $\mathcal{P}$, with base F. Consider an open neighborhood of $F \times [0,1]$, denoted $N_{F\times[0,1]}$. Then the embedding $\sigma((F \times [0,1]) \setminus N_{F\times[0,1]})$ will glue the open lip of $N_{F\times[0,1]}$ to the support P of the plug $\mathcal{P}$. This is done via an *attaching map*, denoted $\alpha : N_{F\times[0,1]} \to N_P$, where N_P is a neighborhood of the boundary of P. The attaching map should also satisfy $\alpha(p,0) = \alpha_-(p)$ and $\alpha(p,1) = \alpha_+(p)$, where α_- and α_+ are the maps on the closure of the transverse boundary of $\mathcal{P}$ from the definition of a flow bordism.

Since all leaves in the parallel boundary are finite, we are able to do this via a leaf-preserving homeomorphism [GKK].

We also address the idea of an *untwisted* plug [GKK]. A plug $\mathcal{P}$ with base F and support P is untwisted if the attaching map extends to a homeomorphism $F \times [0,1] \to P$.

In Chapter 5 we construct a sequence of flow bordisms, which are used in the proof of Theorem 2.6. These flow bordisms will always have all leaves in the parallel boundary finite. Furthermore, the open neighborhoods around the embeddings of the base of the flow bordisms in the proof of Theorem 2.6 will always be foliated with vertical lines. We will therefore have insertibility. All leaves in the parallel boundary will be finite, so we will have attachability. Our attaching maps will extend to homeomorphisms, and our flow bordisms will remain untwisted.

In our constructions, we will only require a flow bordism. That is all that is necessary for our modifications, so it is the only condition that will be checked. It is possible that a flow bordism is not a semi-plug. The cylinder example above, which is foliated only by vertical lines, is a flow bordism, but as it has no stopped set, it is not a semi-plug.

In Chapter 5, we will very carefully construct our flow bordisms. It will be our desire to modify existing foliations. We will take a region of a foliated manifold which is not only homeomorphic to our flow bordism, but which has the same height and radius. Furthermore, we will construct the foliations to be modified by the flow bordism such that the neighborhood around the space where the bordism is to be inserted is foliated entirely by vertical lines. This will automatically satisfy the condition for insertability from [GKK]. Careful choices regarding the size of the bordism will prevent any changes in the topology of the original foliated space after insertion.

If a flow-bordism is a measured, oriented, 1-foliation, then it may be made into a dynamical system, which preserves Lebesgue measure. We need an additional theorem before we prove this.

Let $Q^m = \mathbb{R}^m_{\geq 0}$ be the positive orthant of $\mathbb{R}^m$. A point $x \in Q$ is a *corner of codimension* q if it lies at the intersection of q coordinate hyperplanes [BMPR]. For example, in $\mathbb{R}^3$, the origin would have codimension 3, while points on the x, y, or z axis would have codimension 2.

We have defined corners in terms of the boundary of a flow bordism, by looking at boundary that is neither parallel nor transverse. We can further clarify this by saying that the corners of an m-dimensional manifold M are the subsets of M whose chart maps are open subsets of Q^m.

Let $\partial^q M$ be the set of points in M which are corners of codimension q.

We also need the notion of a *density*. This is a weaker version of a volume form, which is appropriate for non-orientable manifolds. We will not use it here, but it is necessary to state our theorem precisely. For the third theorem that follows, we can assume that the manifold is orientable, and the density may be replaced by a volume form.

We cite three results of increasing strength, which allow the change in measure between manifolds. The first is due to Moser.

Theorem 4.4 ([Mos])**.** Let τ and σ be two volume forms on a compact, connected manifold. We say $\tau \sim \sigma$ if there exists an orientation-preserving automorphism ϕ of M, such that

$$\int_M \tau = \int_{\phi(M)} \phi(\sigma).$$

If $\tau = \sigma$, then $\int_M \tau = \int_M \sigma$. Let $\kappa = \int_M \tau / \int_M \sigma$. Then $\tau \sim \kappa\sigma$.

This states that two volume forms on compact, connected manifolds, with the same total volume, will always be equivalent via a diffeomorphism. This is strengthened in Banyaga.

Theorem 4.5 ([Ba])**.** Let M be an orientable, differentiable n-manifold, compact and connected, with boundary ∂M. Let τ_t be a family of 1-parameter volume-forms. The following conditions are equivalent:

1. $\int_M \tau_0 = \int_M \tau_t$ for all t
2. There exists a family of 1-parameter $(n-1)$-forms α_t such that $\frac{\partial \tau_t}{\partial t} = d\alpha_t$ and $\alpha_t(x) = 0$ for all $x \in \partial M$.

3. There exists an isotopy ϕ_t of M such that

$$\phi_t^*(\tau_t) = \tau_0,\ \phi_0 = \text{ id, and } \phi_t|\partial M = \text{ id}$$

where ϕ_y^* is the pullback.

The additional value in this theorem is that the diffeomorphism between the volume forms may be chosen such that it is the identity on the boundary.

The third version of this theorem comes from Bruveris, et. al., and allows us to consider manifolds with corners.

Theorem 4.6 ([BMPR])**.** Let M be a compact, connected, smooth manifold with corners, possibly non-orientable. Let μ_1, μ_2 be smooth positive densities on M, with $\int_M \mu_1 = \int_M \mu_2$. Then there exists a diffeomorphism $\phi : M \to M$, such that $\phi^*(\mu_1) = \mu_2$. ϕ can be chosen to be the identity on the boundary of M iff $\mu_1 = \mu_2$ on $\partial^{\geq 2} M$.

We can now state an important extension of Theorem 4.2.

Theorem 4.7. Let $\mathcal{P}$ be a flow bordism with support P. If $\mathcal{P}$ is a measured foliation, with transverse measure μ, it may be used to construct a dynamical system which preserves Lebesgue measure.

Proof. Let $(P, \mathcal{P}, \mu)$ be a measured flow bordism. Let V_1 be the Euclidean volume of P. By Theorem 4.2, there exists a measure η on P and a phase map π, such that $(P, \mathbb{R}, \pi, \eta)$ is a measure preserving dynamical system. Let $V_2 = \eta(P)$. Since P is compact and connected, this is well defined, as η will be defined on some finite number of sets in the nice foliation atlas of $\mathcal{P}$. Now let $\kappa = V_1/V_2$, and define a new measure $\eta' = \kappa\eta$.

Now $\eta'(P)$ has the same total volume as the Lebesgue measure of P. We want to make these volumes agree, and need Theorem 4.6 to do so, as the flow bordism may have corners.

In a flow bordism, the set of all corners is a circle in the base, on which both η' and Lebesgue measure λ have measure zero. By Theorem 4.6, there exists a diffeomorphism $\phi : P \to P$, which is the identity on the boundary, and which transforms η' to agree with Lebesgue measure. □

4.3 Suspension foliations

When we encounter PL-dynamical systems in Chapter 5, we will not be able to rely on the notion of a parallel vector field to construct a flow, as we did in the smooth case. Instead, we can use the idea of a suspension foliation. We borrow the notation for this from Richardson [R].

Let M be an n-manifold, and f an bijection on M. Take the quotient of $M \times [0,1]$ under the equivalence relation $(f(x),1) \sim (x,0)$. We denote the resulting quotient space $M_{\sim f}$. We have a natural way to get a 1-foliation of this space.

For $x_0 \in M$, define

- $\mathcal{O}_{x_0} = \{\ldots, f^{-2}(x_0), f^{-1}(x_0), x_0, f(x_0), f^2(x_0), \ldots\}$.
- $L_{x_0} = \{(t,x), t \in [0,1], x \in \mathcal{O}_{x_0}\}$.

Using the orientation induced from [0,1],

$$\mathcal{F} = \cup_{x_0 \in M} L_{x_0}$$

is then an oriented 1-foliation of $M_{\sim f}$.

Note that the smoothness class of the map f determines the smoothness class of the foliation ($C^1, C^\infty, C^\omega, PL$, etc.) We are looking for diffeomorphisms in the smooth cases, or piecewise-linear (PL) homeomorphisms in the PL case. PL homeomorphisms are defined precisely in Chapter 5.

Isotopy has been defined in Chapter 1, but we may sometimes make use of a weaker version, *pseudo-isotopy*. A map $g : M \times [0,1] \to M \times [0,1]$ is a pseudo-isotopy if g is the identity when restricted to $M \times \{0\} \cup \partial M \times [0,1]$. Letting f be the restriction of g to $M \times \{1\}$, we say that f is *pseudo-isotopic to the identity*.

Another way to think of this is, if f is a diffeomorphism (or PL homeomorphism) of M, and there exists a diffeomorphism (again, or PL homeomorphism) g of $M \times [0,1]$ such that for all $x \in M$, $g(x,0) = id(x)$ and $g(x,1) = f(x)$.

In some modern usage, the map f is referred to simply as a pseudo-isotopy. We will refer to it here as a map which is pseudo-isotopic to the identity.

We can similarly say that, if g is an isotopy, and f is the restriction of g to $M \times \{1\}$, then f is *isotopic to the identity*.

If f is isotopic or pseudo-isotopic to the identity, then the support of the foliation on $M_{\sim f}$ is homeomorphic to $M \times S^1$ [GK]. This follows from the fact that, if f is the identity map, then $M_{\sim f} = M \times S^1$.

For most examples, we will want the support of our foliation to be homeomorphic to $M \times S^1$, but this first example shows that it need not always be the case.

Example 4.8. There exists a suspension of a manifold M whose support is not diffeomorphic to $M \times S^1$.

Let $M = [0.1]$, and $f : M \to M$ be given by $f(x) = (1 - x)$. Since $f(0) = 1$ and $f(1) = 0$, this map is not an isotopy or pseudo-isotopy. In fact, $M_{\sim f}$ is a half-twist Möbius band, while $M \times S^1$ is a cylinder. These two spaces are not diffeomorphic.

Theorem 4.9. If f is a volume-preserving homeomorphism of M, then the suspension $M_{\sim f}$ is a measured-foliation.

Proof. Let $f : M \to M$ be volume-preserving, for some measure μ on M. We define a measure μ' on $M_{\sim f}$. Let α be an $n-$dimensional submanifold of $M_{\sim f}$ which is transverse

to the foliation $\mathcal{F}$ on $M_{\sim f}$. Let α' be the projection of α along the leaves of the foliation onto M. Let $\mu'(\alpha) = \mu(\alpha')$. Then for two isotopic transversals α and β, $\alpha' = f^n(\beta')$ for some integer n. As f preserves volume, $\mu(\alpha') = \mu(f^n(\beta'))$, and we conclude $\mu'(\alpha) = \mu'(\beta)$. Therefore, the foliation $(M_{\sim f}, \mathcal{F})$ is measured. □

Chapter 5

Piecewise linear topology, foliations, and dynamics

5.1 PL topology

A *p-simplex* σ is the convex closure of a set of $p+1$ points, $\{v_0, v_1, \ldots, v_p\}$ such that for each $x \in \sigma$, $x = \sum t_i v_i$, where each $t_i \in [0,1]$ and $\sum t_i = 1$. The set $\{v_0, v_1, \ldots, v_p\}$ makes up the vertices of σ, and for each $x \in \sigma$, the set of $\{t_i\}$ are the *barycentric coordinates* of x. We will need a particular point $\beta(\sigma) = \sum \frac{1}{p+1} v_i$, denoted the *barycenter* of σ. A simplex is *spanned* by its vertices, and we write $\sigma = v_0 v_1 \ldots v_p$ to indicate this. For any simplex τ spanned by a subset of $\{v_0, v_1, \ldots, v_p\}$, τ is a *face* of σ. We use the notation $\tau < \sigma$ to indicate that τ is a face of σ.

A *simplicial complex* [Mu] is a collection K of simplices in $\mathbb{R}^n$, such that

1. if $\sigma \in K$, then all faces of σ are in K.

2. If $\sigma, \tau \in K$, and $\sigma \cap \tau \neq \emptyset$, then $\sigma \cap \tau$ is a face of both σ and τ.

We call $|K| = \cup\{\sigma : \sigma \in K\} \subset \mathbb{R}^n$ the *polyhedron* of K. For each $p \geq 0$, we call $K^{(p)} = \{\sigma \in K : \dim \sigma \leq p\}$ the *p-skeleton* of K. For every $\sigma \in K$, the *boundary* of σ is $\partial\sigma = \{\tau < \sigma : \tau \neq \sigma\}$.

We can define a topology to make $|K|$ a topological space. First note that individual simplices are closed by their definition. Define a topology on $|K|$ by letting a subset $A \subset |K|$ be closed if and only if $A \cap \sigma$ is closed in σ for every $\sigma \in |K|$. [Mu]

The space $|K|$ may inherit the subspace topology from $\mathbb{R}^n$, but this need not be the case (see Example 5.1). The topology on K will be the subspace topology inherited from $\mathbb{R}^n$ if K is finite.

Example 5.1. Let K be the collection of 1-simplices of the form $[m, m+1]$, where $m \in \mathbb{Z} \setminus \{0\}$, along with all simplices of the form $[1/(n+1), 1/n]$, where $n \in \mathbb{N}$. Allow the faces defined by these simplices to be in K as well, making it a simplicial complex. As a set, $|K| = \mathbb{R}$, but the topologies are different. The set $\{1/n : n \in \mathbb{N}\}$ is closed in $|K|$, though it is not closed in $\mathbb{R}$ [Mu].

For any simplicial complex K, $|K|$ is always Hausdorff, and if K is finite, then $|K|$ is compact. A simplicial complex is *locally finite* if each vertex in K belongs to only finitely many simplices of K. If K is locally finite, then K is metrizable [Mu].

We may also take a complex K, and subdivide it to create a new complex with the same polyhedron. A complex L is a *subdivision* of K if $|L| = |K|$ and each simplex $\tau \in L$ lies in some simplex $\sigma \in K$. We denote this by $L \prec K$. A simple way to subdivide is the *first barycentric subdivision*. This is achieved inductively. For each 1-simplex σ in K, find its barycenter $\beta(\sigma)$. The subdivision is then $\partial\sigma \cup \{\beta(\sigma)v_i : v_i \in \partial\sigma\}$, where v_i are the faces of $\partial\sigma$, though in this case, they are just the vertices.

Once this is complete, for each 2-simplex $\tau \in K$, find $\beta(\tau)$. Note that $\partial\tau$ will include the subdivision from the previous step. Subdivide τ by taking $\partial\tau \cup \{\beta(\tau)\eta : \eta < \partial\tau\}$. Note that we included not just the vertices of the 1-simplices in the boundary of τ, but all of its faces. The union ensures that we will not count simplices twice in our subdivision.

Proceeding inductively, we have a subdivision of K. The first barycentric subdivision is denoted K^1. The process may be repeated, resulting in K^2. Letting $K^0 = K$, the notation is well defined for all subdivisions, and $(K^{r-1})^1 = K^r$. The polyhedron remains the same for all such subdivisions.

Subdivisions could also be constructed by choosing an interior point other than the barycenter of a simplex. An important result is that any two subdivisions of a simplicial complex have a common subdivision.

Theorem 5.2. Let K be a simplicial complex, with $J \prec K$ and $L \prec K$. Then there exists a common subdivision of J and L.

Proof. Let $\mathcal{C} = \{\sigma \cap \tau : \sigma \in J, \tau \in L\}$. Then each element of $\mathcal{C}$ is a convex region, and a subset of $|K|$. It may not be the case that the elements of $\mathcal{C}$ are simplices. Order the vertices of $\mathcal{C}$, and choose any $c \in \mathcal{C}$. Assuming the boundary of c is subdivided, let v be the first vertex in c, and add the simplex $vw_0w_1 \dots w_i$, where $w_0w_1 \dots w_i$ is a simplex in the boundary of c. Beginning with 1-dimensional elements of $\mathcal{C}$ and proceeding inductively, we get a common subdivision of J and L, without adding new vertices. □

We now define maps between simplicial complexes. Here a straight line segment may intersect more than one simplex, if those simplices are coplanar. Given two simplicial complexes K and L, a map $f : K \to L$ *preserves linearity* if, straight line segments in K are sent to straight line segments in L. f *preserves ratios* if, for $v_1, v_2, v_3 \in K$ collinear points, $d(v_1, v_2)d(f(v_2), f(v_3)) = d(v_2, v_3)d(f(v_1), f(v_2))$, where d is the Euclidean distance. A function is *linear* if is preserves linearity and preserves ratios [B]. $f : K \to L$ is a *simplicial map* if $f : |K| \to |L|$ and for each $\sigma \in K$, $f|_\sigma$ maps linearly onto a simplex in L. A map $f : |K| \to |L|$ is *piecewise linear (PL)* if there are subdivisions $K' \prec K$ and $L' \prec L$ such that $f : K' \to L'$ is simplicial. Two polyhedra $|K|$ and $|L|$ are *piecewise linearly (PL) homeomorphic* if there exist subdivisions $K' \prec K$ and $L' \prec L$ such that $K' \cong L'$. We then write $|K| \cong |L|$.

5.2 PL manifolds

To put a piecewise linear structure on a manifold, we start with a more fundamental idea. First, let the *link* of σ in K be the subcomplexes $\mathrm{Lk}(\sigma, K) = \{\tau \in \mathrm{St}(\sigma, K) : \tau \cap \omega = \emptyset\}$. The link can be thought of as the simplices which are reachable from σ by moving across one simplex. [Mu]

A *combinatorial n-manifold* is a complex K for which the link of each p-simplex is PL homeomorphic to either the boundary of an $(n-p)$-simplex or an $(n-p-1)$-simplex. For example, in a combinatorial 3-manifold, a 0-simplex is a point, a 1-simplex is a line, a 2-simplex is a triangle, and a 3-simplex is a tetrahedron. The link of a 0-simplex would be the 2-simplices which share the 0-simplex as a vertex.

Simplices of the second type are a subcomplex of the boundary of K, and constitute a combinatorial $(n-1)$-manifold. Note that, if K is a combinatorial n-manifold, then $|K|$ is a topological n-manifold.

To define a piecewise linear manifold, we need the notion of triangulation. Given a topological space X, a *triangulation* of X is a complex K and a homeomorphism $f : |K| \to X$. Two triangulations, $f : |K| \to X$ and $g : |L| \to X$ are *equivalent* if there is a PL homeomorphism $h : |K| \to |L|$ such that $g \circ h = f$. A topological space for which a triangularization exists is *triangulable*.

We have two different definitions for a piecewise linear n-manifold. The first, is that a *PL n-manifold* is a topological n-manifold M, with a triangulation $f : |K| \to M$, where K is a combinatorial n-manifold.

An equivalent definition involves an atlas of charts on M, with each embedding piecewise linear. We further require that, for $U, V \in \mathcal{U}$, $\varphi_U(\varphi_V^{-1}) : \varphi_U(U \cap v) \to \varphi_V(U \cap V)$ is also piecewise linear.

Given such an atlas, we can define a PL triangulation of M. For each open set U in the atlas, triangulate its image in $\mathbb{R}^n$[RoSa]. If M is compact, there is a finite subcover of M subordinate to the atlas $\mathcal{U}$, each of which is the pre-image of a simplex in $\mathbb{R}^n$, and so each is a compact polyhedra. Inductively, we can subdivide these until we have a triangulation of M. If M is not compact, there is still a cover of M by compact polyhedra, which is subordinate to $\mathcal{U}$[Br, DS]. We then proceed as in the compact case.

It seems likely that, in general, two triangulations of a manifold will share a common refinement. This was disproved in the general case in [M2]. It is true when the dimension of the manifold is less than or equal to 3. [Mo]

The Cartesian product is not immediately well-defined. In the case of a smooth manifold, $S^1 \times S^1$ is simply the 2-torus. In the PL case, even a simple triangulation of $S^1 \times S^1$ causes problems. We can remedy this by taking multiple barycentric subdivisions. [Br, DS]

Given any two complexes K and L, let σ be a simplex in K, and τ a simplex in L. Let $s = \{s_0, s_1, \ldots, s_n\}$ be the set of vertices in σ and $t = \{t_0, t_1, \ldots, t_m\}$ be the set of vertices in τ.

Define a sequence of ordered pairs of vertices with lexicographical ordering. We have (s_i, t_j) is followed by either (s_{i+1}, t_j) or by (s_i, t_{j+1}). Add any simplices spanned by these sequences of vertices to the triangulation. Any cells which arise during this construction that are not simplices can be addressed with an additional barycentric subdivision prior to the adding of edges. This can always be done with two or fewer subdivisions [Br, DS].

Consider the example of $S^1 \times S^1$. Label the vertices in the first circle v and in the second circle w. If we do not subdivide, the only ordered pair of vertices here is (v_0, w_0), which does not span a simplex, other than itself.

Instead, try a single subdivision. The sequences of vertices are now $((v_0, w_0), (v_0, w_1), (v_1, w_1))$ and $((v_0, w_0), (v_1, w_0), (v_1, w_0))$. This subdivision and the resulting triangulation are shown in Figure 5.1, where we assume the top and bottom edge are identified, as well as the left and right edges.

We will refer to *n-fold simplicial approximations* of PL manifolds. This involves subdividing a m complex into n subcomplexes, which are each PL homeomorphic to the original complex. For example, a n-fold simplicial approximation of a S^1 would involve subdividing a 1-simplex into n identical 1-simplices by the addition of $n - 1$ equally spaced vertices,

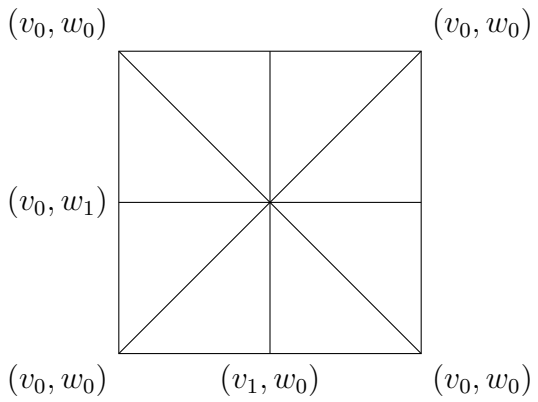

Figure 5.1: Product of $S^1 \times S^1$, triangulated after subdivision.

and identifying the endpoints. An n-fold simplicial approximation of a 2-torus, would involve taking the product of two n-fold approximations of S^1, and triangulating as per the description of the Cartesian product above.

Quotients are also troublesome in triangulated spaces. For example, a 1-simplex σ with the endpoints identified is not PL homeomorphic to any simplicial approximation of S^1 [Br, DS]. Let v_0 and v_1 be the 0-simplices at the endpoints of σ. Any simplicial map from σ which identifies the endpoints must be constant on the interior of σ, and so the resulting space will not be homeomorphic to S^1. We can address this, but it will require subdividing σ prior to making the identifications. Taking 2 barycentric subdivisions, we then have a PL homeomorphism from σ to a 4-fold simplicial approximation of S^1. Figure 5.2 shows how this can be applied to the 2-torus. In Figure 5.2(a), we've taken a quotient of a 4-fold approximation of $S^1 \times [0, 1]$, without proper subdivisions. This is clearly not triangulated. In 5.2(b), we show the same quotient, but with appropriate subdivisions and the resulting triangulation.

Taking the second barycentric subdivision of a triangulable space prior to taking the quotient will ensure that the resulting quotient space is triangulable [Br, DS].

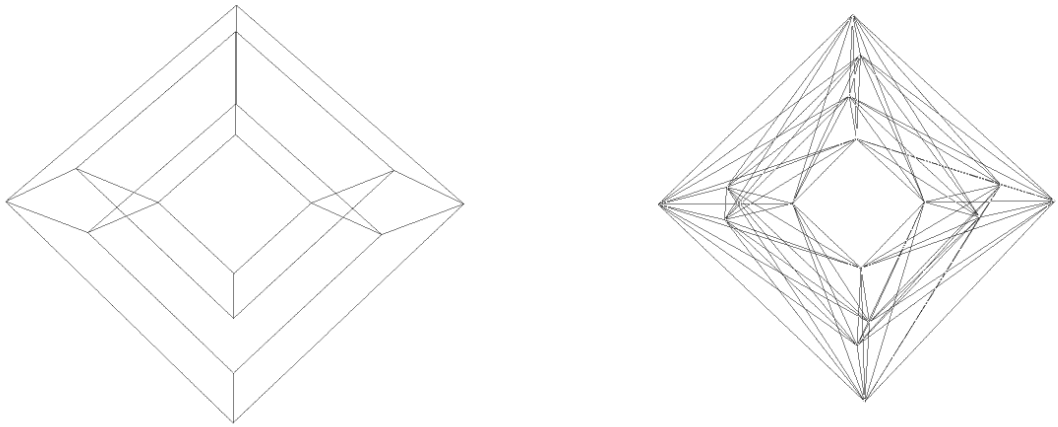

(a) Example of issue with Quotient on PL manifold.

(b) Quotient of $S_1 \times [0,1]$, with $0 \sim 1$, after appropriate subdivisions.

Figure 5.2: Problems and solutions in the quotient of simplicial complexes

5.3 PL dynamics and foliations

We can also extend the notions of a flow and a foliation to PL manifolds. The definition of a flow generalizes naturally. All we ask is that the map π be a piecewise linear homeomorphism on the phase space. A PL foliation is realized when the chart maps for the atlas, as described in section 2.3, are each piecewise linear homeomorphisms.

We present here a few additional examples of PL foliations. These use the suspension from Chapter 4. The notation for leaves and orbits is the same as in section 4.3.

Theorem 5.3. Given a PL manifold K, the suspension of K under some PL-homeomorphism f is still a PL manifold.

Proof. Let K be a PL-manifold, and $f : K \to K$ a PL-homeomorphism. K and $f(K)$ are each triangulations of the same polyhedron, so there exists a common subdivision, which we denote L. Triangulate $L \times [0,1]$, take the second barycentric subdivision, and construct the quotient for the suspension. The result is triangulable, □

For example, the image in Figure 5.2(b) could be thought of as the suspension of a S^1, under the identity map. While the previous example shows the triangulation, the foliation would just consist of straight lines on the boundary, and would be a PL-foliation.

Example 5.4. There exists a PL foliations of the annulus, with all leaves PL-homeomorphic to circles.

This is the similar to the foliation used in Example 4.1. The difference here is that we construct it from a suspension, and it is specifically piecewise-linear. Let $I = [0, 1]$ and take the suspension of I under the identity map. Take a 4-fold covering of the suspension, to get a PL annulus, with inner and outer boundaries made up of squares. The space is triangulable, the identity map is PL, and all leaves are homeomorphic to circles. This is shown with sample leaves in Figure 5.3, with orientation indicated. The inner and outer boundary of this annulus are also leaves.

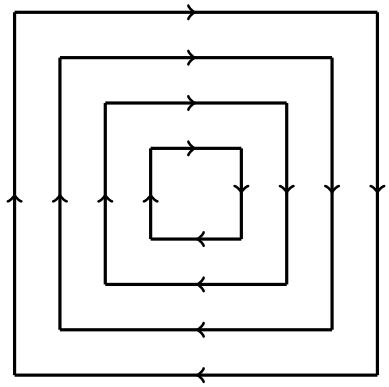

Figure 5.3: PL foliation of the annulus with all leaves homeomorphic to S^1

We can explicitly create a PL dynamical system from the foliation in example 5.4. All that is needed is to choose a triangulation of the annulus such that each of the corners in a leaf is on the edge of a simplex. The thick lines in Figure 5.4 show the boundary of the annulus, while the thinner lines show an appropriate triangulation.

The orbits in the dynamical system arise from the leaves. Introducing a time parameter into the dynamical system is done following the method in example 4.1. Note that we have not confirmed that this is a measured foliation, so that component would be omitted.

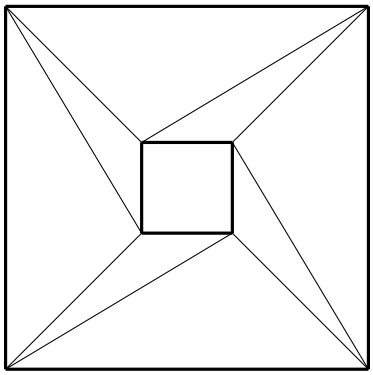

Figure 5.4: Triangulation of an annulus such that the foliation in example 5.4 yields a PL dynamical system

Example 5.5. There exists a PL foliation of the annulus, with only the leaves on the boundary compact.

Begin with a map $g : I \to I$, defined piecewise as

$$g(x) = \begin{cases} \frac{x}{2} & \text{if} \quad x \in [0, 1/2] \\ \frac{3x-1}{2} & \text{if} \quad x \in (1/2, 1] \end{cases}$$

A selection of the leaf $L_{1/2}$ is shown in Figure 5.6.

As g is isotopic to the identity, our suspension is homeomorphic to the annulus. Furthermore, g is PL. We again use a 4-fold covering for convenience, and the resulting foliated annulus is shown in Figure 5.5. The leaves are oriented counterclockwise. As the endpoints of I were fixed under g, we have the inner and outer boundary of the annulus as circles. All other leaves spiral towards the inner boundary and towards the outer boundary. Each leaf, other than the leaves on the boundary, is not compact.

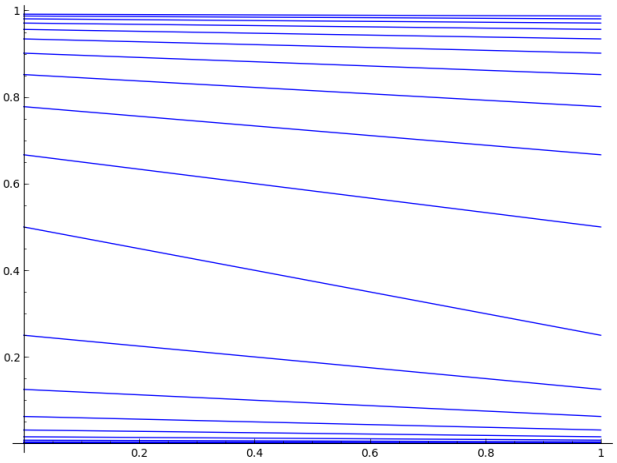

Figure 5.5: The leaf $L_{1/2}$. Note that the points in the orbit $\mathcal{O}_{1/2}$ approach 0 in the forward direction and 1 in the backward direction.

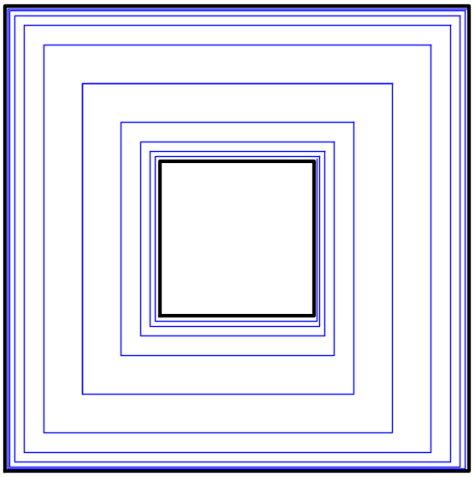

Figure 5.6: PL foliation of an annulus, with only the inner and outer boundary as compact leaves.

Note that the function g is example 5.5 is not unique. Any PL homeomorphism, isotopic to the identity, of I which fixes the endpoints, and for which one interior point limits to 0 under repeated iteration of the map, will result in a foliation of the annulus with only 2 compact leaves. This should come as no surprise, since any such map will be isotopic to g.

5.3.1 Measured PL foliations

A property of PL homeomorphisms we will be interested in, is when these maps are measure preserving. To do this, we will need to define a measure on our PL spaces. Let M be a PL n-manifold. A measure is *simplicial* on M if, for some triangulation T of the manifold, the measure is given by the measure of the linear embedding of an m-simplex of T in $\mathbb{R}^m$. A simplicial measure can then be thought of as a volume form, in the sense of section 2.2, which assigns the m-dimensional Euclidean volume to an m-simplex [A]. Any such volume-form will be piecewise-constant on the entire n-manifold M, since it will return a constant volume on each simplex.

Thanks to G. Kuperberg [GK], we have a theorem which allows us some flexibility in our choice of PL measures. This is a piecewise-linear analog of the results of Moser [Mos], Banyaga [Ba] and Bruveris, et. al, [BMPR], stated earlier as Theorems 4.4-4.6.

Theorem 5.6. Two simplicial measures on a connected, compact, PL-manifold, with the same total volume, are equivalent under a PL homeomorphism. Moreover, any simplicial measure is locally PL-Lebesgue.

This result is strengthened in Henriques and Pak [HP].

Theorem 5.7. Let M_1 and M_2 be two PL-manifolds, possible with boundary, which are PL-homeomorphic and equipped with piecewise-constant volume-forms ω_1, ω_2. If M_1 and M_2 have equal volume, then there exists a volume-preserving PL-homeomorphism $f : M_1 \to M_2$. That is, the pullback of f gives $f^*(\omega_2) = \omega_1$.

Figure 5.7: Area-preserving map for Example 5.5

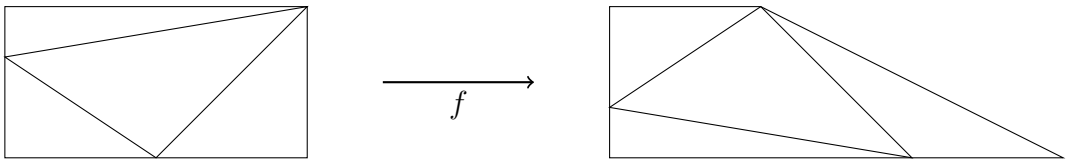

The main difference here is that we have removed the requirement for the manifold to be compact and connected. The pullback here indicates the PL map, defined by $f^*(\omega_2)(\sigma) = \omega_2(f(\sigma))$, where σ is a simplex in M_2.

Regarding the notion of a locally PL-Lebesgue measure [GK], while the simplicial measure may not agree with the Lebesgue measure on the entire PL manifold, when restricted to a single simplex, it will agree with Lebesgue measure.

Given an n-dimensional PL-manifold M and a measure μ on M, a function f defined on M is an *measure-preserving* PL-homeomorphism if there is a triangulation of $f(M)$, whose simplices have the same measure as their pre-image under f.

Example 5.8. Consider the rectangle in the plane with vertices (0,0), (0,1), (2,0), and (2,1), with the measure the usual Euclidean volume on $\mathbb{R}^2$. This clearly has the same area as the trapezoid in the plane with vertices (0,0), (0,1), (3,0), and (1,1). We seek a PL, measure-preserving homeomorphism between them. Begin by triangulating the rectangle with the addition of vertices at (0,2/3) and (1,0). Let f be the function which fixes the vertices (0,0) and (0,1), and maps $(0, 2/3) \to (0, 1/3)$, $(2, 1) \to (1, 1)$, $(1, 0) \to (2, 0)$, and $(2, 0) \to (3, 0)$. Let f preserve linearity on each 1-simplex, and be linear on each 2-simplex. It is easily checked that the areas of the simplices are preserved, hence f is an measure-preserving PL-homeomorphism. This is shown in Figure 5.7.

As stated above, a simplicial measure can be thought of as a piecewise-constant volume form. In the case that our measure is simplicial, we will generally use the term *volume-preserving*, rather than measure-preserving. This is more consistent with the literature on this topic.

We have three results relating to volume-preserving PL foliations which will be useful later.

Lemma 5.9. Let M be a PL n-manifold and $\mathcal{F}$ a measured 1-foliation of M. If M is retriangulated, $\mathcal{F}$ remains measured.

Proof. Let μ be a transverse measure on $\mathcal{F}$, and α a transversal in M. Let β be a transversal in M, isotopic to α, so that $\mu(\alpha) = \mu(\beta)$. Retriangulating M does not affect the flow boxes used in computing the transverse measure of the small transversals which make up α and β, so it is possible to keep μ the same. Therefore, under the retriangulation, $\mu(\alpha) = \mu(\beta)$, and the foliation remains measured. □

Lemma 5.10. Let M be a PL n-manifold, and $\mathcal{F}$ a measured 1-foliation of M. Let $g : M \to M$ be a PL-homeomorphism which preserves simplicial measure on the simplices for some triangulation of M. Then the foliation $g(\mathcal{F})$ is a measured foliation.

Proof. Let μ be a transverse measure on $\mathcal{F}$, with α and β isotopic transversals. Without loss of generality, assume α and β are small, contained in flow boxes U_α and U_β respectively. Let η be the simplicial measure on M, then $\eta(U_\alpha) = \eta(g)U_\alpha)$, and similarly for U_β. Now consider $g(\alpha)$ and $g(\beta)$. Since g is a PL-homeomorphism, $g(\alpha)$ and $g(\beta)$ are still isotopic. If $g(\alpha)$ and $g(\beta)$ did not possess the same transverse measure, there would exists a retriangulation of M on which areas of simplices would not be preserved under g. We conclude that $g(\mathcal{F})$ remains a measured foliation. □

Corollary 5.11. A volume-preserving PL flow bordism $\mathcal{P}$ may be inserted into a foliation of $\mathbb{R}^n$, while preserving Lebesgue measure on $\mathbb{R}^n$.

Proof. Let V represent the total volume of the support P of $\mathcal{P}$. Scale V linearly, so that the total volume of the P is the same as that of the Euclidean volume of the region of $\mathbb{R}^n$ which is being replaced with $\mathcal{P}$. It follows from Theorem 5.7 that the measure on $\mathcal{P}$ may be modified via a PL-homeomorphism to agree with Lebesgue measure. □

5.4 Slanted suspensions

We will require the use of a *slanted suspension* in the following constructions, which is similar to the suspension foliations discussed in Chapter 4. This technique will allow us construct a foliation which gives a proof of Theorem 2.6.

As given in [GKK], for any compact manifold H, let $f : H \times [a, b] \to H \times [a, b]$ be a PL homeomorphism. Fix a real number $l \in (0, 1)$. For each fixed point $x \in H$ and $y \in [a, b]$, let $L_{xy} = \{(x, y + lz, z) : y + lz \in [a, b] \text{ and } z \in [0, 1]\}$. Then $\mathcal{L} = \{L_{xy} : \forall (x, y) \in H \times [a, b]\}$ is a foliation of $H \times [a, b] \times [0, 1]$, with leaves oriented from $H \times [a, b] \times \{0\}$ to $H \times [a, b] \times \{1\}$. The *slanted suspension* of $H \times [a, b]$ with *slant* l is the foliation of the quotient space generated by the equivalence $(f(x, y), 0) \sim (x, y, 1)$, with a foliation $\mathcal{F}$ induced by $\mathcal{L}$. We denote this as $M_{\sim f,l}$.

Example 5.12. For our first example, let H be a single point, and $[a, b] = [0, 1]$. We construct a slanted suspension with a singled fixed circular orbit. Let $f : [0, 1] \to [0, 1]$ be given by

$$f(x) = \begin{cases} 2x - 1 & \text{if } x \in [1/2, 1] \\ \frac{2x}{3} & \text{else} \end{cases}$$

Take the slanted suspension with slant $1/4$. The points 0 and 1 are fixed, under this map. Note that $f(3/4) = 1/2$. This is important, since there is a leaf from $(1/2, 0)$ to $(3/4, 1)$. This leaf comes from the slant, but the point $(3/4, 1)$ has the first coordinate shifted down

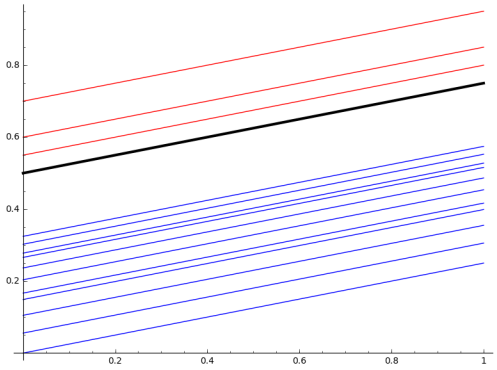

Figure 5.8: Example 5.12. The thick line indicates the fixed circular leaf.

by the same amount as the slant of the suspension. Thus $(3/4, 1)$ is identified with $(1/2, 0)$, creating a fixed circular leaf in the foliation.

Example 5.13. We can use the same choice of H and $[a, b]$, but with a different map, to get a fixed annulus, rather than a fixed circle. Let $f : [0, 1] \to [0, 1]$ be given by

$$f(x) = \begin{cases} 2x - 1 & \text{if } x \in (7/8, 1] \\ x - 1/8 & \text{if } x \in [3/8, 7/8] \\ \frac{2x}{3} & \text{else} \end{cases}$$

Take the slanted suspension of $[0, 1]$ under f with slant $1/8$. For each point $x \in [3/8, 7/8]$ the point $(x, 0)$ has a leaf connecting it to $(x + 1/8, 1)$, but under our map, the points $(x + 1/8, 1)$ and $(x, 0)$ are identified in the suspension. As in the last example, the slant of the suspension, and the amount by which each x is shifted down under f, agree. The black strip indicated in Figure 5.9 is a collection of fixed circular leaves, making up a large fixed annular leaf.

To use the slanted suspension to construct a PL analog of the earlier constructions, we need that the slanted suspension can yield a measurable foliation.

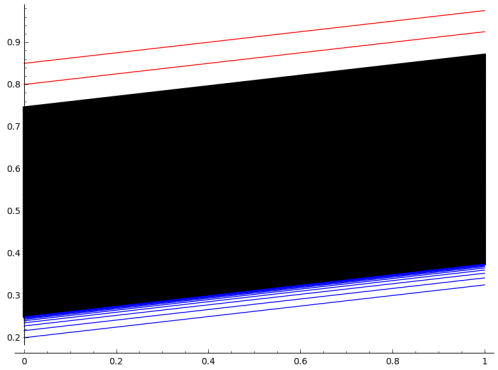

Figure 5.9: Example 5.9. The black strip indicates the annular leaf.

Theorem 5.14. Let M be a 2 dimensional PL-manifold, μ a simplicial measure on M, and f a measure-preserving PL-homeomorphism on M. Then the foliation $M_{\sim,f,l}$ given by the slanted suspension of M under f, with slant l, is measured.

Proof. Let $M_{\sim,f,l}$ be the slanted suspension in the theorem. Let α and β be two isotopic transversals. A transverse measure on the foliation can be given by the extending the measure used on M, as each transversal is isotopic to some subset of M, we assign the transversal the measure of the subset of M to which it is isotopic. Therefore if α is isotopic to β, they are each isotopic to some subset of M, and therefore, the measures of α and β coincide. We conclude that the suspension is measured. □

Just as we have constructed flow bordisms for smooth flows and smooth foliations, we can construct flow bordisms to modify PL-foliations using the slanted suspension. Given an measure-preserving PL-homeomorphism f of a planar region T, which fixes the boundary of T. Depending on our choice of f, it is possible to use the slanted suspension to create a flow bordism, a semi-plug, or a plug.

Theorem 5.15. Let $M = [a, b] \times [c, d]$, and $f : M \to M$ a PL-homeomorphism. Take the slanted suspension of M with slant l. If for all $p \in \partial M$, $f(p) \neq p - l$, then $M_{\sim,f,l}$ may be made into a flow bordism, via a leaf-preserving map $g : M_{\sim,f,l} \to M_{\sim,f,l}$. Furthermore, if $M_{\sim,f,l}$ is a measured-foliation, g may be chosen such that $g(M_{\sim,f,l})$ remains measured.

Proof. Assume that $M_{\sim,f,l}$ is as in the theorem. Denote P to be the support of the foliation $M_{\sim,f,l}$. Then $P = [a,b] \times [c,d] \times [0,1]$, with $[a,b] \times [c,d] \times \{0\} \sim [a,b] \times [c,d] \times \{1\}$. P is then a cylinder with an annular base. We use coordinates (x,y,z), as though we were in the unquotiented space $[a,b] \times [c,d] \times [0,1]$.

F_- is the subset of P with y coordinate c, and F_+ is the subset of P with y coordinate d.

This is because the definition of the slanted suspension requires that $l > 0$. Any leaf passing through F_- will have an increasing y coordinate following the orientation of the leaf, and any leaf through F_+ will have a decreasing y coordinate following the reversed orientation of the leaf. The non-zero slant prevents any portion of the sets we've designated F_- or F_+ from satisfying the definition of parallel boundary.

To create parallel boundary, we are interested in the components of the boundary for which $x = a$ or $x = b$. This is the boundary component which we have not already designated F_- or F_+.

We will retriangulate these boundary components, in order to define a PL-homeomorphism on P which yields parallel boundary on these components. The condition $f(p) \neq p - l$ is essential to guarantee that there are no circular leaves in the boundary, which would prevent the possibility of parallel boundary. This condition is the opposite of what occurred in example 5.12. In that case we specifically created a circular leaf. Here we avoid it. If a circular leaf arose in this portion of the boundary, the remainder of the construction would fail.

Begin with a leaf L_0, through $(a,c,0)$. In the unquotiented space, this leaf will intersect the point $(a,c+l,1)$, and will continue through the point $(a,f(c+1),0)$. In P, this leaf will wrap around the boundary of the cylinder, until identified with the appropriate point. The map we are looking for here is a PL analog of a map which fixes the base of a cylinder, and rotates the top until the leaves are unwound and vertical.

Let $x_0 = c$, $y_0 = c + l$, $x_1 = f(y_0)$, $y_1 = x_1 + l$, and so on, with $x_n = f(y_{n-1})$ and $y_n = x_n + l$. Our condition that avoids circular leaves guarantees that this leaf eventually intersects a point with z coordinate d. Use the sequences x_i and y_i to create vertices in the line segment $[c, d]$ and let $\{z_i\}$ be a common subdivision of $[c, d]$. This allows L_0 to move through a sequence of vertices each time it wraps around the boundary of P. In acting on those vertices, we can see this leaf become vertical through a PL-homeomorphism. Since all leaves on this boundary component are parallel to this leaf, this will allow us to create parallel boundary, while preserving F_- and F_+.

Let w be the largest index in $\{z_i\}$. In the case that f is the identity on the boundary, $w = |d - c|/l$. We work in the unquotiented version of P to create the simplices on which g will act. Subdivide $[0, 1]$ and $[a, b]$ each using w evenly spaced vertices.

We will first triangulate $[c, d] \times [0, 1]$, and use this to define g. This is done by adding edges to make w^2 squares, then adding an edge in each square, moving from lower left to upper right. By lower left we mean the vertex closest to $(c, 0)$, and by upper right, the vertex closest to $(d, 1)$.

Label the vertices $v_0, v_1, \ldots, v_{w-1}, v_w, \ldots v_{w^2}$, moving left to right, and from vertices with second coordinate c to the vertices with second coordinate d.

Let g be the map which fixes $v_0, v_1, \ldots, v_{w-1}$, and shift all other vertices to the left (decreasing their z coordinate), accounting for the identified vertices in the slanted suspension. Once all leaf segments with endpoints on $[a, b] \times \{c\} \times [0, 1]$, are vertical, fix vertices $v_0, v_1, \ldots, v_w, v_{w+1}, \ldots, v_{2w-1}$ and repeat the process. This is shown in the case that $w = 1$ in Figures 5.10-5.14.

g is applied to the vertices of $\{a\} \times [c, d] \times [0, 1]$ and $\{b\} \times [c, d] \times [0, 1]$ simultaneously, creating parallel boundary on both components. Since no vertex is mapped to a vertex with a lower y coordinate, the transverse boundary is preserved, as is the orientation of the leaves intersecting the transverse boundary.

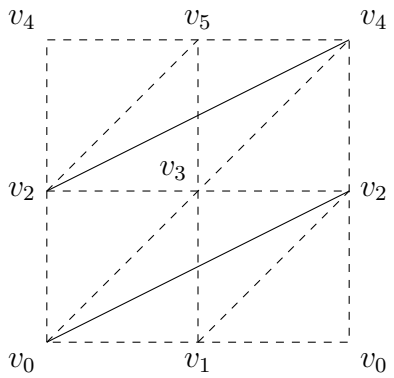

Figure 5.10: Initial triangulation

Figure 5.11: Shift $v_2, \ldots, v_5$ one vertex to the left.

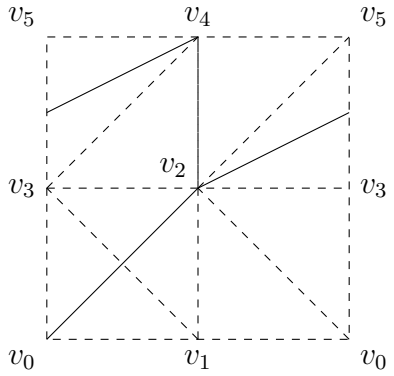

Next, we show how g is defined on all of $M_{\sim,f,l}$. We have already subdivided $[a, b]$ into w evenly spaced vertices, and at each of these we triangulate the copy of $[c, d] \times [0, 1]$ exactly as before. Add further edges so that each of the squares in $c, d] \times [0, 1]$ is now the face of a cube. We can triangulate each face of this cube, and by adding a vertex at the center of the cube, add 3 additional edges connecting opposite vertices of the cube, to fully triangulate the cube. This is shown in Figure 5.15.

g shifts all vertices on copies of $[c, d] \times [0, 1]$ as before, while fixing the newly added center vertices. The advantage of this triangulation is that g preserves area on all 2-simplices, and since the center vertices of each cube are fixed, the heights of the 3-simplices are also preserved, hence the volume of all simplices in the triangulation are preserved.

Figure 5.12: Shift $v_2, \ldots, v_5$ one vertex to the left.

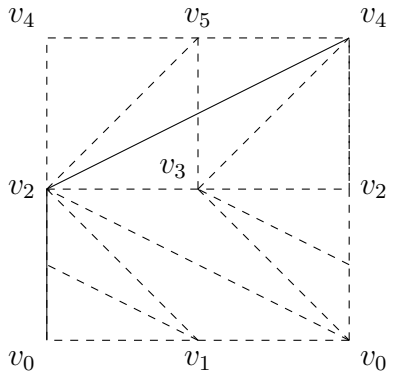

Figure 5.13: Shift v_4 and v_5 one vertex to the left.

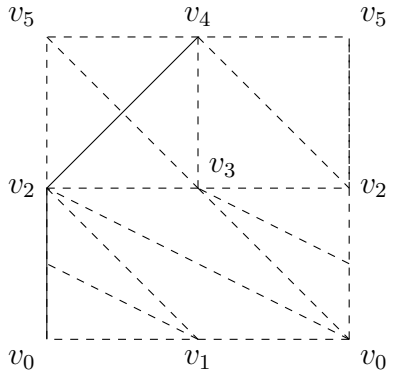

All leaves in $\{a, b\} \times [c, d] \times [0, 1]$ are now vertical line segments, and so this component of the boundary of $g(M_{\sim,f,l})$ is parallel boundary. Since the slope was positive, no leaves will lie entirely in either $(a, b) \times \{c\} \times [0, 1]$, or $(a, b) \times \{c\} \times [0, 1]$, so the entire set $(a, b) \times \{c, d\} \times [0, 1]$ is transverse boundary. We conclude that $g(M_{\sim,f,l})$ is a flow-bordism.

As g preserves volume on individual simplices, the second portion of the proof, follows immediately from lemmas 5.9 and 5.10. □

We have here an example of a flow bordism created from a slanted suspension.

Example 5.16. We begin with a PL homeomorphism from a construction in [GK]. Consider the planar rectangle T with vertices at (0,0),(0,3),(2,3), and (2,0). Construct a triangulation of T and a area-preserving homeomorphism f as in Figure 5.16.

Figure 5.14: Shift v_4 and v_5 one vertex to the left.

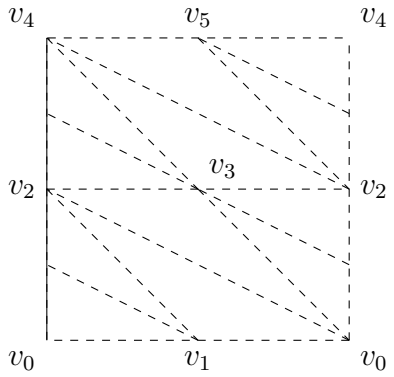

Let $T_{\sim,f,1}$ be the slanted suspension of T with slope 1, under f. Under this suspension, the point $(f(2,2),0) = ((2,1),0)$ is identified with $((2,2),1)$. However, using the foliation with slope 1, this identification determines a circular leaf. Any points along the midline of T (points with x-coordinate 0) will, thanks to the slant of the suspension, be mapped to a leaf which spirals towards the circular leaf.

The boundary is mapped to itself, and the result is a semi-plug with an annular base and a single circular orbit. This can be made into a flow bordism via Theorem 5.15. It is a semi-plug, as leaves passing through the point (1,0) in T will be in the entry stopped set. The mirror-image construction of Wilson [W] will turn this semi-plug into a PL plug. Furthermore, this plug will preserve volume, by Theorem 5.14.

The easiest way to visualize the leaves in this foliation is with an analog of a Poincare return map. We look at the points in $T \times \{1\}$ which lie on the same leaf in the foliation, to see the points along the base of the flow bordism that eventually leave the bordism, and those that are in the stopped set.

In Figure 5.17(a), we see the points on the leaf which originates through the point (1,0) in T. The points shown indicate each time that leaf passes through $T \times \{1\}$. With each intersection, the points y-coordinate increases. We can see the intersection points getting closer to each other, and so, approaching the fixed circular orbit through the point (1,2)

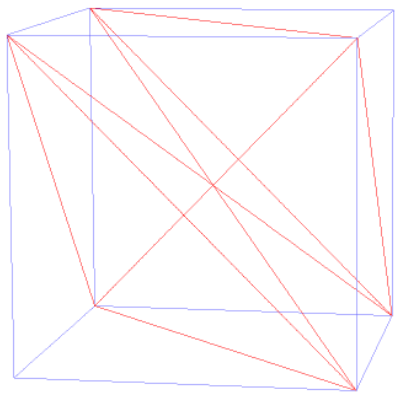

Figure 5.15: Triangulated cube

in T. Since the slope is positive, the iterations of the points intersected by this leaf have increasing y-coordinates. This shows the infinite leaf, so we have a flow bordism.

In Figure 5.17(b), we see points originating at (3/4,0) and (5/4,0). Both of these leaves exit rectangle T after 6 iterations. The positive slant in the suspension ensures that the y-coordinates of these points increase with each iteration. The widening of the base of the triangles closest to the midline of T under the map f ensure that the intersection points move around the fixed circular orbit.

This is indicated as that the points appearing in this figure move around the point (1,2). The leaves which pass through these points then avoid the fixed circular leaf, and are not part of the stopped set.

5.4.1 Dehn Surgery in a PL flow bordism

Given the correct volume-preserving homeomorphism, we can construct a flow bordism with the correct number of circular orbits and, if necessary, the desired stopped sets. Before

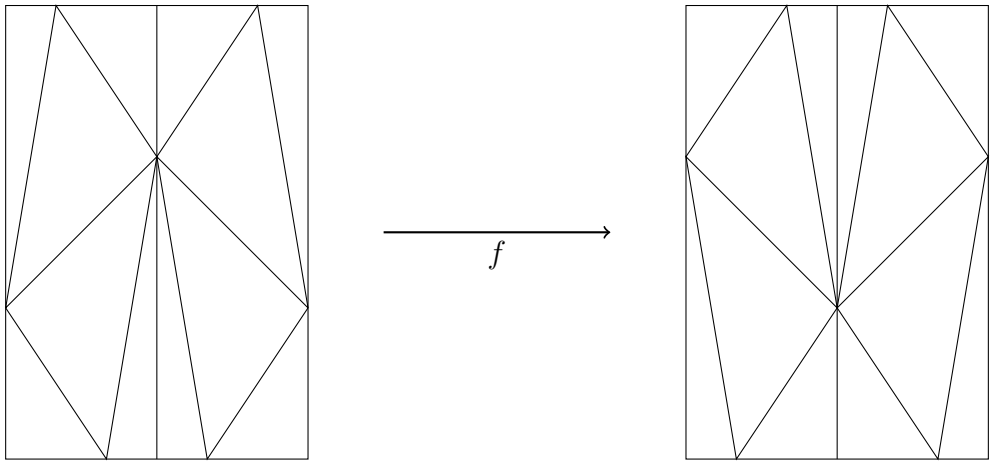

Figure 5.16: Triangulation of T and $f(T)$ in example 5.10

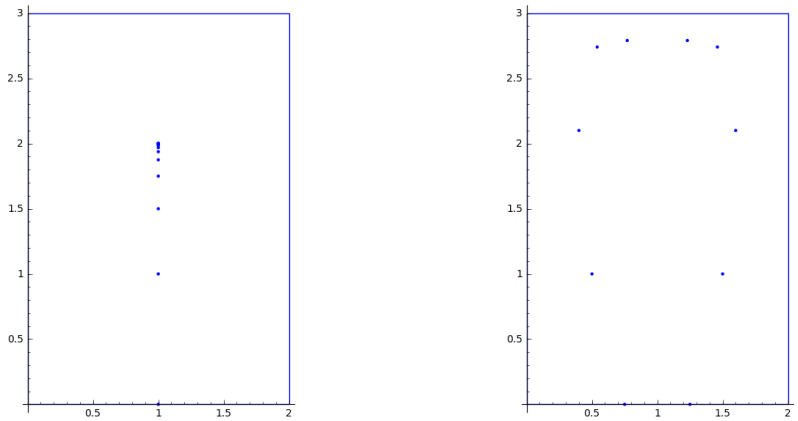

(a) Illustration of a leaf in the stopped set of example 5.16

(b) Illustration of leaves not in the stopped set of example 5.16

Figure 5.17: Points of intersection of leaves with $T \times \{1\}$ in example 5.16.

moving on to the proof of Theorem 2.6, we present the use of the slanted suspension to construct a PL version of the result of Jones and Yorke [JY], stated earlier as Theorem 3.2. This will illustrate the use of the slanted suspension to create a flow bordism, and show how the insertion is carried out. Our proof of Theorem 2.6 will then use the same basic construction, but will show how the flow bordism can be made measure-preserving, and what other conditions need to be satisfied to ensure the entire foliation remains measured. In this construction, we use Dehn surgery to remove a solid torus from the interior of a flow

bordism. The bordism arises from a slanted suspension. As discussed in Chapter 3, we are only interested in the trivial Dehn surgery here, which does not change our manifold. We detail this construction in Theorem 5.17. We will construct PL nested tori, with specific choices of triangulation. We then ensure that our use of Theorem 5.15 creates a torus in the interior of our flow bordism whose border shares that same triangulation. This will permit the choice of appropriate meridians to ensure that no Dehn twists occur during the construction.

Theorem 5.17. There exists a PL 1-foliation of $\mathbb{R}^3$, with each leaf contained in a bounded set.

Proof. We first nest simplicial approximations of tori (which we call PL tori) together, as per Jones-Yorke [JY]. In each torus, there are 16 subdivisions in the triangulation along the major circumference, and 64 subdivisions in the triangulation along the minor circumference. The subdivisions along the major circumference are spaced in intervals of $\pi/8$. Since these simplicial approximations are in $\mathbb{R}^3$, they are always triangulable.[Mo] Let T_0^{PL} be a PL torus, in the xy-plane, centered at the origin, with minor radius $m_0 = 1$ and major radius $M_0 = 4$. Let T_1^{PL} be a PL torus, in the yz-plane, centered at (0,48,0), with minor radius $m_1 = 10$ and major radius $M_1 = 48$. Rotate the entire torus by an angle of $\pi/16$. This ensures that T_0^{PL} is between vertices on the boundary of T_1^{PL}, as shown in Figure 5.18. Note that the smaller torus in this figure has all of its vertices contained one one of the subdivided regions of the larger.

Let T_n^{PL} be a PL torus, in the xy-plane if n is even, and the yz-plane if n is odd, centered at $(0,(4)12^n,0)$, with minor radius $m_n = \frac{5}{2}M_{n-1}$ and major radius $M_n = 12M_{n-1}$. Again, rotate by $\pi/16$ after each construction.

This gives a nested collection of PL tori, which union to $\mathbb{R}^3$.

We can foliate all of $\mathbb{R}^3$ using these PL Tori. If we foliate T_n^{PL} by 16-fold simplicial approximations of circles, stopping all leaves which intersect T_{n-1}^{PL} we will have a singular

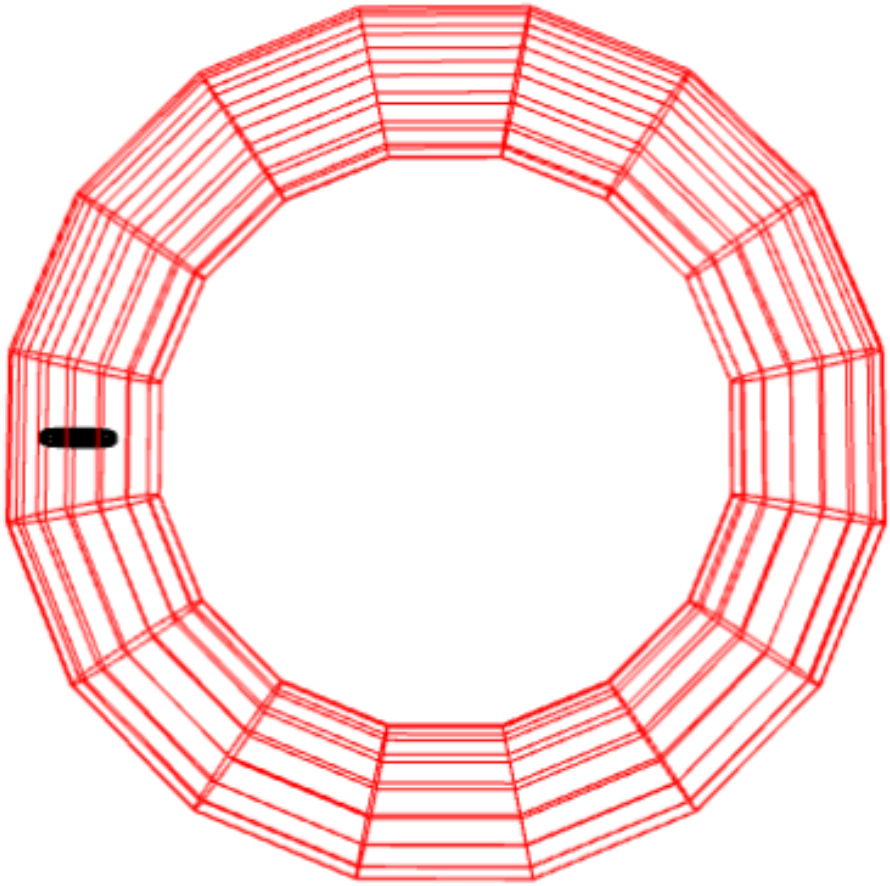

Figure 5.18: T_0^{PL} nested in T_1^{PL}.

foliation. The idea is to then remove all of these singular points by inserting a sequence of flow bordisms. Note that our rotation of each torus ensures that the segments of a leaf in T_n^{PL} which intersect T_{n-1}^{PL} in a singular point consists entirely of vertical lines.

This is why we do not need to use tobrounds in the PL case. We introduced the tobround in Chapter 4 to create vertical trajectories, but the PL-construction and the choice of simplicial approximation avoids this.

Referring again to Figure 5.18, note that all leaves in the segment of T_1^{PL} which contains T_0^{PL} are vertical. Our flow bordism will be constructed so that it is insertible, and therefore embeds transverse to vertical lines. The existing foliation consists of vertical lines, so no modification of leaves is needed during the insertion. Each leaf in the parallel boundary of our flow bordism will be finite, and the parallel boundary of the bordism will be PL homeomorphic to the product of an annulus and an interval. This careful construction will result in a bordism which is insertible, attachable, and untwisted. It is possible that an twist could be added when removing the torus from the interior of the flow bordism. As stated in Chapter 3, the Dehn surgery performed will always have slope 1, so the bordism remains untwisted.

As stated above, the current stage of the construction is a singular foliation. To modify this foliation so that it is non-singular, we will construct a slanted suspension of a rectangle. The key is that this rectangle has a square region in the center, which is shifted down by a fixed quantity l, and that we use the same l for our slant in the suspension.

Let $M = [-3, 3] \times [-2, 2]$, with horizontal axis labeled x and vertical axis labeled z, triangulated as in Figure 5.19.

Let f be the function which shifts the vertices (-1,-1), (-1,1), (1,1), and (1,-1) each down by 1/4, fixing all other vertices, as shown in Figure 5.20.

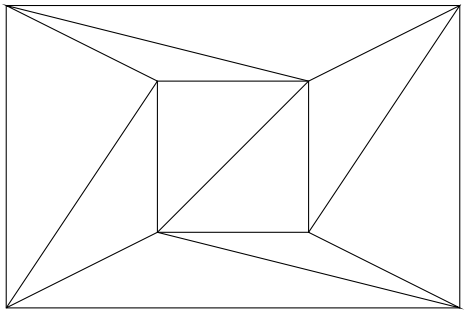

Figure 5.19: M, with simplices indicated

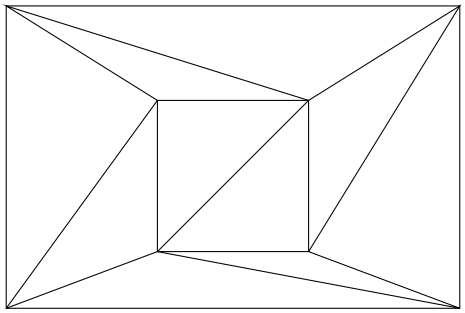

Figure 5.20: $f(M)$, with simplices indicated

Note that this does not preserve the area of each simplex, so it would not be appropriate to use in the proof of Theorem 2.6. Nevertheless, it is a PL-homeomorphism, so we can use this to create the slanted suspension $M_{\sim,f,1/4}$.

The support of $M_{\sim,f,1/4}$ is a cylinder, with an annular base, which we denote P. In taking the quotient, we have $P = \{(x, y, z) : 1 \leq \sqrt{x^2 + y^2} \leq 7, -2 \leq z \leq 2\}$. This does require a change of coordinates from the notation in the definition of the slanted suspension, but agrees with the coordinates we've given M above. We will proceed from here in the usual Cartesian coordinates.

Visualization of the leaves in $M\sim, f, 1/4$ is done with the return map, as in example 5.16. We look at the points where leaves intersect $M \times \{1\}$ in the unquotiented space. For any point (x, z) in the square at the center of M, $f(x, z) = (x, z - 1/4)$. However, the slant of $1/4$, guarantees that there is a leaf connecting $(f(x, z), 0)$ and $(x, z, 1)$. We conclude that all leaves passing through that central square are circular. The square is PL-homeomorphic

to S^1, so we have the PL analog of a foliation of a torus by circular leaves at the center of P. This is analogous to the constructions in examples 5.12 and 5.13. We avoid this situation in the parallel boundary, but it is useful to us in the interior of the bordism.

In Figure 5.21 we show leaves which approach the torus in the center of the bordism, and leaves which pass around the torus.

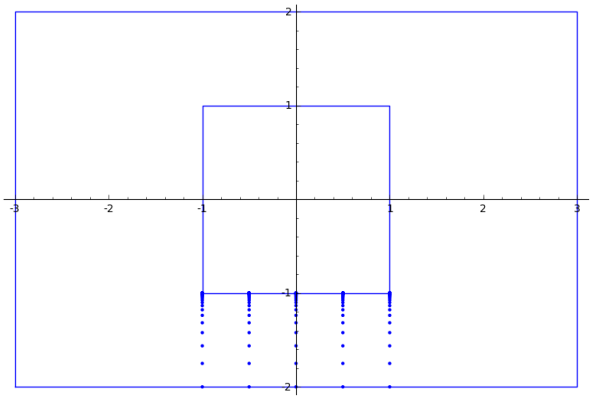

(a) Illustration of a leaf approaching the square region in M

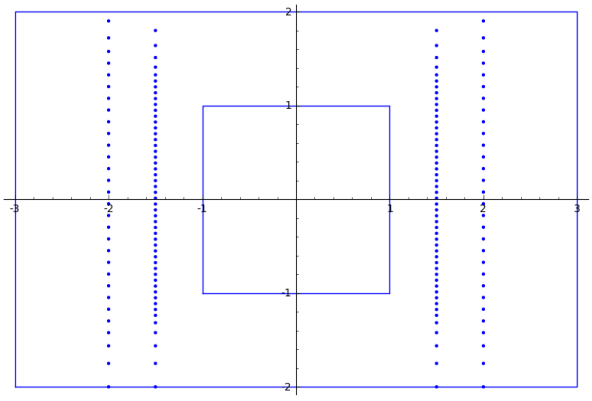

(b) Illustration of leaves not approaching the square region in M.

Figure 5.21: Points of intersection of leaves with $M \times \{1\}$ in Theorem 5.17.

Let $P_0 = P$, with the foliation inherited from $M_{\sim,f,1/4}$. P_n is the support of the slanted suspension obtained by scaling up M so that the square in the center is bounded by vertices $(-m_n, -m_m)$ and (m_n, m_n), taking the slanted suspension with slant $\frac{m_n}{4}$, under the appropriately scaled f.

The sizes of the nested tori are chosen so that there is room to insert each P_n

As constructed, $M_{\sim,f,1/4}$ is not a flow bordism, but this can be remedied by applying the function g of Theorem 5.15. This gives us the parallel boundary we need. The idea from here is to create a sequence of flow bordisms P_n, by scaling P, such that the PL torus in the center of each P_n is not only PL-homeomorphic to T^{PL}_{n-1}, but the exact same size, as given by having coordinates that only differ by a linear translation. The foliation of the boundary of T^{PL}_{n-1} will be by circular leaves, as is the foliation of the PL-torus inside P_n.

Insertion proceeds as follows. First, remove the open torus from the center of P_n, leaving the boundary of a torus, foliated by circular leaves. By our construction, the area in T^{PL}_n into which we want to embed the base of P_n is foliated by vertical leaves. Therefore the insertion can be easily carried out. Furthermore, the parallel boundary of P_n consists of vertical leaves, which have finite length, and so we have an attaching map. Finally, the boundary of T^{PL}_{n-1} is identical to the boundary of the region insider P_n after the open torus is removed. This scaling of the flow bordisms ensure that the subdivisions of the PL-tori above will match with the subdivisions introduced in the application of Theorem 5.15. Remove the boundary of T^{PL}_{n-1} during the insertion map. Then the insertion does not affect the leaves in the interior of T^{PL}_{n-1}.

It is this point when we need to ensure that our meridians match in the Dehn surgery used for the insertion. We have already scaled the PL torus in the center of P_n. In our construction of T^{PL}_{n-1}, we chose a 16 vertices along the major radius and 64 vertices along the minor radius. The use of Theorem 5.15 allows for the same choice of subdivision on the torus in the interior of P_n, and therefore, the boundary of this torus can be chosen to have the same triangulation as T^{PL}_{n-1}. We then have only to choose our meridians. For the meridian on T^{PL}_{n-1}, we can think of each T^{PL}_i as being described by cylindrical coordinates. We use two options here. If i is even, let the coordinates be (r, θ, z) with $x = r\cos\theta$ and $y = r\sin\theta$. If i is odd, use coordinates (r, θ, x), with $z = r\cos\theta$ and $y = r\sin\theta$. Changes in the θ coordinate were already assumed with the rotation by $\pi/16$ in our construction of

each T_i^{PL} above. Choose the meridian to be the 64-fold approximation of S_1 with coordinate $\theta = 0$, prior to any rotation of the torus. This clearly bounds a solid disc in T_i^{PL}. For the longitude on the torus in the interior of P_n, choose the 64-fold approximation of S_1 which exists as the boundary of the square with vertices $(-m_n, -m_m)$ and (m_n, m_n), with third coordinate 0, prior to the quotient in the slanted suspension. This clearly also bounds a disc, and so is a meridian. Since both tori have the same triangulation, we can see that the mapping of one meridian to the other in the insertion of our flow bordism will only affect the trivial Dehn surgery, and that this insertion will not affect the topology of the underlying manifold, that is, $\mathbb{R}^3$.

Each P_n can therefore be inserted around each $T^{PL}n - 1$, yielding a foliation of $\mathbb{R}^3$, which has removed all previously indicated singular points, and in which each leaf remains bounded within one of the PL-tori. □

We have a corollary to Theorem 4.7 which will be useful in finishing our last proof.

Corollary 5.18. A PL flow bordism, with an invariant transverse measure, admits a PL dynamical system, which preserves measure.

Proof. The proof follows immediately from the proof of Theorem 4.7, with a few small changes. First, we assume the measures used are simplicial. Second, we assume the nice foliation atlas has chart maps which are PL homeomorphisms. Finally, rather than using Theorem 4.6, we use Theorem 5.7. □

This is a helpful result, as it allows us prove Theorem 2.6 by essentially repeating the construction from Theorem 5.17, but with a different PL-homeomorphism in the slanted suspension.

We now move on to a proof of Theorem 2.6.

5.5 Proof of Theorem 2.6

Proof. For this construction, we will start with the same nested PL-tori as in Theorem 5.17, again denoted $\{T_n^{PL} : n \in 0, 1, \ldots\}$. We also begin with the same region $M = [-3, 3] \times [-2, 2]$ as the starting point for the slanted suspension.

The difference here is that M has a different triangulation, and that the PL-homeomorphism f preserves the area on the 2-simplices in M. We then take the slanted suspension of M, with slant $1/4$, which by Theorem 5.13, is a measured foliation.

Next, we apply a PL homeomorphism, as per Theorem 5.15, to the slanted suspension $M_{\sim,f,1/4}$, to get a flow bordism. Next apply Lemmas 5.9 and 5.10 to ensure that the foliation remains measured. The support of the flow bordism is the same cylinder with annular base, which was denoted P in Theorem 5.17.

We can build a sequence of carefully constructed flow bordisms from here. Each is built specifically to be insertible, attachable, and untwisted, with size specific to each of the PL-tori T_n^{PL}. The repeated insertion of these bordisms creates a measured foliation of $\mathbb{R}^3$, with all leaves contained in bounded sets. An application of corollary 5.18 finishes the proof.

Let $M = [-3, 3] \times [-2, 2]$. Triangulate M, and let $f : M \to M$ be the PL homeomorphism, which preserves area on 2-simplices, and shifts the vertices of the shaded region down $1/4$. The vertices are labeled in Figures 5.22 and 5.23, while the areas of the simplices are shown in Figures 5.24 and 5.25.

Take the slanted suspension $\mathcal{P} = M_{\sim,f,1/4}$ of M with slant $1/4$. We immediately have several of the properties we need to get a PL analog of the construction in Theorem 2.5.

First, since f preserves area on 2-simplices, $\mathcal{P}$ is a measured foliation, by Theorem 5.13. Denote the support of $\mathcal{P}$ by P. Then $P = \{(x, y, z) : 1 \leq \sqrt{x^2 + y^2} \leq 7, -2 \leq z \leq 2\}$, just as in the Theorem 5.17.

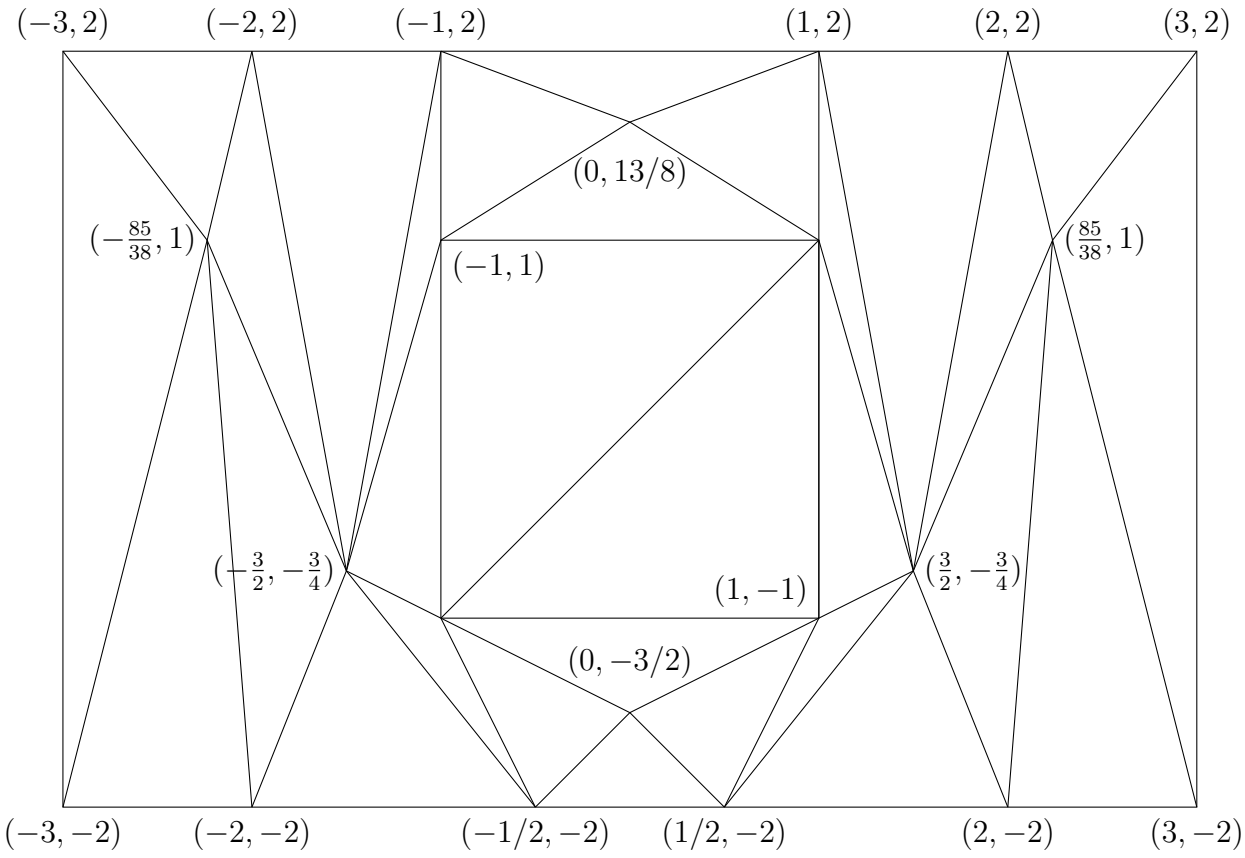

Figure 5.22: M with vertices indicated

The region $[-1,1]\times[-1,1]\times[0,1]$ forms a PL-torus foliated by simplicial approximations of circular leaves when the quotient is applied. This gives a simplicial approximation of a solid torus with major radius 4 and minor radius 1, which is contained in P. Figure 5.26 shows an approximate version of this, though it has been smoothed for clarify.

Note that the leaf in the boundary of P shown in Figure 5.26 indicates that this component of the boundary is not parallel boundary.

We will apply Theorem 5.15 to remedy the issue with the parallel boundary. Since the slant is $l = 1/4$, the height of M is 4, and f is the identify on the boundary, $w = 16$. We therefore use a 16-fold covering to retriangulate P. Figure 5.27 shows this applied to $[-2,2] \times [0,1]$ in the unquotiented space. This is analogous to the process described in

Theorem 5.15. We will fix each of the vertices with index 0-15 in Figure 5.27, and shift each of the remaining vertices one to the left. Next, fix all vertices with index 0-31, and repeat the shifting for all higher indexed vertices. As per the details of Theorem 5.15, this process will eventually result in a foliation by vertical leaves, which preserving the area of each simplex in Figure 5.27.

We can break down P into 3 boundary components. The first, is when $z = -2$. This is our transverse boundary oriented inwards, F_-. The second is when $z = 2$, which is F_+, the transverse boundary oriented outwards. The remaining boundary component, usually referred to as the sides of the cylinder, is not currently parallel boundary. Apply Theorem 5.15 to get remedy this, as shown in Figure 5.32. The support remains P, and we denote the new foliation of P by $\mathcal{S}$. We therefore have that $\mathcal{S}$ is a measured flow bordism, as proven in Theorem 5.15. Note also that all of the circular leaves on the simplicial approximation of the torus contained in P were parallel to the 1-simplices which were only shifted to the left in the application of Theorem 5.15. Therefore, these leaves remain circular, as in Figures 5.26 and 5.32.

We can determine the entry stopped set in $\mathcal{P}$, which will have measure zero.

As in Theorem 5.17, all points in the square bounded by (-1,-1) and (1,1) lie on circular leaves. Additionally, the points (0, -3/2) and (0, 13/8) give rise to circular leaves. Their image under f decreases the second coordinate by the same amount as the slant of the suspension. As stated in Theorem 5.17, this is analogous to the construction from Examples 5.12 and 5.13.

The entry stopped set F_- is only the simplicial approximation of the circle in P corresponding to the point (0,-2) in M, crossed with [0,1], and with endpoints identified. For any volume form in $\mathbb{R}^3$, the simplicial measure of a circle is zero, hence the entry stopped set has measure zero.

For any other point in M with first coordinate not 0, the first coordinate is changed during the application of f. Therefore the leaf which intersects these points cannot simply have an increasing second coordinate. They move either left or right while the second coordinate increases, causing the points which intersect $M \times \{1\}$ to move around the center square. This is shown in Figures 5.23-5.31

The exit stopped set it determined similarly. The point (0, 13/8) lies on a circular leaf. The leaf through the point (0,2) will approach (0, 13/8), while all other leaves, when traced with the reversed orientation, will avoid the square in the center of M. Therefore F_+ is a circle lying on the component of the boundary of P with $z = 2$. For the same reason as above, the exit stopped set has measure zero.

As stated earlier, we are beginning with the nested PL tori from Theorem 5.17.

Insertion follows as described in the proof of Theorem 5.17.

To use the flow bordism $\mathcal{S}$ to make this into a non-singular foliation, first remove the interior of the minimal torus from the center of $\mathcal{S}$, and scale it to create a sequence of flow bordisms, $\mathcal{S}_n$, where the removed torus in $\mathcal{S}_n$ is PL-homeomorphic to T_n^{PL}, and the total volume of the removed torus in $\mathcal{S}_\setminus$ is the same as that of T_n^{PL}. The support of $\mathcal{S}$ was retriangulated during the construction of the parallel boundary. In doing so, the region left after removing the interior torus is now bounded by the product of a 16-fold simplicial approximation of S^1 and a 64-fold simplicial approximation of S^1. Lemma 5.9 assured that the foliation $\mathcal{S}$ remained measured during this process.

Once scaled up, the height of the support of each $\mathcal{S}_n$ will be twice the minor radius of the torus contained inside that support. The base remains transverse boundary, and our existing foliation of T_{n+1}^{PL} ensures that all leaves in that neighborhood of T_n^{PL} are already vertical. Therefore the conditions for insertion from section 4.2 are satisfied. The conditions for each bordism to be attachable and untwisted are satisfied for the same reasons as in Theorem 5.17. The choice of triangulation for the torus in the interior of $\mathcal{S}_n$ can be chosen

just as in Theorem 5.17. This ensures that our Dehn surgery is trivial and does not cause any issues. It is the careful construction of both the bordism, and the foliation on the nested tori which is to be modified that permits this.

Let ω be the simplicial measure on $\mathbb{R}^3$ given by the usual Euclidean volume form. Then each T_n^{PL} has measure equal to its Lebesgue measure. We have constructed $\mathcal{S}_n$ in such a way that the vertices on the torus contained in $\mathcal{S}_n$ are mapped exactly to the vertices on the boundary of T_{n-1}^{PL}. The leaves in the parallel and transverse boundary of $\mathcal{S}_n$ match with the leaves in the existing foliation of the nested PL-tori. The regions where the boundaries meet can be given a common subdivision using Theorem 5.2.

Each $\mathcal{S}_n$ is measured, so we let ω_n be the simplicial measure on $\mathcal{S}_n$. Our condition on the scaling of $\mathcal{S}_n$ will give ω and ω_n the same total volume on $\mathcal{S}_n$. In the parlance of Theorem 5.7, let M_1 be the support of $\mathcal{S}_n$, and M_2 be the subset of T_n^{PL} which contains T_{n-1}^{PL} and is PL-homeomorphic to the support of $\mathcal{S}_\backslash$. Then there exists a volume preserving PL-homeomorphism f from M_1 to M_2, which pulls back the volume form ω_n to ω.

Since $\mathcal{S}$ was measured, $\mathcal{S}_n$ is measured. By the argument above, insertion of $\mathcal{S}_n$ preserves the usual Lebesgue measure on $\mathbb{R}^3$. For the portion of each T_n^{PL} which was not modified by insertion, it is foliated by simplicial approximations of circles, and a foliation by circles is measured. Therefore, this constructions is a measured foliation of $\mathbb{R}^3$.

Corollary 5.18 is enough to ensure that the foliation in each $\mathcal{S}_n$ will create a PL dynamical system. To extend this to the rest of T_n^{PL}, we need a whose trajectories are simplicially approximated by the leaves in T_n^{PL}. Take the closure of $T_n^{PL} \backslash \mathcal{S}_n$. This satisfies the conditions of Corollary 5.18, so it also yields a PL dynamical system.

By construction, the foliations on the boundary of $\mathcal{S}_n$ and on $T_n^{PL} \setminus \mathcal{S}_n$ agree, and since our dynamics are only required to be PL, the dynamical systems created both in and out of the flow bordism agree at the switching manifold.

Therefore, the measured foliation yields a measure-preserving dynamical system, and our theorem is satisfied. □

Figure 5.23: $f(M)$ with vertices indicated

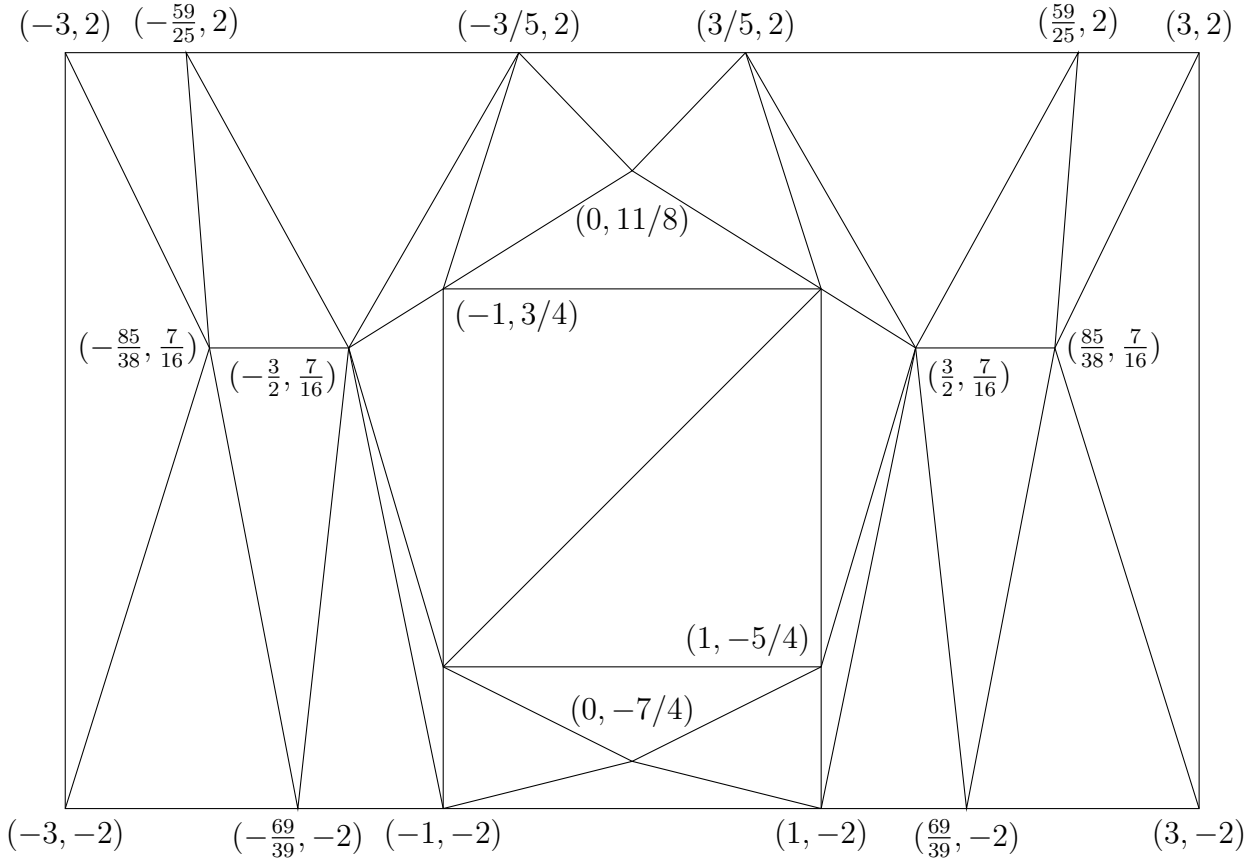

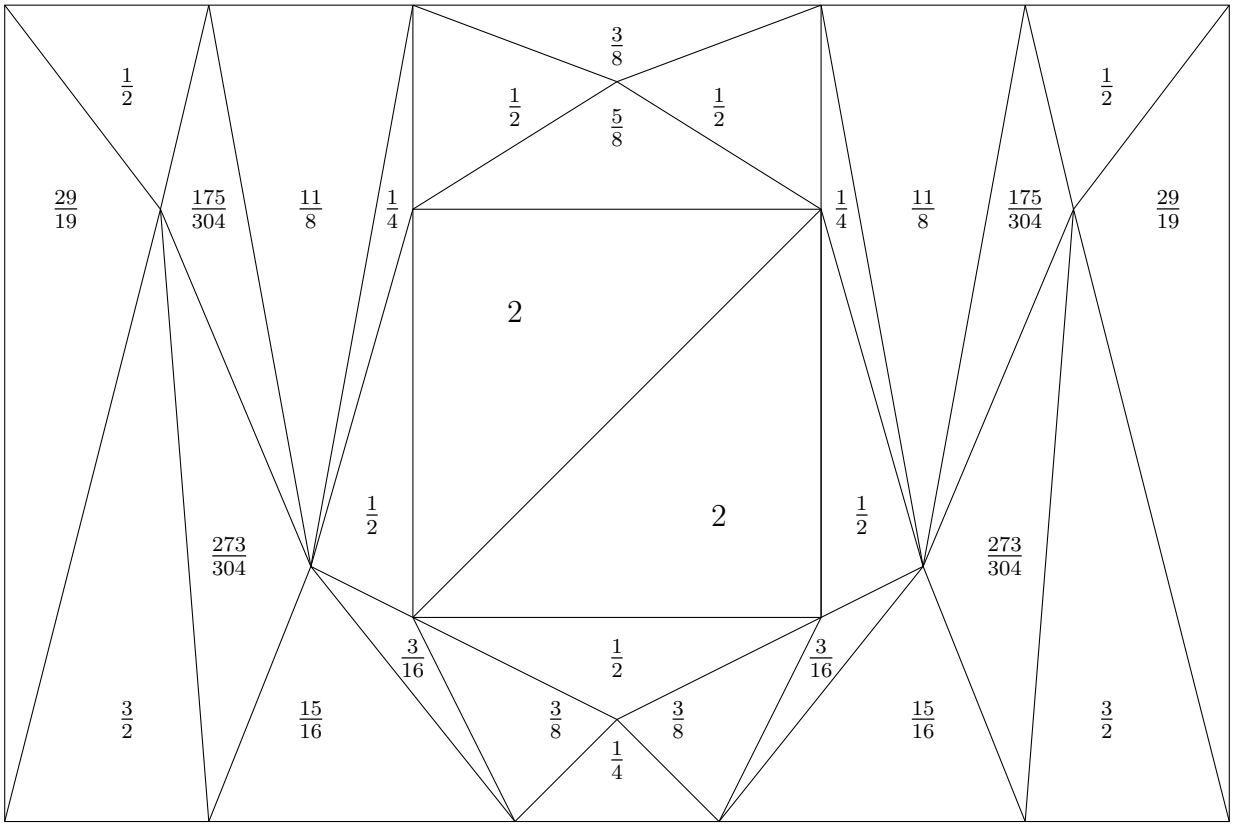

Figure 5.24: M with areas of simplices indicated. The sum of the areas on the simplices is 24.

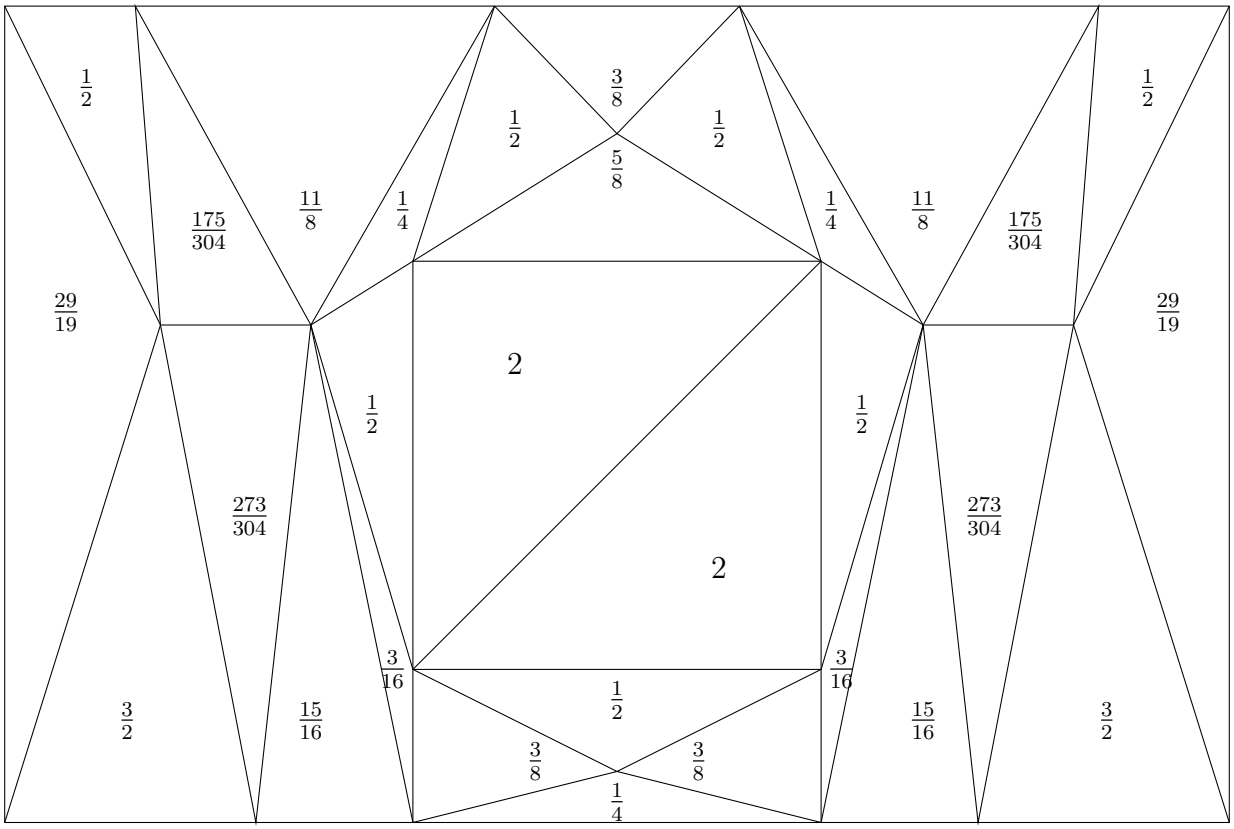

Figure 5.25: $f(M)$ with area of simplices indicated. The sum of the areas on the simplices is 24.

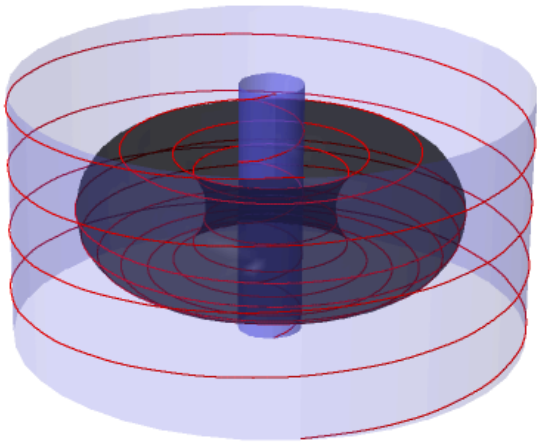

Figure 5.26: Support P of the slanted suspension of M, with torus in the interior, and a sample leaf shown on the boundary.

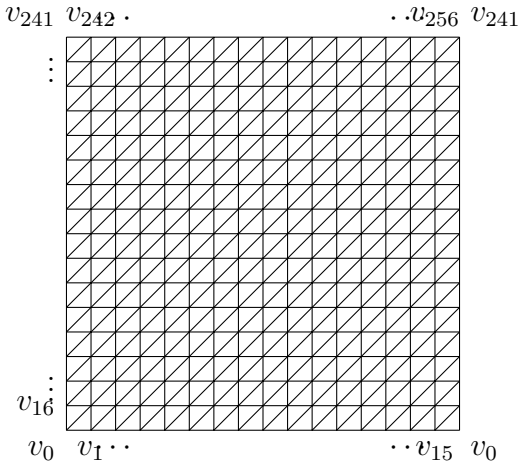

Figure 5.27: Triangulation of a cylinder with labeled vertices. The vertical axis is scaled down by a factor of 4.

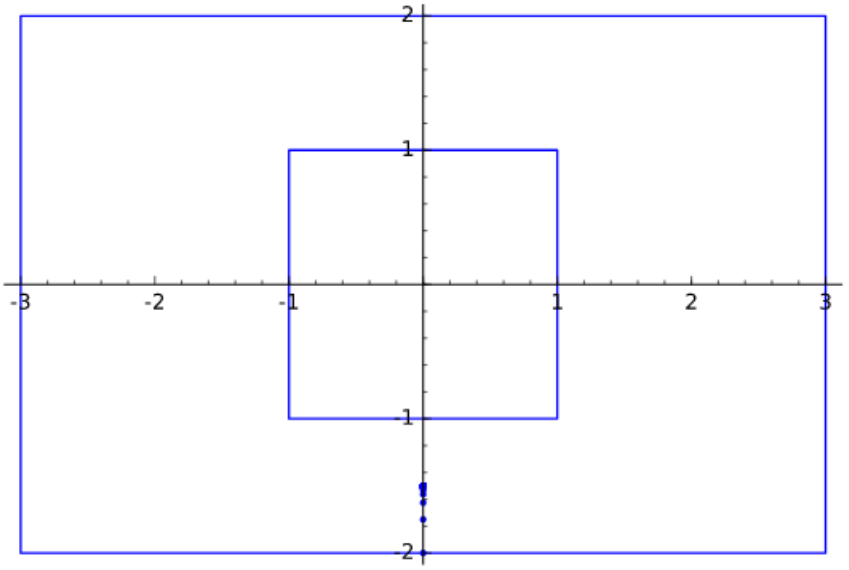

Figure 5.28: Sequence of points in $M \times \{1\}$ arising from a leaf in the entry stopped set.

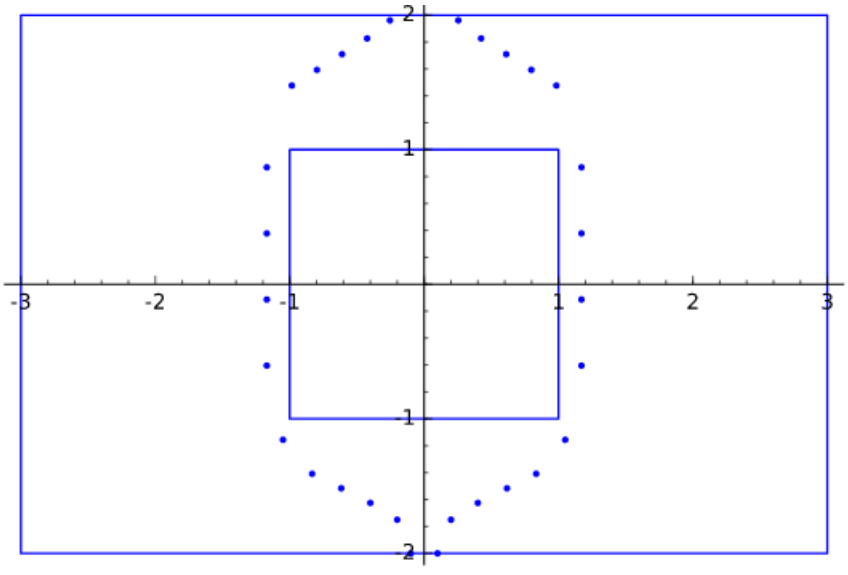

Figure 5.29: Trajectories originating at (0.1,-2) and (-0.1,-2)

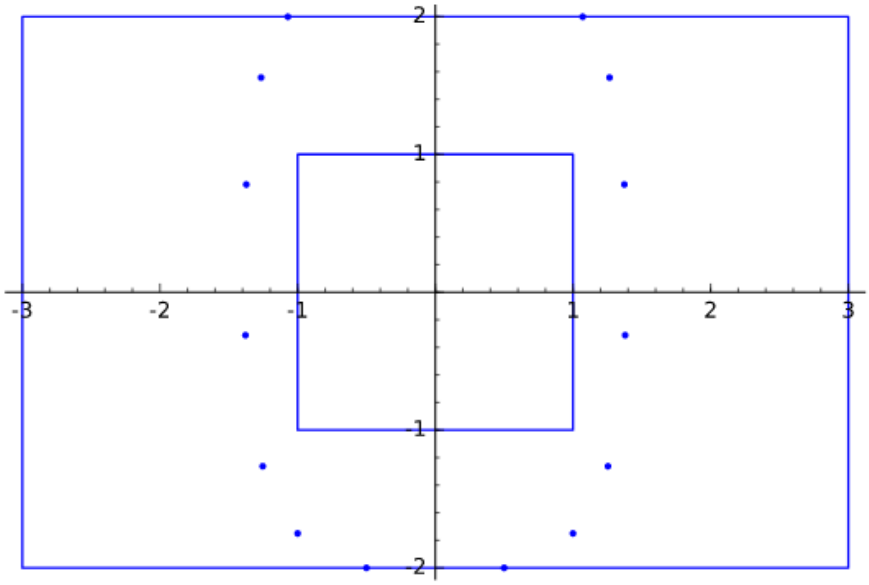

Figure 5.30: Trajectories originating at (1/2,-2) and (-1/2,-2)

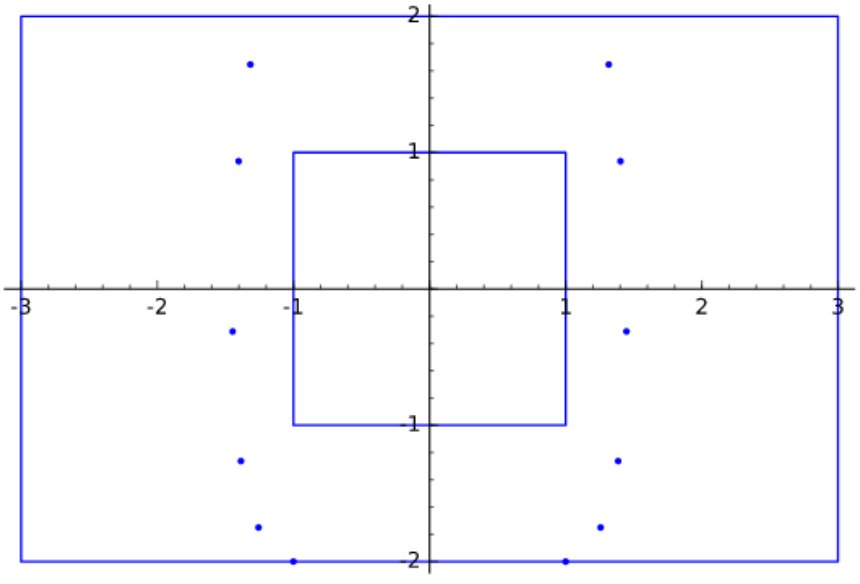

Figure 5.31: Trajectories originating at (1,-2) and (-1,-2)

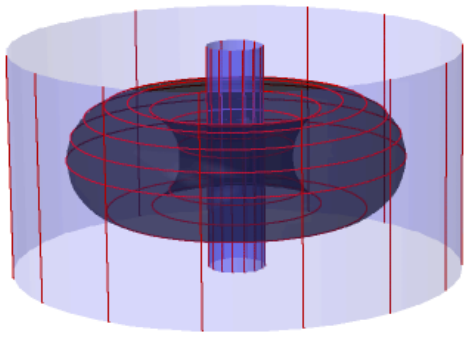

Figure 5.32: Parallel boundary after application of Theorem 5.14

References

[Ac] Acheson, D.J., *Elementary Fluid Dynamics*, Clarendon Press, Oxford, 1990.

[A] Akin, E., *Simplicial Dynamical Systems*, AMS, Providence, 1999.

[Ba] Banyaga, A., *Formes-volume sur les variétés a bord* Enseignement Math. (2), 20:127131, 1974.

[BS] Bhatia, N.P. and Szegö, G.P., *Stability Theory in Dynamical Systems*, Springer-Verlag, New York, 1967.

[B] Bing, R.H., *The Geometric Topology of 3-Manifolds*, AMS, Providence, 1983.

[B2] Bing, R.H., *The Elusive Fixed Point Property*, The American Mathematical Monthly, **76** (1969), no. 2, 119-132.

[B3] Bing, R.H., *Challenging Conjectures*, The American Mathematical Monthly, **74** 1967, no. 1, part 2, 56-64.

[Bo] Borsuk, *Sur on continu acyclique qui se laisse transformer topologiquement en luí-même sans points invariants*, Fund. Math., **24**, 1935, 51-58.

[BM] Brechner, B., Mauldin, R.D., *Homeomorphisms of the plane*, Pacific Journal of Mathematics, **59**, 1975, no. 2, 375-381.

[BMPR] Bruveris, M., Michor, P., Parusinski, A., Rainer, A., *Moser's theorem on manifolds with corners* `arxiv.org:1604.07787v1`

[Br, DS] Bryant, J.L., Piecewise Linear Topology, in *Handbook of Geometric Topology*, (Daverman, R.J., Sher, R.B, editors), North Holland, Amsterdam, 2002.

[CC] Candel, A. and Conlon L., *Foliations I*, AMS, Providence, 2000.

[CL] Coddington, E. and Levinson, N. *Theory of Ordinary Differential Equations*, McGraw-Hill Book Company, New York, 1955.

[DBCK] diBernardo, M., Budd, C.J., Champneys, A.R., Kowalczyk P., *Piecewise-smooth Dynamical Systems*, Springer, London, 2008.

[FLP] Fathi,A., Laudenbach,F., and Poénaru, V., *Thurston's Work on Surfaces*, translated by Djun Kim and Dan Margalit, Mathematical Notes, 48, Princeton University Press, 2012.

[G] Gordon, C., *Dehn Surgery and 3-Manifolds*, IAS/Park City Mathematics Series, Volume 16, 2006.

[GP] Guillemin, V., Pollack, A., *Differential Topology*, AMS Chelsea Publishing, Providence, 1974.

[HP] Henriques, A., Pak, I., *Volume-preserving PL-maps between polyhedra*, in *Lectures on Discrete and Polyhedral Geometry*, `http://www.math.ucla.edu/ pak/geompol8.pdf`.

[Hi] Hirsch, M. *Differential Topology*. Springer-Verlag, New York, 1976.

[HSD] Hirsch, M., Smale, S., Devaney, R., *Differential Equations, Dynamical Systems, and an Introduction to Chaos*, Elsevier Academic Press, Oxford, UK, 2004.

[H, LN] Hurder, S. Lectures on Foliation Dynamics, in *Foliations: Dynamics, Geometry, and Topology*, (Lopez, J.A., Nicolau, M. editors), Springer, Basel, 2014.

[J] Janna, W.S. *Introduction to Fluid Mechanics*, CRC Press, Boca Raton, 2010.

[JY] Jones, G.S. and Yorke, J.A. *The existence and non-existence of critical points in bounded flows*, Journal of Differential Equations, **6**, 1969, 236-246.

[HK] Khudaverdian, H.M., *Riemannian Geometry*, University of Manchester, `www.maths.manchester.ac.uk/ khudian/Teaching/Geometry/GeomRim11/riemgeom11.pdf`.

[GK] Kuperberg, G. *A volume-preserving counterexample to the Seifert conjecture*, Comment. Math. Helv. **71**, 1996, no. 1, 70-97.

[KK] Kuperberg, K. *A smooth counterexample to the Seifert conjecture*, Annals of Mathematics, **140**,1994,723-732.

[GKK] Kuperberg, K. and Kuperberg, G. *Generalized counterexamples to the Seifert conjecture*, Annals of Mathematics, Second Series, **143, No. 3**, 1996, 547-576.

[KR] Kuperberg K. and Reed C., *A rest point free dynamical system on* $\mathbb{R}^3$ *with uniformly bounded trajectories*, Fund. Math., **114** 1981, 229-234.

[Ku] Kulczycki, M. *A note on special measure-preserving dynamical systems in metric spaces*, Topology Proceedings, **27**, 2003, no. 1, 211-216.

[L] Lickorish, W.B.R., *A representation of orientable combinatorial 3-manifolds*, Annals of Math., **76**, 1962, no. 3, 531-540.

[Ma] Mauldin, D., Ed., *The Scottish Book: Mathematics from the Scottish Cafe*, Boston: Birkhäuser, 1981.

[M] Milnor, J. *On the concept of attractors*, Communications in Mathematical Physics, **99**, 1985, 177-195.

[M2] Milnor, J., *Introductory Dynamics Lectures*, Stony Brook University, `http://www.math.stonybrook.edu/ jack/DYNOTES/`.

[Mo] Moise, E., *Geometric Toplogy in Dimensions 2 and 3*, Springer-Verlag, New York, 1977.

[Mo2] Moise, E. *Affine Strutures in 3-Manifolds, IV. Piecewise Linear Approximations of Homeomorphisms*, Annals of Mathematics, **55**, no. 2, 1952, 215-222.

[Mos] Moser, J., *On the volume elements of a manifold*, Transactions of the American Mathematical Society, **120**, 1965, 286-294.

[Mu] Munkres, J., *Elements of Algebraic Topology*, Perseus, Cambridge, 1984.

[P] Plante, J., *Foliations with measure preserving holonomy*, Annals of Mathematics, vol. 102, no. 2, 1975, 327361.

[R] Richardson, K., *Suspension Foliations: Interesting Examples of Topology and Geometry*, Notes from Jeju National University colloquium, Korea, 2009.

[RoSa] Rourke, C.P., Sanderson, B.J., *Introduction to Piecewise-Linear Topology*, Springer-Verlag, New York, 1972.

[Ro] Royden, H.L., Fitzpatrick, P.M., *Real Analysis, 4th edition*, Pearson, Boston, 2010

[RS] Ruelle, D. and Sullivan, D. *Currents, flows, and diffeomorphisms*, Topology, **14**, 1975, 319-327.

[Sp] Spivak, M. *Calculus on Manifolds*, W.A. Benjamin, Reading, 1965.

[T] Tamura, I. *Topology of Foliations:An Introduction*, AMS, Providence, 1992.

[W] Wilson, F.W. *On the minimal sets of non-singular vector fields*, Ann. of Math., **84**, 1966, 529-536.

[Wa] Walczak, P., *Dynamics of foliations, groups and pseudogroups*, Birkhuser Verlag, 2004.